REGULATION OF LIPID OXIDATION DURING THERMOGENESIS AT HIGH ALTITUDE IN DEER MICE

REGULATION OF LIPID OXIDATION DURING THERMOGENESIS AT HIGH ALTITUDE IN DEER MICE

By Sulayman A. Lyons, B.Sc.

A Thesis

Submitted to the School of Graduate Studies

In Partial Fulfillment of the Requirements for the Degree

Doctor of Philosophy

McMaster University

DOCTOR OF PHILOSOPHY (2022) MCMASTER UNIVERSITY

(Department of Biology) Hamilton, Ontario

TITLE: Regulation of lipid oxidation during thermogenesis at high altitude in deer mice

AUTHOR: Sulayman A. Lyons

Hons. B.Sc. (McMaster University)

SUPERVISOR: Dr. Grant B. McClelland

NUMBER OF PAGES: xv, 186

LAY ABSTRACT

Thermogenesis, the metabolic production of heat, allows endotherms to maintain stable body temperatures in cold environments. However, it was not yet understood how small mammals fuel and sustain heat production in the cold and low oxygen environment of high altitude. My thesis has uncovered how deer mice native to high altitudes have adapted to burning fats at high rates in hypoxia to sustain thermogenesis. My findings show that high delivery rates of fats to heat-generating tissues are responsible for the elevated rates of heat production in high altitude deer mice. My work contributes to our understanding of the inner workings of the fat pathways and how it has evolved to ensure survival in extreme environmental conditions.

ABSTRACT

Organisms are constantly balancing energy demand with an adequate supply of oxygen and substrates to sustain metabolic activity. Thermogenesis is an important metabolic process by which endotherms predominately burn lipids to regulate and maintain their body temperatures by balancing heat loss with heat production. Due to their high rates of heat loss, small winter-active mammals, like the North American deer mouse (*Peromyscus maniculatus*), are constantly challenged with thermogenesis. Deer mice are also native to high-altitude environments, conditions that further complicate the process of thermogenesis due to the inherent reduced oxygen availability. How metabolic substrates are used for fuelling and sustaining thermogenesis at high altitude remains unclear. The goal of my thesis was to examine how lipid metabolism has evolved to sustain heat production in animals living in high-altitude environments. This was achieved by using deer mice native to high- and low-altitudes acclimated to either standard lab conditions or simulated high altitude (cold hypoxia). I demonstrate that during thermogenic capacity (cold-induced $\dot{V}O_2max$), high-altitude deer mice have higher thermogenic lipid oxidation rates compared to their lowland counterparts, which is further increased after cold hypoxia acclimation. Interestingly, these high rates of lipid oxidation were associated with higher circulatory delivery rates of fatty acids and triglycerides to thermo-effector tissues. Specifically, I show that after a bout of cold-induced $\dot{V}O_2max$, fatty acid uptake occurs primarily in the skeletal muscle in control acclimated high-altitude deer mice, and then shifts to brown adipose tissue following acclimation to high altitude conditions. These findings clearly show that in high-altitude deer mice, maximal thermogenesis is reliant on elevated delivery of circulatory lipids to muscle and brown

adipose tissue. This research further sheds light on the mechanistic underpinnings responsible for enhanced thermogenic capacity of high-altitude deer mice and capacity for the highest lipid oxidation rates observed in any mammal.

ACKNOWLEDGEMENTS

Bismillah ar-Rahman ar-Rahim. My days, it is so wild to think that 6 years has already gone by, and it is the end of truly a remarkable experience that was only possible because of my mentors, friends and family.

Grant, there isn't enough space to express my gratitude and appreciation towards you as both a mentor and friend after all these years. You are an incredible researcher, you are family oriented, and you are kind – all things I aspire to be. Thank you so much for taking me under your wing and sharing your passion for substrate metabolism. Thank you for always motivating me to achieve more, sharing my enthusiasm for science and new ideas, being my Pictionary partner, and ruler of all Dad jokes. Graham, thank you so much for giving me the opportunity to get into the lab for my honours thesis project; it was truly the first step that got me hooked on research. I have always admired your enthusiasm for research and have always appreciated your feedback. Greg, thank you for playing an integral role for providing unique perspectives that was critical for advancing my project.

Thank you to all the past and present members of the McClelland and Scott labs, especially Sajeni, Cayleih, Catie, Oliver, Soren, Neal, Lauren and Claire B. I would not be the researcher I am today if it weren't for you all. I have been so fortunate to be surrounded by such brilliant minds, kind, and fun people. Thank you for making my graduate experience the best one. I also must thank Megan and Dawn from the CAF for being integral for animal care. My project would not have existed if it weren't for their consistent and amazing work.

I would like to thank my beautiful family for supporting me on this journey on becoming a “professional student”. Thank you, Mom and Dad, for always teaching me to chase my dreams and not being afraid to put in the work because it always pays off. Ibo and Yasmine, it’s been so amazing seeing you both achieve all that you have. It encourages me to keep shooting for the stars. To my new family, Jack, Mary, and Matthew, thank you for all the love and support you have provided me throughout my graduate career, and for what the future holds. Emily, I am so proud of you. Thank you for supporting me day in and day out, being my personal editor, and listening to me ramble on about my research more than anyone else. You could probably also just add Ph.D. beside the M.D. you already have! I love you so much.

I can’t wait to see what the future has in store. And so we go. *Ameen.*

TABLE OF CONTENTS

LIST OF FIGURES AND TABLES

LIST OF ABBREVIATIONS AND SYMBOLS

A.s.l.: Above sea level

AMPK: AMP-activated protein kinase

ATP: Adenosine triphosphate

BAT: Brown adipose tissue

CH: Cold hypoxia

CoA: Coenzyme A

COX: Cytochrome c oxidase

CPM: Counts per minute

CPT: Carnitine palmitoyltransferase

CS: Citrate synthase

FA: Fatty acids

FABP: Fatty acid binding protein

FAT/CD36: Fatty acid translocase cluster of differentiation 36

HA: High altitude

He: Helium

HOAD: β-hydroxyacyl-CoA dehydrogenase

iBAT: interscapular brown adipose tissue

IMTG: Intramuscular triglyceride

ingWAT: Inguinal white adipose tissue

LA: Low altitude

LPL: Lipoprotein lipase

N_2: Nitrogen

NADH: Nicotinamide adenine dinucleotide + hydrogen

NEFA: Non-esterified fatty acid

NiAc: Nicotinic acid

NST: Non-shivering thermogenesis

O_2: Oxygen

RER: Respiratory exchange ratio

S.e.m.: Standard error of the mean

ST: Shivering thermogenesis

TCA: Tricarboxylic acid cycle

TG: Triglyceride

THL: Tetrahydrolipstatin

TN: Thermoneutral

UCP-1: Uncoupling protein-1

VLDL: Very-low density protein

Vmax: Apparent maximal enzyme activity

$\dot{V}O_2$: Rate of oxygen consumption

$\dot{V}O_2max$: Maximal oxygen consumption rate

WAT: White adipose tissue

WN: Warm normoxia

DECLARATION OF ACADEMIC ACHIEVMENT

This thesis is organized in a sandwich format consisting of five chapters, as recommended, and approved by members of my supervisory committee and by McMaster University. Chapter 1 is a general overview of background material, outlined aims and objectives, and hypotheses tested. Chapter 2 through 4 are manuscripts that are published, or ready to be submitted for publication in a peer reviewed scientific journal. Chapter 2 is referred to as Lyons et al., (2021) and Chapter 3 is referred to as Lyons and McClelland, (2022). Chapter 5 summarizes the major findings of this thesis, places these findings in a context of the current literature, and provides ideas for future research directions.

CHAPTER 1 **GENERAL INTRODUCTION**

CHAPTER 2 **LIPID OXIDATION DURING THERMOGENESIS IN HIGH-ALTITUDE DEER MICE (*PEROMYSCUS MANICULATUS*)**

Authors: Sulayman A. Lyons, Kevin B. Tate, Kenneth C. Welch Jr., and Grant B. McClelland.

Status: Published May 18, 2021

Journal: *American Journal of Physiology: Regulatory, Integrative, and Comparative Physiology*

Comments: This study was conducted by S.A.L. and K.B.T under the supervision of G.B.M. Co-author K.C.W. provided technical and logistical support. S.A.L. wrote the manuscript.

CHAPTER 3 **THERMOGENESIS IS SUPPORTED BY HIGH RATES OF CIRCULATORY FATTY ACID AND TRIGLYCERIDE DELIVERY IN HIGHLAND DEER MICE**

Authors: Sulayman A. Lyons and Grant B. McClelland.

Status: Published June 14, 2022

Journal: *Journal of Experimental Biology*

Comments: This study was conducted by S.A.L. under the supervision of G.B.M. S.A.L. wrote the manuscript.

CHAPTER 4 **HIGHLAND DEER MICE REDIRECT TISSUE FATTY ACID UPTAKE TO SUPPORT THERMOGENESIS AFTER COLD HYPOXIA ACCLIMATION.**

Authors: Sulayman A. Lyons and Grant B. McClelland.

Status: Manuscript prepared for the submission to the *American Journal of Physiology: Regulatory, Integrative, and Comparative Physiology*

Comments: This study was conducted by S.A.L. under the supervision of G.B.M. S.A.L. wrote the manuscript.

CHAPTER 5 **GENERAL DISCUSSION**

APPENDIX A. **SUPPLEMENTAL MATERIALS**

CHAPTER 1: GENERAL INTRODUCTION

1.1 INTRODUCTION

The ability of animals to survive in extreme environments, all while balancing energy supply and demand, has always fascinated physiologists. Depending on the aerobic metabolic demand or functional needs of the organism, the oxygen (O_2) and metabolic substrate pathways are adjusted and maintained to ensure the effective delivery of both O_2 and metabolic fuel (Weibel et al., 1996). The oxygen cascade is a singular pathway, with equal rates of O_2 flux along all steps of the pathway (from the environment, to circulation, to tissue mitochondria), while substrate pathways are more complex due to the ability to store metabolic substrates for future use. Active tissues have multiple sources of fuel for ATP production, both intracellular and originating from specialized storage organs (McClelland et al 2017; McClelland & Scott, 2019). These circulating carbohydrates, intracellular carbohydrates, circulating lipids, and intracellular lipids, all converge at the site of oxidation (Taylor et al., 1996). Researchers have been challenged with developing innovative technologies, intricate techniques, and experimental design paradigms to determine how substrates are regulated to fuel metabolic demands. Most work on fuel use has been studied in humans within the fields of biomedicine and exercise physiology; however, there is a dearth of research demonstrating ***how*** the regulation of fuel use has evolved to function in mammals.

Substrate use has been studied for decades in mammals, particularly humans, dogs, goats, and rodents; however, much less is known about how substrate use has evolved in mammals. Studying animals living in challenging environments offers a deeper

understanding of how effective fuel supply and oxidation support survival in the wild. One environment where it would be expected for substrate pathways to have evolved to function in extreme metabolic conditions would be high altitude. High altitude is home to endotherms that are faced with the great metabolic challenge of maintaining stable body temperatures in an environment where both O_2 availability and temperatures are persistently low (McClelland & Scott, 2019). These high-altitude natives have evolved adaptations that ensure an adequate supply of both O_2 and metabolic fuels to survive the cold-alpine environment. These adaptive traits have fascinated both comparative and environmental physiologists alike. A great deal of work has assessed the O_2 pathway, and how highland natives have increased oxygen transport capacities from the environment to working tissues, compared to lowlanders (Storz et al., 2019). For example, highlanders have higher aerobic capacities resulting from their more oxidative phenotype (greater hemoglobin O_2 binding affinities, greater cardiac output, greater muscle capillarity, and greater proportion of oxidative fibres) compared to lowlanders (Lui et al., 2015; Storz et al., 2010; Tate et al., 2017). Surprisingly, little is known about how the substrate pathways have adapted to adequately supply metabolic activities, such as locomotion or heat production, in cold hypoxic environments. The **goal** of this thesis was to further understand how energy supply has evolved to power and sustain heat production in high-altitude populations of deer mice.

1.1 LITERATURE REVIEW

To understand the regulation of lipid oxidation in thermoregulating deer mice, it is important to review 1) the major metabolic fuels, 2) the metabolic conditions in which fuels are used, 3) the mechanisms of thermogenesis, and 4) deer mouse adaptations to high altitude.

Metabolic Fuels

Mammals use three main sources of fuel to supply energy in the form of adenosine triphosphate (ATP): carbohydrates, proteins, and lipids. The focus of this thesis pertains to the lipid metabolic pathway, so carbohydrates and proteins are only briefly discussed here. Most of the research in this literature review is based on studies in humans, rats, mice, goats, and dogs.

Carbohydrates, which account for one percent of the body's total energy reserves, can be stored in the form of glycogen in the liver and muscle tissue (Brooks & Mercier, 1994). In the liver, glycogen is broken down into glucose and is transported through the circulation in the plasma. Working tissues, such as muscle, take up circulating glucose via glucose transporters, and use it to fuel ATP production in the mitochondria (Brooks & Mercier, 1994; Weber & Haman, 2004). Carbohydrates are preferentially oxidized during high intensity aerobic exercise (>65% VO_2max) as they provide a high ATP yield per mol of O_2 (Brand, 1994; Lau et al., 2017; Weber et al., 1996). Carbohydrates are also used to produce ATP via anaerobic glycolysis, in O_2-limiting conditions, such as all out sprinting exercise (Hargreaves & Spriet, 2018).

Proteins account for 14 percent of the body's total energy reserves. Proteins are water soluble and are transported to the liver, where amino acid deamination occurs to convert them into tricarboxylic acid (TCA) cycle intermediates or pyruvate (Weber & Haman, 2004). Protein oxidation mainly occurs during rest or low intensity exercise. Deamination yields ammonia, a toxic metabolic bi-product that must be eliminated and as a result, protein oxidation is minimal and often considered negligible during mammalian exercise (Weber & Haman, 2004).

Lipids account for 85 percent of the body's total energy reserves and are predominately stored in adipose and muscle tissue (Brooks & Mercier, 1994; McClelland, 2004, Weber 2011). In white adipose tissue (WAT), lipids are stored as triglycerides (TG). TGs are broken down by lipases (adipose tissue lipase, hormone sensitive lipase, and monoglyceride lipase) into fatty acids (FA) and glycerol, via lipolysis. Liberated FAs are shuttled out of WAT via fatty acid translocase CD36 (FAT/CD36) and are transported in the circulation bound to albumin within the plasma. TGs are also transported in circulation bound to lipoproteins (very low-density lipoproteins; VLDLs). Uptake of circulating FAs occurs via FAT/CD36 expressed on cellular membranes. Once inside the cell, FAs are bound to fatty acid binding protein (FABP) and can be shuttled to be stored as TG within the tissue or be converted to fatty-acyl CoA via acyl-CoA synthetase and be shuttled towards the mitochondria to be oxidized for ATP production. FAs are shuttled into the mitochondria via FAT/CD36 and carnitine palmitoyltransferase (CPT), where they undergo beta-oxidation to become acetyl CoA, and enter the TCA cycle to produce NADH, which goes on to be oxidized by the electron transport chain and produce ATP

(McClelland, 2004; Stephens, 2018). Lipids are very energy dense molecules, providing three times the ATP per mol of substrate compared to carbohydrates (Brand, 1994) and are preferentially oxidized during periods of rest, up to moderate exercise intensities (~65% VO_2max) (Brooks & Mercier, 1994). During running exercise, maximal rates of lipid oxidation occur between 40 and 60% of VO_2max (Brooks & Mercier, 1994; Weibel et al., 1996).

Metabolic Fuel Use

The proportion of fuels that contribute to ATP production for working tissues is largely dependant on the intensity and duration of metabolic activity (Hargreaves & Spriet, 2018). As mentioned previously, lipids provide most of the energy supply during low to medium intensity exercise activities (<60% VO_2max) (Brooks & Mercier, 1994; Weber et al., 1996). At rest and low exercise intensities, most lipids oxidized are derived from the circulation (Weber, Brichon, et al., 1996). As exercise intensity increases, FAT/CD36 is transported from the cytosol to the sarcolemmal membrane to increase FA uptake from the circulation (Bonen et al., 1999; Glatz et al., 2010; McClelland, 2004; Weber & Haman, 2004). Also, during moderate intensity exercise, the proportion of lipids derived from intramuscular stores increases (McClelland, 2004; Weber et al., 1996). Once the exercise intensity exceeds 60%VO_2max, the "crossover concept" dictates an increased reliance on carbohydrate oxidation, and a decreased reliance on lipid oxidation (Figure 1.1, Brooks & Mercier, 1994; Weber et al., 1996).

During rest, the oxidation of carbohydrates is suppressed by the products of lipid oxidation. The accumulation of citrate within the TCA cycle, derived from FAs, inhibits phosphofructokinase, one of the many enzymes responsible for the conversion of glucose into pyruvate during glycolysis (McClelland, 2004). This inhibition of phosphofructokinase prevents the breakdown of carbohydrates for oxidation, allowing the cell to rely on lipid oxidation for the generation of ATP and spare glycogen stores for future instances of greater ATP demand.

At high exercise intensities, lipid oxidation is inhibited by increased ATP demand through two possible mechanisms. The first occurs through increased activation of AMP-activated protein kinase (AMPK). AMPK phosphorylates acetyl-CoA carboxylase, promoting the conversion of acetyl-CoA to malonyl-CoA, which inhibits CPT1 function, thus preventing FA uptake into the mitochondria (Båvenholm et al., 2000; Stephens, 2018). The inhibitory effects of malonyl-CoA on CPT1 function are greater for the CPT1α subunits, which are mainly found in the liver, compared to CPT1β subunits, which are mainly found in muscle and BAT (Lopez et al., 2007). The second mechanism is the result of increased glycolysis and acetyl-CoA production within the mitochondria. Increased concentrations of acetyl-CoA promote its own conversion to acetyl-carnitine via carnitine acetyl transferase. This build up of acetyl-carnitine uses up the free carnitine that is used to shuttle FAs into the mitochondria via CPT, thus hindering FAs ability to be oxidized (Roepstorff et al., 2005; Stephens, 2018) and increasing the reliance on carbohydrates during high intensity exercise.

It is important to note that most work in this field has studied lipid metabolism in the context of exercise, while there is less work done on lipid regulation in the context of thermogenesis.

Shivering and Non-Shivering Thermogenesis

Thermogenesis is an aerobic process that allows endotherms to maintain stable body temperatures by balancing heat lost to the external environment with endogenous heat production. The onset of thermogenesis occurs when the ambient temperature falls below an animal's thermoneutral zone (Scholander et al., 1950). Warm-sensitive neurons in the periphery relay information to the preoptic area within the rostral hypothalamus, which acts through the sympathetic nervous system to coordinate a thermogenic response and restore thermal homeostasis (Boulant, 2000). Animals thermoregulate using two major mechanisms: shivering thermogenesis (ST) and non-shivering thermogenesis (NST). ST is the process of producing heat through muscular contractions that provide no beneficial locomotory work. There are 2 types of shivering observed in humans. The first is a constant low frequency shivering, primarily achieved by oxidative fibres that can oxidize lipids readily. The second type is a high frequency burst shivering, achieved by glycolytic fibres primarily using carbohydrates (Haman, et al., 2002; Haman et al., 2004; Weber & Haman, 2004; Vaillancourt et al., 2009). NST is the process of metabolic heat production without muscular contraction. Small endotherms are known to rely on NST more heavily than larger endotherms because their larger surface area to volume ratios dictate rapid loss of body heat to the environment. In placental mammals, NST is primarily derived

from the specialized thermo-effector organ, brown adipose tissue (BAT). Increased heat production from BAT is thought to be adaptive by allowing muscle function to shift from shivering to locomotion. BAT generates heat through the futile cycling of protons across the mitochondrial membrane via uncoupling protein 1 (UCP1). The uncoupling of mitochondrial fuel oxidation and respiration from ATP production increases the activity of electron-generating cycles (such as the TCA cycle and beta oxidation) and increases the flow of electrons along the electron transport chain, generating heat (Cannon & Nedergaard, 2004; Zhang & Wang, 2006; Xue et al., 2009). The increased flow of electrons along the electron transport chain is derived from the catabolism of metabolic substrates. BAT-mediated NST relies primarily on lipids, and also carbohydrates, as a source of fuel (Meyer et al., 2010; Grimpo et al., 2014). It has been suggested that increasing BAT thermogenic activity facilitates the switch from carbohydrate use to lipid use for heat production and serves as a carbohydrate sparing strategy (Meyer et al., 2010). Furthermore, as ST and NST predominantly rely on lipids as a source of fuel, thermogenesis may be considered equivalent to low/moderate intensity exercise.

Deer Mouse Adaptations to High Altitude

The North American deer mouse has the highest altitudinal gradient of any north American mammal (Hock, 1964). It is thought that populations of deer mice moved up in altitude over multiple generations to reduce the competition of resources between other species. For example, rats are known to outcompete mice for territory and resources, however, rats do not inhabit altitudes greater than 2,500m a.s.l., while mice have been

found to live over 4,000m (Jochmans-Lemoine et al., 2015). Given that only specific populations of mice live at high altitude, these mice must have acquired adaptations to ensure survival and maintain fitness in these environments. Deer mice living at high-altitude are faced with 2 major stressors: low partial pressures of oxygen and low ambient temperatures. A specific trait linked with their survivability is thermogenic capacity, or the maximal capacity to produce heat (Hayes & O'Connor, 1999). Indeed, highland deer mice have many underlying traits that contribute to their ability to sustain the oxygen-demanding process of thermogenesis in a cold, hypoxic environment.

Highland native deer mice, when compared to their lowland conspecifics, rely more on greater tidal volumes rather than breathing frequency, a more effective strategy in hypoxia (Ivy & Scott, 2017), have greater oxygen loading and carrying capacities (Storz et al., 2010; Lui et al., 2015), have greater cardiac outputs (Tate et al., 2017), have greater capillarity in locomotory tissue (Lui et al., 2015), have greater proportion of oxidative fibres (Lui et al., 2015; Dawson et al., 2018), and have more mitochondria, with higher respiratory capacities, localized towards the periphery of the muscle cell (Mahalingam et al., 2017). All of these adaptations coincide with the higher running VO_2max, in hypoxic conditions, observed in highland deer mice (Lui et al., 2015; Lau et al., 2017). Furthermore, while acclimation to hypoxia also increased hypoxic running VO_2max in both highland and lowland deer mice (Lui et al., 2015), highland deer mice demonstrate an increased carbohydrate oxidation and a greater reliance on carbohydrates during exercise at 75% of VO_2max (Lau et al., 2017).

Thermoregulation is challenging for small, winter-active mammals, such as deer mice, due to their large surface area to volume ratio, resulting in high rates of heat loss. Furthermore, high altitude poses the additional challenge of hypobaric hypoxia on the oxygen demanding process of thermogenesis. The capacity to thermoregulate has been shown to be under directional selection at high altitude, correlating to greater survival in deer mice (Hayes & O'Connor, 1999). The mechanisms that underlay this increased heat production are not fully understood; however, increased thermogenic capacity has been associated with an increased aerobic muscle phenotype, and higher capacities for lipid oxidation in the muscle (Cheviron et al., 2012). Studies on deer mice suggest that during maximal rates of heat production (cold-induced VO_2max), lipid use predominates over other fuel sources (e.g. carbohydrates, proteins), as respiratory exchange ratios (RER) approached ~0.71, a value indicative of lipid oxidation (Cheviron et al., 2012). It has also been observed that highland native deer mice have higher cold-induced VO_2max compared to their lowland conspecifics, despite having the same RERs. These findings suggest that highlanders have higher lipid oxidation capacities than lowlanders (Cheviron et al., 2012). These high rates of lipid oxidation would not have been predicted from current models of exercise fuel use, where metabolic rates close to running VO_2max are supported exclusively by carbohydrate oxidation (RER ~1) (Roberts et al., 1996; Schippers et al., 2012; 2014; Lau et al., 2017). Thus***, it is unclear how these high metabolic rates for thermogenesis are dominated by lipid metabolism***.

1.2 AIMS AND OBJECTIVES

Differences in capacity along the lipid metabolic pathway, from storage, mobilisation, transport, uptake, and oxidation, are not characterized in high-altitude adapted mammals. The differences in lipid oxidation capacities observed between highlanders and lowlanders may be explained by differences in specific regulatory steps or shared among multiple steps along the lipid metabolic pathway. The **primary objective** of this work was to understand how the lipid metabolic pathway has adapted and functions to sustain thermogenesis in highland deer mice. Furthermore, my research sought to uncover the role of phenotypic plasticity on the lipid metabolic pathway in response to simulated high-altitude conditions (cold hypoxia).

To address these objectives, I used first- and second-generation deer mice native to high- (Mt. Evans CO, 4350m,) and low-altitude (Lincoln NE, 430m; Kearney NE, 656m). All experimental mice were born and raised in warm normoxic conditions (~23^{o}C, 21kPa O_2), on a 12:12-h light-dark photoperiod, with food and water *ad libitum*. All experiments were completed with male and female mice at least 6 months of age. The major acclimation groups in my thesis are: 1) controls, where mice were kept in normal living conditions (~23^{o}C, 21kPa O_2), 2) cold-hypoxia (CH) conditions (5^{o}C, 12kPa O_2), simulating high altitude for 6-8 weeks, or 3) thermoneutral (TN) conditions (30^{o}C, 21kPa O_2) for 6-8 weeks.

Using this experimental design and implementing techniques ranging from the whole-animal level to the cellular level, I conducted 3 major studies to measure lipid metabolism and characterize the structural and regulatory components of the lipid oxidation pathway. These studies addressed the **overarching hypothesis** that highland

native deer mice have evolved increased lipid use to supply the energy necessary for sustaining thermogenesis at high altitude. The following 3 chapters allowed me to test the proposed objectives and hypothesis.

1.3 CHAPTER GOALS & HYPOTHESIS

Chapter 2. Lipid Oxidation during Thermogenesis in High-Altitude Deer Mice (*Peromyscus maniculatus*)

The goal of this study was to assess how substrate use at both moderate and maximal intensities of thermogenesis may differ in highland and lowland deer mice, and the strictly lowland white-footed mouse. I also determined the role of phenotypic plasticity of substrate use after acclimation to cold hypoxia (CH), conditions simulating high altitude.

Hypothesis 1. Moderate and maximal rates of thermogenesis are predominately supported by lipid metabolism in deer mice and rates of lipid oxidation are higher in deer mice native to high altitude.

Hypothesis 2. High-altitude deer mice respond to chronic cold hypoxia with a greater increase in lipid oxidation during thermogenesis than low-altitude deer mice.

Chapter 3. Thermogenesis is supported by high rates of circulatory fatty acid and triglyceride delivery in highland deer mice

The aim of this study was to quantify the various structures along the lipid oxidation pathway- storage, mobilization, transport, uptake, and oxidation. This study provided insight about the key components of the lipid pathway that contribute to the differences in

whole-animal lipid oxidation rates between highland and lowland deer mice, and acclimation to simulated high altitude.

Hypothesis 1. Differences between highland and lowland deer mice in whole-animal lipid oxidation are due to differences in the structural components of the lipid mobilisation-delivery-transport-oxidation pathway.

Hypothesis 2. Acclimation to simulated high altitude augments the capacity of the lipid metabolic pathway.

Chapter 4. Highland deer mice redirect tissue fatty acid uptake to support thermogenesis after cold hypoxia acclimation.

One challenge of correlating lipid oxidation and tissue metabolic properties is isolating the contribution of a tissue to total energy consumption. During exercise, substrates and oxygen are predominately consumed by working skeletal muscle. Thermogenesis, however, occurs in both skeletal muscle and BAT. The goal of this study was to determine the contribution of various tissues (including muscle and BAT) to heat production in highland and lowland deer mice, acclimated to either thermoneutral or cold hypoxic conditions.

Hypothesis 1. Heat production is contributed mainly by BAT in highland deer mice relative to lowland deer mice.

Hypothesis 2. Simulated high-altitude conditions increases BAT activity and shifts the uptake of fatty acids from muscles to BAT during thermogenesis.

Figure 1.1

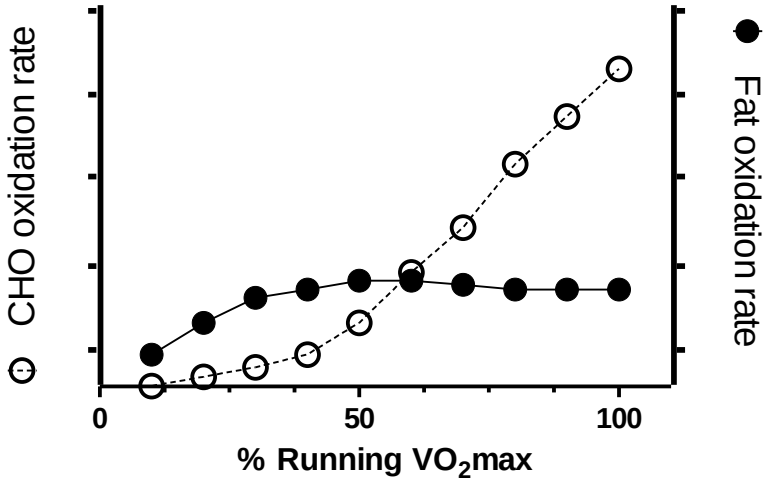
CHO oxidation rate
Fat oxidation rate
0
50
100
% Running VO2max

Figure 1.1. Substrate oxidation rates at varying exercise intensities. The combination of metabolic substrates oxidized during running exercise is largely dependent on intensity. In mammals, fat oxidation (filled circles) dominates energy provision from low to moderate exercise intensities, while carbohydrate oxidation (CHO; open circles) is greater during high intensity exercise. Peak rates of fat oxidation occur between 40 and 60% of running VO_2max (Roberts *et al.*, 1996).

1.4 REFERENCES

Båvenholm, P. N., Pigon, J., Saha, A. K., Ruderman, N. B., & Efendic, S. (2000). Fatty acid oxidation and the regulation of malonyl-CoA in human muscle. *Diabetes*, *49*(7), 1078-1083. https://doi.org/10.2337/diabetes.49.7.1078

Bonen, A., Dyck, D. J., Ibrahimi, A., & Abumrad, N. A. (1999). Muscle contractile activity increases fatty acid metabolism and transport and FAT/CD36. *American Journal of Physiology - Endocrinology and Metabolism*, *276*(4), 642–649. https://doi.org/10.1152/ajpendo.1999.276.4.e642

Boulant, J. A. (2000). Role of the Preoptic-Anterior Hypothalamus in Thermoregulation and Fever. *Clinical Infectious Diseases*, *31*(Supplement_5), S157–S161. https://doi.org/10.1086/317521

Brand, M. D. (1994). The stoichiometry of proton pumping and synthesis in mitochondria. *The Biochemist*, *16*, 20–24.

Brooks, G. A., & Mercier, J. (1994). Balance of carbohydrate and lipid utilization during exercise: the "crossover" concept. *Journal of Applied Physiology*, 76(6), 2253-2261. https://doi.org/10.1152/jappl.1994.76.6.2253

Cannon, B., & Nedergaard, J. (2004). Brown Adipose Tissue: Function and Physiological Significance. *Physiological Reviews*, *84*(1), 277–359. https://doi.org/10.1152/physrev.00015.2003

Cheviron, Z. A., Bachman, G. C., Connaty, A. D., McClelland, G. B., & Storz, J. F. (2012). Regulatory changes contribute to the adaptive enhancement of thermogenic capacity in high-altitude deer mice. *Proceedings of the National Academy of Sciences*, *109*(22), 8635–8640. https://doi.org/10.1073/pnas.1120523109

Dawson, N. J., Lyons, S. A., Henry, D. A., & Scott, G. R. (2018). Effects of chronic hypoxia on diaphragm function in deer mice native to high altitude. *Acta Physiologica*, *223*(1). https://doi.org/10.1111/apha.13030

Glatz, J. F. C., Luiken, J. J. F. P., & Bonen, A. (2010). Membrane fatty acid transporters as regulators of lipid metabolism: Implications for metabolic disease. *Physiological Reviews*, *90*(1), 367–417. https://doi.org/10.1152/physrev.00003.2009

Grimpo, K., Völker, M. N., Heppe, E. N., Braun, S., Heverhagen, J. T., & Heldmaier, G. (2014). Brown adipose tissue dynamics in wild-type and UCP1-knockout mice: in vivo insights with magnetic resonance. *Journal of Lipid Research*, *55*(3), 398–409. https://doi.org/10.1194/jlr.M042895

Haman, F., Legault, S. R., & Weber, J. M. (2004). Fuel selection during intense shivering in humans: EMG pattern reflects carbohydrate oxidation. *Journal of Physiology*, *556*(1), 305–313. https://doi.org/10.1113/jphysiol.2003.055152

Haman, F., Péronnet, F., Kenny, G. P., Massicotte, D., Lavoie, C., Scott, C., & Weber, J.-

M. (2002). Effect of cold exposure on fuel utilization in humans: plasma glucose, muscle glycogen, and lipids. *Journal of Applied Physiology*, *93*(1), 77–84. https://doi.org/10.1152/japplphysiol.00773.2001

Hargreaves, M., & Spriet, L. L. (2018). Exercise metabolism: Fuels for the fire. *Cold Spring Harbor Perspectives in Medicine*, *8*(8), 1–16. https://doi.org/10.1101/cshperspect.a029744

Hayes, J. P., & O'Connor, C. S. (1999). Natural Selection on Thermogenic Capacity of High-Altitude Deer Mice. *Evolution*, *53*(4), 1280. https://doi.org/10.2307/2640830

Hock, R. J. (1964). The Physiological Effects of High Altitude 59-68. Pergamon Press, Oxford.

Ivy, C. M., & Scott, G. R. (2017). Ventilatory acclimatization to hypoxia in mice: Methodological considerations. *Respiratory Physiology and Neurobiology*, *235*, 95–103. https://doi.org/10.1016/j.resp.2016.10.012

Jochmans-Lemoine, A., Villalpando, G., Gonzales, M., Valverde, I., Soria, R., & Joseph, V. (2015). Divergent physiological responses in laboratory rats and mice raised at high altitude. T*he Journal of Experimental Biology*, 218(7), 1035-1043. https://doi.org/10.1242/jeb.112862

Lau, D. S., Connaty, A. D., Mahalingam, S., Wall, N., Cheviron, Z. A., Storz, J. F., … McClelland, G. B. (2017). Acclimation to hypoxia increases carbohydrate use during exercise in high-altitude deer mice. *American Journal of Physiology - Regulatory, Integrative and Comparative Physiology*, *312*(3), R400–R411. https://doi.org/10.1152/ajpregu.00365.2016

López-Viñas, E., Bentebibel, A., Gurunathan, C., Morillas, M., de Arriaga, D., Serra, D., ... & Gómez-Puertas, P. (2007). Definition by functional and structural analysis of two malonyl-CoA sites in carnitine palmitoyltransferase 1A. *Journal of Biological Chemistry*, 282(25), 18212-18224. https://doi.org/10.1074/jbc.M700885200

Lui, M. A., Mahalingam, S., Patel, P., Connaty, A. D., Ivy, C. M., Cheviron, Z. A., … Scott, G. R. (2015). High-altitude ancestry and hypoxia acclimation have distinct effects on exercise capacity and muscle phenotype in deer mice. *American Journal of Physiology - Regulatory, Integrative and Comparative Physiology*, *308*(9), R779–R791. https://doi.org/10.1152/ajpregu.00362.2014

Mahalingam, S., McClelland, G. B., & Scott, G. R. (2017). Evolved changes in the intracellular distribution and physiology of muscle mitochondria in high-altitude native deer mice. *Journal of Physiology*, 595(14), 4785-4801. https://doi.org/10.1113/JP274130

McClelland, G. B. (2004). Fat to the fire: The regulation of lipid oxidation with exercise and environmental stress. *Comparative Biochemistry and Physiology - B Biochemistry and Molecular Biology*, *139*(3), 443–460.

https://doi.org/10.1016/j.cbpc.2004.07.003

McClelland, G. B., Lyons, S. A., & Robertson, C. E. (2017). Fuel use in mammals: Conserved patterns and evolved strategies for aerobic locomotion and thermogenesis. *Integrative and Comparative Biology*, *57*(2), 231–239. https://doi.org/10.1093/icb/icx075

McClelland, G. B., & Scott, G. R. (2019). Evolved Mechanisms of Aerobic Performance and Hypoxia Resistance in High-Altitude Natives. *Annual Review of Physiology*, *81*(1), 561–583. https://doi.org/10.1146/annurev-physiol-021317-121527

Meyer, C. W., Willershauser, M., Jastroch, M., Rourke, B. C., Fromme, T., Oelkrug, R., … Klingenspor, M. (2010). Adaptive thermogenesis and thermal conductance in wild-type and UCP1-KO mice. *AJP: Regulatory, Integrative and Comparative Physiology*, *299*(5), 1396–1406. https://doi.org/10.1152/ajpregu.00021.2009

Roberts, T. J., Weber, J. M., Hoppeler, H., Weibel, E. R., & Taylor, C. R. (1996). Design of the oxygen and substrate pathways. II. Defining the upper limits of carbohydrate and fat oxidation. *Journal of Experimental Biology*, *199*(8), 1651–1658.

Roepstorff, C., Halberg, N., Hillig, T., Saha, A. K., Ruderman, N. B., Wojtaszewski, J. F. P., … Kiens, B. (2005). Malonyl-CoA and carnitine in regulation of fat oxidation in human skeletal muscle during exercise. *American Journal of Physiology - Endocrinology and Metabolism*, *288*(1), 133–142. https://doi.org/10.1152/ajpendo.00379.2004

Schippers, M. P., LeMoine, C. M. R., & McClelland, G. B. (2014). Patterns of fuel use during locomotion in mammals revisited: The importance of aerobic scope. *Journal of Experimental Biology*, *217*(18), 3193–3196. https://doi.org/10.1242/jeb.099432

Schippers, M. P., Ramirez, O., Arana, M., Pinedo-Bernal, P., & McClelland, G. B. (2012). Increase in carbohydrate utilization in high-altitude andean mice. *Current Biology*, *22*(24), 2350–2354. https://doi.org/10.1016/j.cub.2012.10.043

Scholander, P. F., Hock, R., Walters, V., & Irving, L. (1950). Adaptation to cold in arctic and tropical mammals and birds in relation to body temperature, insulation, and basal metabolic rate. *The Biological Bulletin*, 99(2), 259–271. https://doi.org/10.2307/1538742

Stephens, F. B. (2018). Does skeletal muscle carnitine availability influence fuel selection during exercise? *Proceedings of the Nutrition Society*, *77*(1), 11–19. https://doi.org/10.1017/S0029665117003937

Storz, J. F., Runck, A. M., Moriyama, H., Weber, R. E., & Fago, A. (2010). Genetic differences in hemoglobin function between highland and lowland deer mice. *Journal of Experimental Biology*, 213(15), 2565-2574. https://doi.org/10.1242/jeb.042598

Tate, K. B., Ivy, C. M., Velotta, J. P., Storz, J. F., McClelland, G. B., Cheviron, Z. A., &

Scott, G. R. (2017). Circulatory mechanisms underlying adaptive increases in thermogenic capacity in high-altitude deer mice. *The Journal of Experimental Biology*, 220(20), 3616–3620. https://doi.org/10.1242/jeb.164491

Taylor, C. R., Weibel, E. R., Weber, J. M., Vock, R., Hoppeler, H., Roberts, T. J., & Brichon, G. (1996). Design of the oxygen and substrate pathways. I. Model and strategy to test symmorphosis in a network structure. *Journal of Experimental Biology*, *199*(8), 1643–1649. https://doi.org/10.1242/jeb.199.8.1643

Vaillancourt, E., Haman, F., & Weber, J. M. (2009). Fuel selection in Wistar rats exposed to cold: Shivering thermogenesis diverts fatty acids from re-esterification to oxidation. *Journal of Physiology*, *587*(17), 4349–4359. https://doi.org/10.1113/jphysiol.2009.175331

Weber, J. M., Brichon, G., Zwingelstein, G., Mcclelland, G., Saucedo, C., Weibel, E. R., & Taylor, C. R. (1996). Design of the oxygen and substrate pathways. IV. Partitioning energy provision from fatty acids. *Journal of Experimental Biology*, *199*(8), 1667–1674. https://doi.org/10.1242/jeb.199.8.1667

Weber, J. M., & Haman, F. (2004). Oxidative fuel selection: adjusting mix and flux to stay alive. *International Congress Series*, *1275*, 22–31. https://doi.org/10.1016/j.ics.2004.09.043

Weber, J. M., Roberts, T. J., Vock, R., Weibel, E. R., & Taylor, C. R. (1996). Design of the oxygen and substrate pathways. III. Partitioning energy provision from carbohydrates. *Journal of Experimental Biology*, *199*(8), 1659–1666. https://doi.org/10.1242/jeb.199.8.1659

Weibel, E. R., Taylor, C. R., Weber, J. M., Vock, R., Roberts, T. J., & Hoppeler, H. (1996). Design of the oxygen and substrate pathways. VII. Different structural limits for oxygen and substrate supply to muscle mitochondria. *Journal of Experimental Biology*, *199*(8), 1699–1709. https://doi.org/10.1242/jeb.199.8.1699

Xue, Y., Petrovic, N., Cao, R., Larsson, O., Lim, S., Chen, S., … Cao, Y. (2009). Hypoxia-Independent Angiogenesis in Adipose Tissues during Cold Acclimation. *Cell Metabolism*, *9*(1), 99–109. https://doi.org/10.1016/j.cmet.2008.11.009

Zhang, X. Y., & Wang, D. H. (2006). Energy metabolism, thermogenesis and body mass regulation in Brandt's voles (Lasiopodomys brandtii) during cold acclimation and rewarming. *Hormones and Behavior*, *50*(1), 61–69. https://doi.org/10.1016/j.yhbeh.2006.01.005

CHAPTER 2: LIPID OXIDATION DURING THERMOGENESIS IN HIGH-ALTITUDE DEER MICE (*PEROMYSCUS MANICULATUS*)

Modified and reproduced with permission from Lyons, S. A., Tate, K. B., Welch Jr, K. C., & McClelland, G. B. (2021). *Am. J. Physiol.-Reg. I.* 320(5), R735–R746. doi: 10.1152/ajpregu.00266.2020

2.1 ABSTRACT

When at their maximum thermogenic capacity (cold-induced $\dot{V}O_2max$), small endotherms reach levels of aerobic metabolism as high, or even higher, than running $\dot{V}O_2max$. How these high rates of thermogenesis are supported by substrate oxidation is currently unclear. The appropriate utilization of metabolic fuels that could sustain thermogenesis over extended periods may be important for survival in cold environments, like high altitude. Previous studies show that high capacities for lipid use in high-altitude deer mice may have evolved in concert with greater thermogenic capacities. The purpose of this study was to determine how lipid utilization at both moderate and maximal thermogenic intensities may differ in high- and low- altitude deer mice, and strictly low-altitude white-footed mice. We also examined the phenotypic plasticity of lipid use after acclimation to cold hypoxia (CH), conditions simulating high altitude. We found that lipids were the primary fuel supporting both moderate and maximal rates of thermogenesis in both species of mice. Lipid oxidation increased 3-fold in mice from 30°C to 0°C, consistent with increases in oxidation of [^{13}C]-palmitic acid. CH acclimation led to an increase in [^{13}C]-palmitic acid oxidation at 30°C but did not affect total lipid oxidation. Lipid oxidation rates at cold-induced $\dot{V}O_2max$ were two- to four-fold those at 0°C and increased further after CH acclimation, especially in high-altitude deer mice. These are the highest mass-specific lipid oxidation rates observed in any land mammal.

Uncovering the mechanisms that allow for these high rates of oxidation will aid our understanding of the regulation of lipid metabolism.

2.2 INTRODUCTION

Homeothermic endothermy is a distinctive feature of mammals that is crucial for their survival in cold environments. However, thermal tolerance and thermogenic capacity are performance traits that not only vary with body size but also with individual and population differences in thermal history (23, 31, 54). For instance, small mammals have greater thermoregulatory costs compared to larger species due to a higher surface area for heat loss relative to volume used for heat production. This can be especially challenging for species that are active during colder parts of the year, necessitating high rates of thermogenesis to remain active when temperatures are low (15, 28). Past research has uncovered many details on how these species can maintain high rates of O_2 delivery to thermogenic tissues (21). However, it remains unclear how metabolic substrates are utilized to support high rates of thermogenesis in mammals or if fuel use patterns change seasonally.

Thermogenesis is an aerobic process that allows endotherms to maintain stable body temperatures by balancing heat lost to the external environment with endogenous heat production. The onset of thermogenesis occurs when the ambient temperature falls below an endotherm's thermoneutral zone (54) and can occur in two major ways, shivering and non-shivering thermogenesis (NST). Shivering thermogenesis increases metabolic demand via muscular contractions that provide heat but no beneficial locomotory work,

while NST produces heat through the futile cycling of protons across the mitochondrial membrane via uncoupling protein 1 in brown adipose tissue (BAT) (12). While shivering is fueled by both carbohydrates and lipids, depending on shivering intensity (25), NST is primarily fueled by lipids (8, 32). Furthermore, prolonged cold exposure increases shivering capacity (45) and elevate BAT metabolic activity (5, 62).

Endogenous lipid stores are large in mammals (~80% available energy reserves) and it has been speculated that lipids may be used to sustain heat production (63). Data from rats show that during modest cold exposure (5^{o}C), lipid oxidation supports over 50% of the metabolic demand of shivering thermogenesis (61). However, we are not aware of any study examining fuel use for thermogenesis in smaller mammals, such as mice. It is well-characterized in mammals that maximal rates of lipid oxidation during locomotion occur at moderate intensities of aerobic exercise (10, 53, 65), and these rates do not vary even if fat availability is artificially elevated (26). Although during exercise higher mass-specific rates of lipid oxidation are observed in mice compared to larger species, they too demonstrate an upper limit to lipid use at submaximal exercise intensities (33, 53, 60). Interestingly, during cold-induced V̇O2max (also referred to as summit metabolism) small endotherms often reach levels of aerobic metabolism higher than $\dot{V}O_2max$ elicited by exercise (15, 27, 37). This suggests that metabolism supporting even moderate rates of thermogenesis may be higher than those during aerobic exercise, when lipid oxidation plateaus or even declines (64). Whether small mammals can sustain sufficient rates of lipid oxidation to support even these moderate rates of thermogenesis is unclear.

High-altitude environments can be cooler year-round than lower elevations of the same latitude. Yet, populations of small mammals native to high altitude, such as deer mice, remain active in the cold, maintaining higher daily energetic costs compared to low altitude conspecifics, even during summer months (28). There is also evidence of directional selection for greater cold-induced $\dot{V}O_2max$ in deer mice at high altitude (29), and thermogenic capacity in hypoxia is higher in high-altitude deer mice compared to lowland conspecifics (18, 19, 57). This superior aerobic capacity at high altitude is the product of environmentally induced phenotypic plasticity overlaid upon fixed population differences (19, 34, 58). While the oxygen transport pathway from the external environment to muscle tissues have been extensively examined in mammals living at high altitude (38), fuel use has received much less attention. However, work examining exercise metabolism in high altitude conditions suggests a greater reliance in carbohydrates to support submaximal locomotion, presumably as an oxygen-saving strategy. This has been demonstrated in two species in the genus *Phyllotis* native to the high Andes (53) and in deer mice native to the Rocky Mountains, born and raised at low altitude and acclimated to chronic hypoxia (33). However, how metabolic fuel use may have evolved at altitude to support the high rates of thermogenesis is currently not well understood.

It would be unlikely that a preferential utilization of carbohydrate oxidation occurs to support the high rates of thermogenesis at high altitude, given mammals have limited glycogen reserves (37), and the prolonged nature of thermoregulation would quickly deplete these stores. Indeed, after a 6-week acclimation to low altitude conditions, wild

high-altitude native deer mice showed respiratory exchange ratios (RER= $\dot{V}CO_2/\dot{V}O_2$) at cold-induced $\dot{V}O_2max$ in hypoxia suggestive of a high reliance on lipids (18). These high proportions of lipid use may be largely influenced by NST activity in BAT. Moreover, the higher thermogenic capacities in high-altitude mice suggests a corresponding elevated rate of lipid oxidation. Phenotypic differences between low- and high-altitude deer mice in the gastrocnemius, a muscle used in thermogenesis (44), suggest higher capacities for fatty acid oxidation at high altitude, presumably to support high rates of shivering (18, 33).

Whether moderate and/or maximal rates of heat production are supported solely by lipids or a combination of metabolic fuels has not been explored in either low or high-altitude deer mice. Moreover, it is unclear if lipid oxidation rates follow the same population differences in aerobic capacity, or if this fuel utilization for heat production is affected by acclimation to simulated high-altitude conditions.

To address these issues, we used deer mice (*Peromyscus maniculatus*) native to high altitude and compared them to a low-altitude population and to a closely related strictly low-altitude species, the white-footed mouse (*P. leucopus*). Mice were born and raised in common low-altitude conditions and acclimated as adults to cold hypoxia simulating high altitude. We tested the hypothesis that moderate and maximal rates of thermogenesis are predominately supported by lipid metabolism in deer mice and rates of lipid oxidation are higher in deer mice native to high altitude. High-altitude deer mice are also predicted to respond to chronic cold hypoxia with a greater increase in lipid oxidation during thermogenesis than low-altitude mice.

2.3 METHODS

Animals and experimental design

Male and female deer mice and white-footed mice used in this study were first generation descendants of wild-caught *P.m. rufinus* trapped at the summit of Mount Evans CO (4,350m a.s.l.) and *P.m. nebracensis and P. leucopus* trapped at low altitude at Nine-mile Prairie, NE, USA (320m a.s.l.). Mice were born and raised at McMaster University (~90m a.s.l.) in common laboratory conditions of ~23^{o}C, light cycle of 12:12h light:dark, food and water ad libitum. All mice were at least 6 months of age before the start of experiments. This experimental design allows us to separate the effects of altitude ancestry and environment on physiological traits (18, 33, 34, 58). All procedures were approved by the McMaster University Animal Research Ethics Board in accordance with guidelines from the Canadian Council on Animal Care.

Acclimation Conditions

First generation high-altitude (HA) and low-altitude (LA) deer mice were randomly divided into two acclimation groups and kept for 6 to 8 weeks in either, 1) warm normoxia (WN), at 23^{o}C and 760mmHg (21kPa O_2) - our common laboratory conditions, or 2) cold hypoxia (CH), at 5^{o}C and 480mmHg (12kPa O_2) using hypobaric chambers (35) housed in a climate controlled room to simulate an altitude of 4300m a.s.l. Mice in the CH group were first placed in a cold room for 24 hours at normobaria to adjust to the cold before being placed in the hypobaric chambers. Mice in CH were returned to

normobaria in cold for a brief period (<1h) twice a week to clean cages and replenish food and water (57, 58).

Respirometry

Open-flow respirometry was used to determine rates of oxygen consumption ($\dot{V}O_2$) and CO_2 production ($\dot{V}CO_2$). For each mouse, $\dot{V}O_2$ and $\dot{V}CO_2$ were measured at thermoneutral temperatures (30^{o}C) (16) and moderate cold temperatures (0^{o}C) using a PTC-1 Portable Controlled Temperature Cabinet (Sable Systems, Las Vegas, NV) in random order. Mice were made post-absorptive by a 4-6 hour fast, weighed and placed in a respirometry chamber (~500ml). Dry (Drierite, Hammond, OH) and CO_2 free (Soda Lime and Ascarite, Thomas Scientific, NJ) air was flowed (pushed) into the respirometry chamber at 600ml min^{-1}, using a mass-flow controller (Sable Systems). Excurrent air was subsampled at a rate of ~200ml min^{-1}, dried using pre-baked Drierite (67), and passed through O_2 and CO_2 analyzers (Sable Systems). Fractional incurrent O_2 (F_{iO_2}) and CO_2 (F_{iCO_2}) were recorded at the beginning and end of the trial by flowing air through an empty respirometry chamber. After mice adjusted to the chamber for 20 minutes, fractional excurrent concentrations of O_2 (F_{eO_2}) and CO_2 (F_{eCO_2}) were determined for 20 minutes and $\dot{V}O_2$ and $\dot{V}CO_2$ were calculated using equation 3b from Withers (68). Body temperatures were measured before and after all experimental trials using a rectal probe thermometer (RET-3-ISO, Physitemp). Resting $\dot{V}O_2$ was defined as the lowest, most stable reading during a 1.5 min interval during the last 20 minutes of the trial. Whole-animal rates of substrate oxidation were calculated using the indirect calorimetry

equations from Frayn (22) assuming a minimal contribution of protein oxidation in the post absorptive state (11, 24). Protein oxidation has been shown to contribute only ~5% to energy production during exercise in post-absorptive mammals. Thus, we assumed no contribution of protein oxidation when calculating rates of fuel oxidation. Thermal conductance (C) was calculated based on equations from Scholander et al. (54).

Hypoxic cold-induced $\dot{V}O_2$max reported here are from Tate et al. (58) with an additional 5 HA and 5 LA mice in WN and 9 HA and 9 LA mice in CH. Cold-induced $\dot{V}O_2$max was determined by flowing heliox (21% O_2, 79% He or 12% O_2, 88% He), at 1000ml min^{-1} using mass flow meters and controllers (Sierra Instruments, Monterey, CA, USA; MFC-4, Sable Systems, NV, USA), through copper coils housed inside a temperature control cabinet and into a glass respirometry chamber (~500ml) cooled to ~-10^{o}C. Heliox induces greater heat loss at warmer temperatures and avoids the risk of cold injury to the animals (17, 51). Mice were exposed to these conditions for ~15 minutes and cold-induced $\dot{V}O_2$max was defined as the peak value of $\dot{V}O_2$ averaged over a 10-15 second period (50, 57).

All mice were given at least 48 hours to recover before another submaximal or cold-induced $\dot{V}O_2$max trial was performed.

^{13}C Stable Isotope Breath Analysis

Using indirect calorimetry can provide an estimate of whole-body lipid oxidation rate. While these rates are still very informative, they do not directly quantify the rate of oxidation of specific fuels or sources. We labelled endogenous fat stores with [^{13}C]-

palmitate and quantified rates of [^{13}C]-palmitate oxidation by collecting exhaled $^{13}CO_2$ and measuring $\dot{V}CO_2$, as previously described for other species (40, 43). Using this approach, we could quantify how the rate of oxidation of labelled lipid stores specifically varied with ancestry, acclimation or acute thermal challenge. Briefly, labelled food was prepared by completely dissolving 0.5g of [1-^{13}C]-palmitic acid (Cambridge Isotope Laboratories, Inc) in 95% ethanol to coat 0.5kg of rodent chow (front and back). The chow was then baked at 60^{o}C overnight. A subset of mice was fasted up to a maximum of 24 hours with full access to water to heavily deplete endogenous lipid stores (41, 55). After the 24-hour fast, or once mouse weight was ~80% of their original body mass, animals were provided the ^{13}C-labelled chow for at least 10 days to replenish and ensure sufficient labeling of endogenous lipid stores. Mice were given labelled chow until all breath sampling trial data were collected.

Breath samples were collected from animals before and after [^{13}C]-palmitic acid enrichment of fat stores. Food was removed 4 hours prior to collection of breath $^{13}CO_2$ to prevent recently ingested ^{13}C from influencing our determination of endogenous lipid use (42). During respirometry trials at 30^{o}C and 0^{o}C, a 12ml subsample of excurrent air was collected from these mice using a gas-tight glass syringe and transferred to a 12ml glass exetainer (Labco). Breath samples were analyzed for δ^{13}C signatures by cavity ring-down spectroscopy using the Picarro G2201-I Isotopic Analyzer (Picarro, Inc., Santa Clara, CA, USA). Using the techniques and equations provided by Dick et al. (20) and McCue et al. (40), δ^{13}C signatures were used to calculate [^{13}C]-palmitic acid oxidation (43).

Measurement of Plasma Fatty Acids

Blood samples were obtained from the submandibular vein immediately following indirect calorimetry trials at 30°C and 0°C. Blood was immediately centrifuged at 10,000 × g for 5 min to separate red cells from plasma. Plasma was quickly frozen in liquid nitrogen and stored until further analysis. To quantify free fatty acids, 20µl of plasma were combined with 10µl of internal standard (C17:0, 0.6mg ml^{-1}) in 1ml of 2,2-dimethoxypropane and vortexed. This was followed by the addition of 40µl of HCl (12M) and the methylation of free fatty acids was left to proceed for 1h. The reaction was stopped with the addition of 20µl of pyridine and vortexed. Next, 750µl of iso-octane and 500µl of dH_2O was added to the samples, and then centrifuged at 10,000 × g for 5 min. The resultant upper phase was transferred to a new tube, and the process was repeated for the bottom layer. The top phases were combined and completely dried under N_2. The sample was re-suspended in 50µl of iso-octane and transferred to an autosampler tube. Another 50µl of iso-octane was added to the original sample tube to re-suspend any remaining contents and was also transferred to the autosampler tube and was completely dried under N_2. The final sample was re-suspended in 50µl of iso-octane (36).

Samples were analyzed using an Agilent Technologies 6890N gas chromatograph with a 30m fused silica capillary column (DB-23, Agilent Technologies), flame ionization detector and equipped with an automatic injection system (Agilent Technologies 7683B Series). Helium was used as the carrier gas at a constant pressure and column velocity of 44cm s^{-1}, with 4µl of sample injected into the column. The conditions used during analysis were the following: oven temperature initially programmed for 4min at 160°C,

ramped to 220°C at a rate of 2°C min^{-1} and held at 220°C for 2 min, then ramped to 240°C at 10°C min^{-1}, and held at 240°C for 7 min. Post-run was 130°C for 4 min. The detector temperature was 250°C. Identities of fatty acid methyl esters were compared to the retention times of a standard FAME mix (C8-C24, Sigma). We excluded analysis of fatty acids less than 16 carbons as we did not attempt to minimize volatilization (47).

Statistics

Linear mixed effects models were used to test for effects of population, acclimation, and experimental temperature. Analyses were performed using the lme4 package (3) in R v.4.0.0 (59). We assessed the potential interactions between fixed factors, including body mass as a covariate and the random effects of family, sex and age. If the variance explained by random effects did not approach significance ($p>0.05$), we removed them and reran the analysis. Except for body mass, all other dependant variables were reduced to 3-way analysis of variance (ANOVA)s, with mass as a covariate where appropriate. Additionally, within each experimental temperature (30°C and 0°C), and cold-induced $\dot{V}O_2max$ condition (normoxia and hypoxia), 2-way ANOVAs were performed assessing the interaction between population and acclimation. Pairwise, Holm Sidak post hoc tests were performed to assess significant interactions (30). All statistical analyses were performed on the absolute values of the traits that were not corrected for body mass, but some data are presented as relative to body mass by convention to the literature ($\dot{V}O_2$, $\dot{V}O_2max$, ventilatory volumes, [^{13}C]-palmitate oxidation, lipid oxidation and thermal

conductance). All data are presented as mean ± sem. A statistical significance value was set at $P<0.05$.

2.4 RESULTS

Body Mass

White-footed mice weighed 29% more than both HA and LA deer mice, regardless of acclimation environment ($p<0.05$) (Table 2.1). However, there was no significant difference in mass between HA and LA deer mice ($p>0.05$) (Table 2.1).

Respiration in thermoneutral and moderate cold temperatures

To determine if altitude ancestry or acclimation to CH influences metabolic rate during submaximal thermogenesis, we measured $\dot{V}O_2$ at thermoneutrality (30ºC) and during a moderate cold exposure (0ºC) in LA and HA deer mice and white-footed mice. We found that $\dot{V}O_2$ was 3-fold greater at 0ºC compared to 30ºC for all individuals, regardless of population and acclimation environment ($p<0.05$). HA and LA deer mice had greater $\dot{V}O_2$ than white-footed mice at both 30ºC and 0ºC ($p<0.05$), but there were no differences in $\dot{V}O_2$ between HA and LA deer mice ($p>0.05$). Furthermore, acclimation did not significantly influence $\dot{V}O_2$ ($p>0.05$) (*Fig. 2.1A*). We calculated RER during these submaximal rates of thermogenesis and found it was unaffected by ambient temperature ($p>0.05$). While all mice tested at 0ºC had similar RERs regardless of population or acclimation ($p>0.05$), at 30ºC white-footed mice acclimated to CH had higher RER than those housed in WN ($P<0.05$). The range of RERs observed in all trials were between

0.70 to 0.80 across all groups, suggesting that lipids were the primary source of fuel in thermoneutral conditions and with moderate cold exposure (*Fig. 2.1B*).

Whole animal lipid oxidation rates during submaximal thermogenesis

Since lipid oxidation is the primary fuel for both shivering and non-shivering thermogenesis in rodents (18, 61), we determined if altitude ancestry or acclimation environment influenced this trait in moderate cold conditions. Using indirect calorimetry, we calculated whole-animal lipid oxidation rates and observed an increase from 30°C to 0°C ($p<0.05$). Across all temperatures, LA deer mice had greater lipid oxidation rates compared to white-footed mice ($p<0.05$), but not compared to HA deer mice ($p>0.05$). At 30°C, both HA and LA deer mice had greater lipid oxidation rates compared to white-footed mice ($p<0.05$). Interestingly, CH acclimation did not affect whole-animal rates of lipid oxidation ($p>0.05$) (*Fig. 2.2A*).

Thermal conductance during submaximal thermogenesis

Thermal conductance was calculated to determine if changes in rates of heat loss occurred due to exposure to colder ambient temperatures with CH acclimation (*Table 2.1*). We found that thermal conductance was reduced as ambient temperature decreased from 30°C to 0°C ($F_{1,79} = 147.67$, $P<0.001$), while controlling for any influence of body mass ($F_{1,79} = 21.16$, $P<0.001$). Across all temperatures, white-footed mice had greater thermal conductance compared to HA and LA deer mice ($F_{2,79} = 16.43$, $P<0.001$), which

led to greater changes in body temperature after moderate cold exposure ($p<0.05$). Acclimation to CH had no effect on thermal conductance ($F_{1,79} = 0.866$, $P=0.355$) (*Table 2.1*).

[^{13}C]- palmitic acid oxidation

We directly quantified the oxidation of an individual fatty acid by labelling the fat stores in a subset of LA and HA deer mice using [^{13}C]-palmitate and trapping exhaled $^{13}CO_2$ during submaximal thermogenic trials. We found, similar to whole-animal lipid oxidation, that [^{13}C]-palmitate oxidation rates increased 3-fold as ambient temperatures declined from 30^{o}C to 0^{o}C ($p<0.05$). However, in contrast to whole-animal lipid oxidation rates, CH acclimation led to an increase in [^{13}C]-palmitate oxidization ($p<0.05$). Specifically, at 30^{o}C [^{13}C]-palmitate oxidation increased in CH acclimated HA mice compared to their WN controls ($p<0.05$) (*Fig. 2.2B*).

Circulating plasma non-esterified fatty acids

To understand if substrate use was reflected in changes of circulating plasma non-esterified fatty acids (NEFAs), we determined levels of total and individual circulating NEFAs (*Fig. 2.2C and Fig. 2.3*). Overall, plasma concentrations of total circulating NEFAs did not change as ambient temperature decreased ($p>0.05$), nor were there any significant effects of population ($p>0.05$) or acclimation ($p>0.05$) (*Fig. 2.2C*).

Similar to total NEFA, plasma concentrations of palmitate (16:0) and stearate (18:0) showed no differences between populations, acclimation or with changes in ambient temperature ($p>0.05$; *Fig. 2.3A and Fig. 2.3C*). In contrast, palmitoleate (16:1) was ~47% higher in LA deer mice than HA deer mice at 30°C ($p<0.05$). The concentration of palmitoleate was also significantly higher in CH acclimated mice at 0°C ($p<0.05$; *Fig. 2.3B*). Elaidate (18:1n9t) concentrations were found to be higher in HA deer mice, while oleate (18:1n9c) concentrations were higher in LA deer mice ($p<0.05$; *Fig. 2.3D; Fig. 2.3E*). Concentrations of oleate were also significantly greater in CH acclimated mice at 0°C but significantly greater in WN animals at 30°C ($p<0.05$) (*Fig. 2.3E*). Linoleate (18:2n6c) concentrations were relatively constant with no significant effect of acclimation or temperature ($p>0.05$); however, generally HA mice had higher levels of linoleate compared to LA mice ($p<0.05$; *Fig. 2.3F*).

Whole animal lipid oxidation at cold-induced $\dot{V}O_2max$

Thermogenic capacity was assessed by measuring cold-induced $\dot{V}O_2max$. We determined $\dot{V}O_2$ and lipid oxidation rates at $\dot{V}O_2max$ in both normoxia and hypoxia. After accounting for differences in body mass ($F_{1,135} = 16.93$, $P<0.001$), we found that $\dot{V}O_2max$ was higher in normoxia compared to hypoxia ($F_{1,135} = 353.22$, $P<0.001$). After CH acclimation, $\dot{V}O_2max$ increased ($F_{1,135} = 201.44$, $P<0.001$), but there were no significant population differences ($F_{2,135} = 2.80$, $P=0.064$) (*Fig. 2.4A*).

RER at $\dot{V}O_2max$ was higher in normoxia compared to hypoxia ($F_{1,136} = 9.46$, $P<0.001$). There was a significant population × acclimation × test condition interaction in

RER ($F_{1,136}$ =3.80, P=0.025), where WN HA mice tested in normoxia had greater RERs than WN HA mice, CH white-footed mice and WN white-footed mice when tested in hypoxia ($p<0.05$). In normoxia, there was a significant population × acclimation interaction ($F_{2,40}$ = 4.10, P=0.024), where CH acclimation led to a decrease in RER in HA mice ($p<0.05$), while WN LA mice had lower RERs than WN HA mice ($p<0.05$). In hypoxia, RER was not different among populations or with acclimation environment (*Fig. 2.4B*).

Whole-animal lipid oxidation rates at $\dot{V}O_2max$ were higher in normoxia compared to hypoxic conditions ($p<0.05$). In addition, mice acclimated to CH had greater lipid oxidation rates compared to WN individuals ($p<0.05$). In normoxia, HA deer mice acclimated to CH displayed higher lipid oxidation rates compared to WN white-footed mice ($p<0.05$). In hypoxia, HA deer mice had higher lipid oxidation rates than LA mice, and CH acclimation led to an increase lipid oxidation ($p<0.05$; *Fig. 2.4C*).

2.5 DISCUSSION

The main objective of this study was to determine the substrate utilization necessary to support both moderate and maximal intensities of thermogenesis in LA and HA native *Peromyscus* mice and how this utilization is influenced by acclimation to CH, simulating high altitude. We found that both deer mice and white-footed mice significantly increase whole body lipid oxidation rates from thermoneutral (30°C) to moderate cold (0°C) to support heat production. At 0°C, lipid oxidation accounted for the majority of total $\dot{V}O_2$ but did not differ among the three mouse populations. There was also no effect of CH

acclimation on the proportional use of lipid oxidation at this moderate cold exposure. However, when the oxidation of a major circulating free fatty acid was measured directly through $^{13}CO_2$ production, we found CH acclimation led to a significant increase in palmitate oxidation at 30°C when compared to WN acclimated controls. At cold-induced $\dot{V}O_2max$ under hypoxia, we found whole-animal lipid oxidation rates were elevated two- to four-fold above moderate cold in WN and CH acclimated HA deer mice, respectively. This population also showed a significant effect of CH acclimation leading to higher whole-animal lipid oxidation at $\dot{V}O_2max$ in normoxia. These results demonstrate that lipid oxidation is the major fuel supporting thermogenesis in deer mice, even at maximal cold-induced metabolic rates. Indeed, rates of lipid oxidation that support heat production at 0°C are similar or greater than maximal rates observed during moderate exercise intensities (33). Furthermore, oxidation rates to support maximal thermogenesis were 2.5 to 5.2-fold greater than maximal rates of lipid oxidation during exercise (21; *Fig. 2.5*) and the highest mass-specific lipid oxidation rates reported for any mammal (1, 33, 49, 61).

Submaximal and Maximal Thermogenic Metabolism

Thermoregulation allows for endotherms to balance rates of heat production and heat loss to maintain consistent body temperatures (54). To maintain stable body temperatures as ambient temperatures decrease, there must be an increase of both $\dot{V}O_2$ and substrate availability to match the increased metabolic demand of thermoregulation (38, 57). We observed as the need for heat generation increased, there was an increase in metabolic rate, but RERs remained constant and between 0.7 and 0.8 in all mice. Mice also showed

a decline in thermal conductance that reduced rates of heat loss as ambient temperature decreased from thermoneutral (30°C) to moderate cold (0°C) temperatures (*Fig. 2.1; Table 2.1*), consistent with previous studies on small mammals (13, 14, 16, 48, 69). Interestingly, when exposed to moderate cold, both HA and LA deer mice had the same $\dot{V}O_2$ and RERs, suggesting a specific amount of energy and fuel required for submaximal thermogenic demand, which was maintained even after acclimation to CH.

When cold-induced $\dot{V}O_2max$ was stimulated, RER remained low suggesting fuel utilization did not change between moderate and maximal thermogenic requirements, despite the large change in metabolic rate (*Fig. 2.4A,B*). Previous research has shown an adaptive advantage for high aerobic capacity in HA deer mice (29), and that wild HA mice maintain higher hypoxic $\dot{V}O_2max$ than their LA conspecifics when tested in their native environments (19). We did not find a significant difference in thermogenic capacity between laboratory born and raised HA and LA mice (*Fig. 2.4A*). These results are consistent with previous measurements of hypoxic $\dot{V}O_2max$ in WN and CH acclimated deer mice (57, 58). However, when deer mice were acclimated to warm hypoxia, HA mice did show higher hypoxic $\dot{V}O_2max$ than both LA deer mice (57), and white-footed mice (58). Although the combined effects of cold hypoxia can have opposing effects on thermogenesis in laboratory mice (5), we found CH acclimation significantly increased $\dot{V}O_2max$ in all populations. Given the evidence that higher thermogenic capacities are under directional selection in deer mice at high altitude (29), having the ability to elevate thermogenic capacity in response to cold would be adaptive for surviving alpine environments.

Whole animal lipid oxidation rates

The substrates used by mammals to support thermogenesis, and the rate they are oxidized to support heat production, has received little attention. Here we provide data on substrate use during moderate cooling and at peak thermogenesis in *Peromyscus*. All mice fuelled submaximal thermogenesis primarily with lipids, which contributed between 70 to 93% of total metabolism. At thermoneutrality, lipids supported only 59% of total energy requirements in white-footed mice after CH acclimation (*Fig. 2.1B*). Nonetheless, these mice used lipid oxidation to a proportionally greater extent to power thermogenesis than previously observed in rats exposed to 5^{o}C (*Fig. 2.5;* 43).

During moderate rates of thermogenesis, lipid oxidation rates were equivalent to maximal rates observed during aerobic locomotion in the same species (*Fig. 2.*5; 22). Data from a number of low altitude native mammals (humans, mice rats, goats and dogs) show that substrate use during exercise follows a predictable pattern, where rates of lipid oxidation plateau at moderate intensities (52). At higher exercise intensities, lipid use does not increase, even when fatty acid availability is artificially increased (26). However, we show that during thermogenesis in deer mice, lipid oxidation continues to increase and support higher metabolic rates to levels that are 5-fold higher than those observed during exercise in this species (*Fig. 2.5*). These high rates of lipid oxidation support both the activation of BAT metabolism and high rates of muscle shivering. The degree that these tissues rely on either endogenous or circulatory sources of lipid fuel is currently unclear. It is important to note that we determined lipid oxidation by indirect

calorimetry, which can become unreliable when animals leave steady state conditions at higher metabolic rates (49). However, given the linear relationship between $\dot{V}O_2$ and total ventilation across a range of thermogenic intensities (48) and ventilatory equivalents that never reach anaerobic threshold (46, 70), our data suggests that thermoregulating mice in this study were in steady state metabolism, even at cold-induced $\dot{V}O_2$max (*Fig. 2.S1, Table 2.S1 and Table 2.S2;* Supplemental Material for this article can be found online at https://doi.org/10.6084/m9.figshare.13564784).

The oxidation of [^{13}C]-palmitate was also directly quantified during moderate cold exposures. From thermoneutral to moderate cold, we observed a three-fold increase of [^{13}C]-palmitate oxidation (*Fig. 2.2B*), directly reflecting the increase in whole-animal lipid oxidation (*Fig. 2.2A*). However, while total lipid oxidation was unaffected by acclimation in HA mice, [^{13}C]-palmitate oxidation was higher in CH acclimated HA mice. Interestingly, plasma concentrations of palmitate did not track changes in its oxidation but remained stable with acute changes in temperature and with CH acclimation (*Fig. 2.3A*). This mismatch between whole-body palmitate oxidation and circulating palmitate concentrations with thermogenic demand may shed some light on how fatty acids are utilized to match demand for heat production. While difficulty in interpreting experimentally induced changes in blood metabolites has been highlighted by others (39), we suggest two potential explanations for our data. The first explanation suggests that rates of palmitate disappearance into active tissues are tightly matched with rates of appearance into plasma. The second explanation suggests CH leads to greater use of palmitate from endogenous lipid stores within thermo-effector tissues, such as muscle

and/or BAT. Measuring flux of circulating fatty acids, along with the oxidation of both circulatory and intracellular sources of lipid will provide a deeper understanding of how lipid depots are used during thermogenesis.

Total plasma NEFA levels also remained constant, a reflection of changes in those individual fatty acids with high percent contributions to total NEFA (e.g., palmitate and stearate) (*Fig. 2.2C; Fig. 2.3*). However, HA mice showed higher plasma concentrations of elaidate and linoleate, but lower concentrations of palmitoleate and oleate, compared to LA deer mice (*Fig 2.3*). Acclimation to CH led to a selective increase in plasma levels of palmitoleate and oleate at 0^{o}C and a decrease in oleate at 30^{o}C. These findings suggest a population, acclimation, and temperature-specific mobilization of specific NEFA in deer mice.

At peak rates of thermogenesis, lipids were the predominant fuel used by all mice, regardless of altitude ancestry. Lipids constituted 67 to 100% to total oxygen use, regardless of acclimation environment (*Fig. 2.4B*). In hypoxia, highlanders showed higher lipid oxidation rates than lowland deer mice at $\dot{V}O_2$max, which further increased with CH acclimation (*Fig. 2.4C*). The capacity for high rates of lipid oxidation is likely an important feature of the HA phenotype, and along with an elevated $\dot{V}O_2$max (29), increases the probability of winter survival in HA deer mice. Similar to differences in $\dot{V}O_2$max (19), lipid oxidation in hypoxia was higher in HA deer mice due to a combined effect of phenotypic plasticity, overlaid upon genetic differences in maximal rates of fuel use. When the constraint of hypoxia was removed and thermogenic capacity was

determined in normoxia, lipid oxidation at $\dot{V}O_2$max increased with CH in highlanders, to the highest mass-specific rates recorded for any mammal (*Fig. 2.4C*).

Mice used proportionally more lipids in hypoxia than in normoxia, with this fuel accounting for almost 100% of $\dot{V}O_2$ in some instances. These observations may appear paradoxical, given the higher ATP yield per mole of O_2 afforded by carbohydrate oxidation (9, 63) and their increased use with exercise observed in highland native mice (33, 53). However, the efficiency advantage of carbohydrates as a fuel is likely outweighed by the need of critical tissues for this limited resource (35). Instead, mobilization and utilization of lipids is increased in response to a prolonged need for metabolic heat production, even in face of low O_2 availability. Lipid reserves are in abundance in mammals (36) and could sustain prolonged thermogenesis at an ecologically relevant alpine ambient temperature of 0^{o}C (Western Regional Climate Centre), for up to 71 hours, assuming ~4g of stored lipids (20% of a 20g mouse). Our findings also suggest that even at maximal rates of heat production, onboard lipids would last up to 16 hours until fully depleted. These liberal estimates assume all lipids are accessible to the thermo-effector tissues. Nevertheless, mice are capable of oxidizing lipids at very high rates by delivering fatty acids to working mitochondria. How this process occurs is a fruitful area of future research.

The Lipid Oxidation Pathway

Elevated rates of lipid oxidation to support moderate and maximal rates of heat production require sufficient capacities for mobilization, transport, and oxidation to

supply free fatty acids to working mitochondria. During exercise, maximal lipid oxidation is thought to be limited by fatty acid uptake across the sarcolemma of working muscle (64, 66) and mitochondrial membranes (4, 56). Both of these potential limitations may be bypassed during thermogenesis. Unlike exercise, where skeletal muscle accounts for ~80% of O_2 and substrate use (2), thermogenesis in small mammals involves both shivering by skeletal muscle and non-shivering thermogenesis, principally in BAT. Perhaps thermogenic tissues increase reliance on intracellular stores of lipids for fuelling thermogenesis. For example, BAT increases intracellular lipolysis with cold stress in both humans and rats (7, 8, 32). Alternatively, cold stress may stimulate increased blood flow and increased capacity for fatty acid uptake for BAT and shivering muscle (6). Acclimation to CH would further amplify these differences by increasing BAT activity and increasing capacity for lipid transport and oxidation in BAT and muscle. Thus, differences in fuel use between exercise and thermogenesis may involve the relative contributions of these energy consuming tissues involved (21, 42). Indeed, further research is needed to understand the mechanisms involved and determine how these components of the lipid oxidation pathway are regulated during thermogenesis.

2.6 PERSPECTIVES AND SIGNIFICANCE

We report that lipid oxidation is the primary fuel supporting both moderate and maximal rates of thermogenesis in both deer mice and white-footed mice. Rates of lipid oxidation also reflect the higher thermogenic capacity in hypoxia of HA deer mice, suggesting capacity for high lipid use has also evolved in this environment. In addition, we show that rates of lipid oxidation during thermogenesis are much higher than during

exercise and report the highest mass-specific rates, observed in any land-dwelling mammal, to our knowledge. These results highlight a need to understand how lipid oxidation is regulated during high rates of metabolic heat production. For example, it is unknown how the limitation to maximal lipid oxidation observed during exercise is circumvented when animals are thermoregulating. We suggest the increased reliance on BAT activity is an important driver for the high reliance on lipid use during thermogenesis; however, NST occurring in BAT accounts for ~50-60% of cold-induced $\dot{V}O_2max$ in deer mice (62) suggesting lipids used for shivering is more than twice that is observed during exercise (33). Rates of lipid use by shivering muscles are likely much higher than those observed during exercise. How these higher rates of oxidation are achieved are currently unclear. Animals in chronically cold environments, such as the high alpine, would also require a consistent supply of dietary nutrients to maintain the observed elevated daily metabolic rates (28). However, we know little about food sources available to HA deer mice or how they may differ from those at lower elevations. These next steps will provide a deeper understanding of how thermoregulation can raise the ceiling for fat oxidation, and ultimately provide more insight as to how these deer mice can survive the challenging environment of high-altitude.

2.7 ACKNOWLEDGEMENTS

The authors would like to thank G. Scott and C. Ivy for technical assistance and use of plethysmography equipment. We would also like to thank M. McCue for technical advice on stable isotope analysis and M. Dick for technical assistance with stable isotope

analysis. Current address for K. Tate is the Department of Biology, Texas Lutheran University, Seguin, TX 78155, USA.

2.8 FIGURES AND TABLES

Table 2.1

Table 1. *Body mass, change in body temperature, and thermal conductance of first-generation laboratory born and raised highland and lowland Peromyscus mice, acclimated to control (23°C, 21kPa O_2; WN) or cold hypoxia (5°C, 12 kPa O_2; CH), exposed to ambient temperatures of 30°C and 0°C*

	Lowland (*P. leucopus*)				Lowland (*P. maniculatus*)				Highland (*P. maniculatus*)			
	Warm normoxia		Cold hypoxia		Warm normoxia		Cold hypoxia		Warm normoxia		Cold hypoxia	
	30°C	0°C	30°C	0°C	30°C	0°C	30°C	0°C	30°C	0°C	30°C	0°C
Mass, g	21.7 ± 1.7†	23.6 ± 1.6†	26.3 ± 0.6†	26.6 ± 0.9†	20.4 ± 1.2	19.9 ± 1.2	16.9 ± 0.6	17.2 ± 0.6	20.5 ± 1.3	20.7 ± 1.2	18.4 ± 0.7	18.8 ± 0.8
ΔT_b, °C	−0.31 ± 0.5	−2.11 ± 0.9†	0.61 ± 0.61	−1.04 ± 0.4†	0.64 ± 0.33	0.57 ± 0.33	1.24 ± 0.35	0.18 ± 0.27	0.13 ± 0.42	0.60 ± 0.35	0.93 ± 0.56	1.24 ± 0.45
C, mL·O_2·g^{-1}·h^{-1}·$°C^{-1}$	0.28 ± 0.01†	0.17 ± 0.01*†	0.24 ± 0.01†	0.16 ± 0.01*†	0.39 ± 0.02	0.23 ± 0.02*	0.39 ± 0.02	0.23 ± 0.01*	0.39 ± 0.03	0.20 ± 0.01*	0.39 ± 0.03	0.20 ± 0.02*

Values are presented as means ± SE. C, thermal conductance; ΔT_b, body temperature; WN, warm normoxia. Symbols representing significant differences result from Holm Sidak post hoc tests ($P < 0.05$). †Significantly different from highland and lowland deer mice within a given test temperature. *Significantly different from 30°C.

Figure 2.1

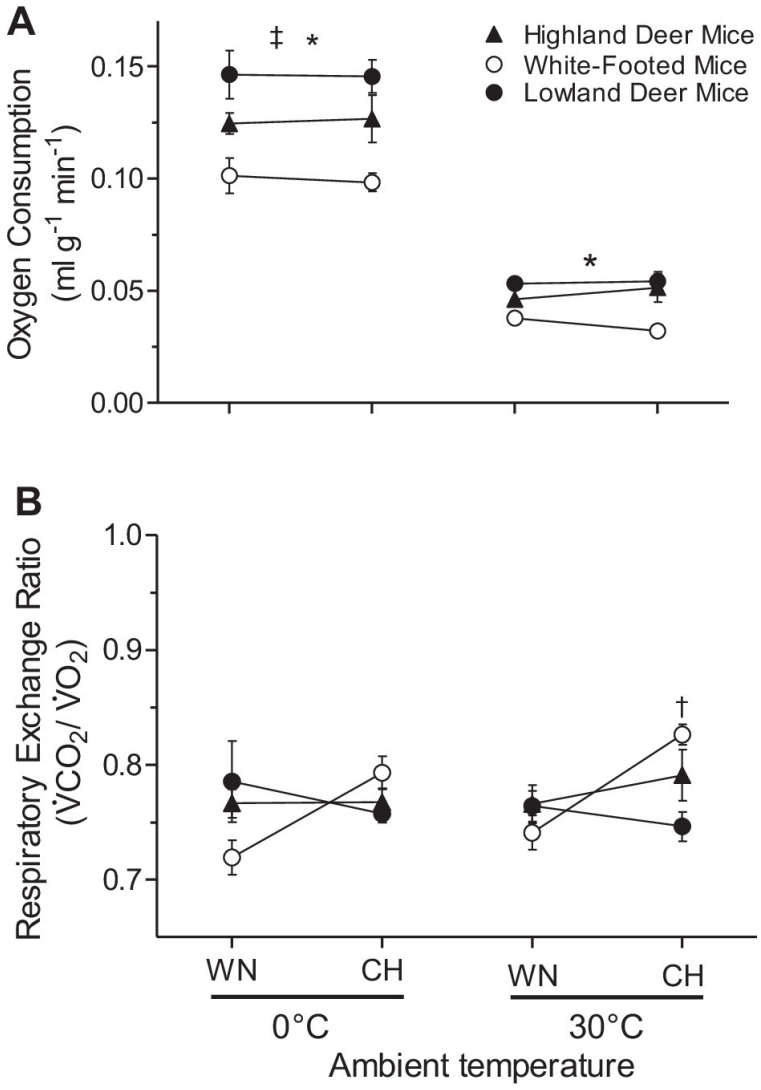
A
B
Highland Deer Mice
White-Footed Mice
Lowland Deer Mice
Oxygen Consumption (ml g-1 min-1)
0.15
0.10
0.05
0.00
‡
*
*
Respiratory Exchange Ratio (V̇CO2/V̇O2)
1.0
0.9
0.8
0.7
†
WN
CH
WN
CH
0°C
30°C
Ambient temperature

Figure 2.1. Oxygen consumption ($\dot{V}O_2$) (in ml g^{-1} min^{-1}) (A) and Respiratory Exchange Ratio (RER= $\dot{V}CO_2/\dot{V}O_2$) (B) of first-generation laboratory born and raised highland and lowland *Peromyscus mice*, acclimated to control warm normoxia (23ºC, 21 kPa O_2; WN) or cold hypoxia (5ºC, 12 kPa O_2; CH), and then exposed acutely to ambient temperatures of 30ºC and 0ºC. A) $\dot{V}O_2$ showed a significant effect of ambient temperature ($F_{1,79}$ = 376.12, P<0.001), and population ($F_{2,79}$ = 11.48, P<0.001), while controlling for differences in body mass ($F_{1,79}$ = 16.08, P<0.001). At 0ºC there was a significant population effect ($F_{2,39}$ = 5.69, P=0.007). At 30ºC there was a main effect of population on $\dot{V}O_2$ ($F_{2,39}$ = 7.59, P=0.002). B) For RER there was a significant population x acclimation interaction ($F_{2,80}$ = 6.12, P=0.003). At 30ºC there was a significant population x acclimation interaction ($F_{2,40}$ = 4.33, P=0.020). Symbols representing significant differences result from Holm Sidak post hoc tests (p<0.05). ‡Significant difference between test temperatures. *Highland and lowland deer mice are significantly different than white-footed mice. †Significant difference between CH lowlanders and CH white-footed mice at 30ºC. N=5 for WN and CH white-footed mice; N= 10 and 9 for WN and CH lowland deer mice, respectively; N= 9 and 8 for WN and CH highland deer mice, respectively. Data are presented as mean ± SEM.

Figure 2.2

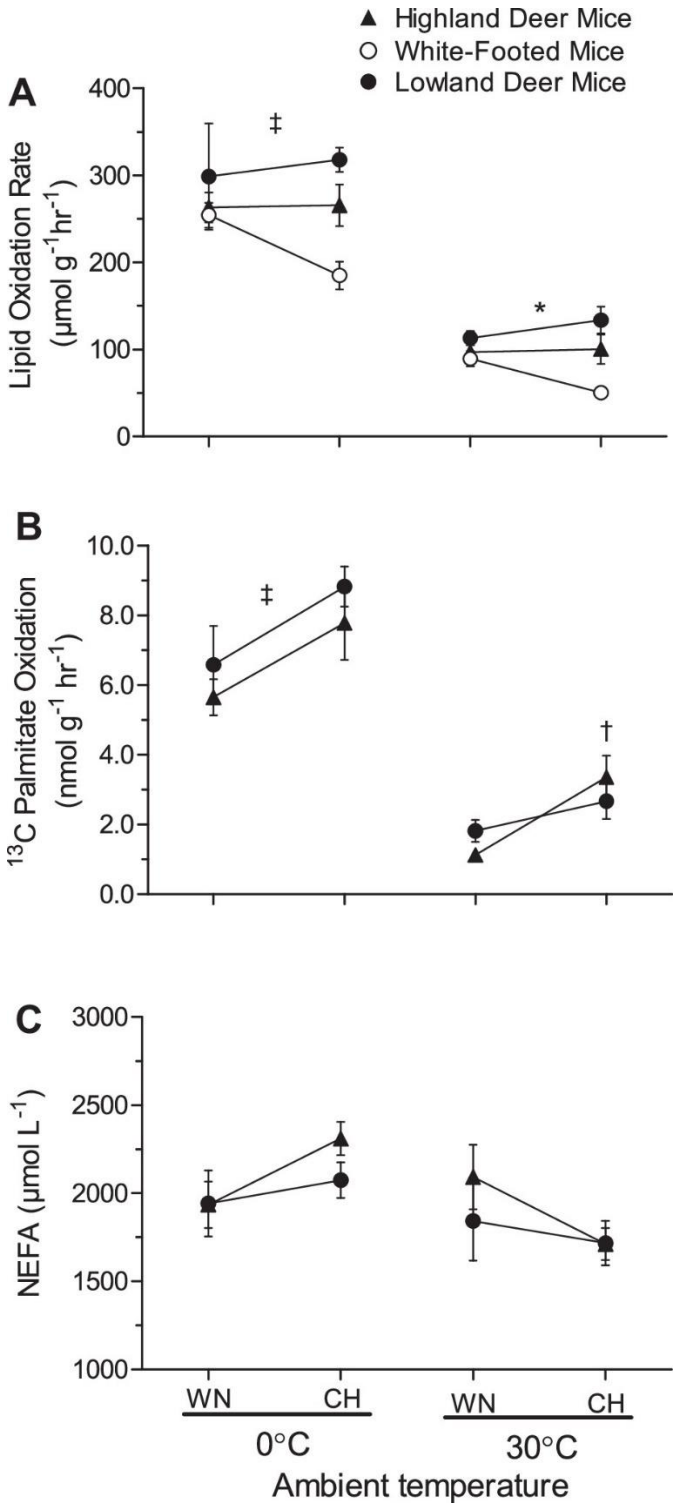
Highland Deer Mice
White-Footed Mice
Lowland Deer Mice
A
Lipid Oxidation Rate (µmol g-1hr-1)
400
300
200
100
0
‡
*
B
13C Palmitate Oxidation (nmol g-1 hr-1)
10.0
8.0
6.0
4.0
2.0
0.0
‡
†
C
NEFA (µmol L-1)
3000
2500
2000
1500
1000
WN
CH
WN
CH
0°C
30°C
Ambient temperature

Figure 2.2. Whole-animal lipid oxidation rates (in µmol g^{-1} h^{-1}) (A), rates of [^{13}C]-palmitate oxidation (in nmol g^{-1} h^{-1}) (B) and concentrations of circulating plasma Non-Esterified Fatty Acids (NEFAs, in µmol L^{-1}) (C) of first-generation laboratory born and raised highland and lowland *Peromyscus mice,* acclimated to control warm normoxia (23ºC, 21 kPa O_2; WN) or cold hypoxia (5ºC, 12 kPa O_2; CH), and exposed acutely to ambient temperatures of 30ºC and 0ºC. A) Whole-animal lipid oxidation rate showed a significant effect of ambient temperature ($F_{1,79}$ = 123.77, P<0.001) and population ($F_{2,79}$ = 3.51, P=0.035) while controlling for differences in body mass ($F_{1,79}$ = 3.95, P=0.050). At 30ºC there was a significant population effect ($F_{2,39}$ = 5.88, P=0.006) while controlling for body mass ($F_{1,39}$ = 0.236, P=0.630). B) [^{13}C]-palmitate oxidation showed a significant effect of ambient temperature ($F_{1,35}$ = 157.30, P<0.001) and acclimation ($F_{1,35}$ = 12.21, P=0.001) while controlling for body mass ($F_{1,35}$ = 0.044, P=0.835). At 30ºC there was a significant population x acclimation interaction ($F_{1,17}$ = 6.59, P=0.020), and significant acclimation effect ($F_{1,17}$ = 14.82, P=0.001), all while controlling for body mass ($F_{1,17}$ = 0.000, P=0.999). Symbols representing significant differences result from Holm Sidak post hoc tests (p<0.05). ‡Significant difference between test temperatures. *Highland and lowland deer mice are significantly different than white-footed mice. †Significant difference between highland acclimation groups at 30ºC. A) N=5 for WN and CH white-footed mice; N= 10 and 9 for WN and CH lowland deer mice, respectively; N= 9 and 8 for WN and CH highland deer mice, respectively. B) N=7 and 5 for WN and CH lowland deer mice, respectively; N= 8 and 4 for WN and CH highland deer mice, respectively. C) N=8-9 for WN and 5 for CH lowland deer mice, respectively; N= 9-10 and 4 for WN and CH highland deer mice, respectively. All data are presented as mean ± SEM.

Figure 2.3

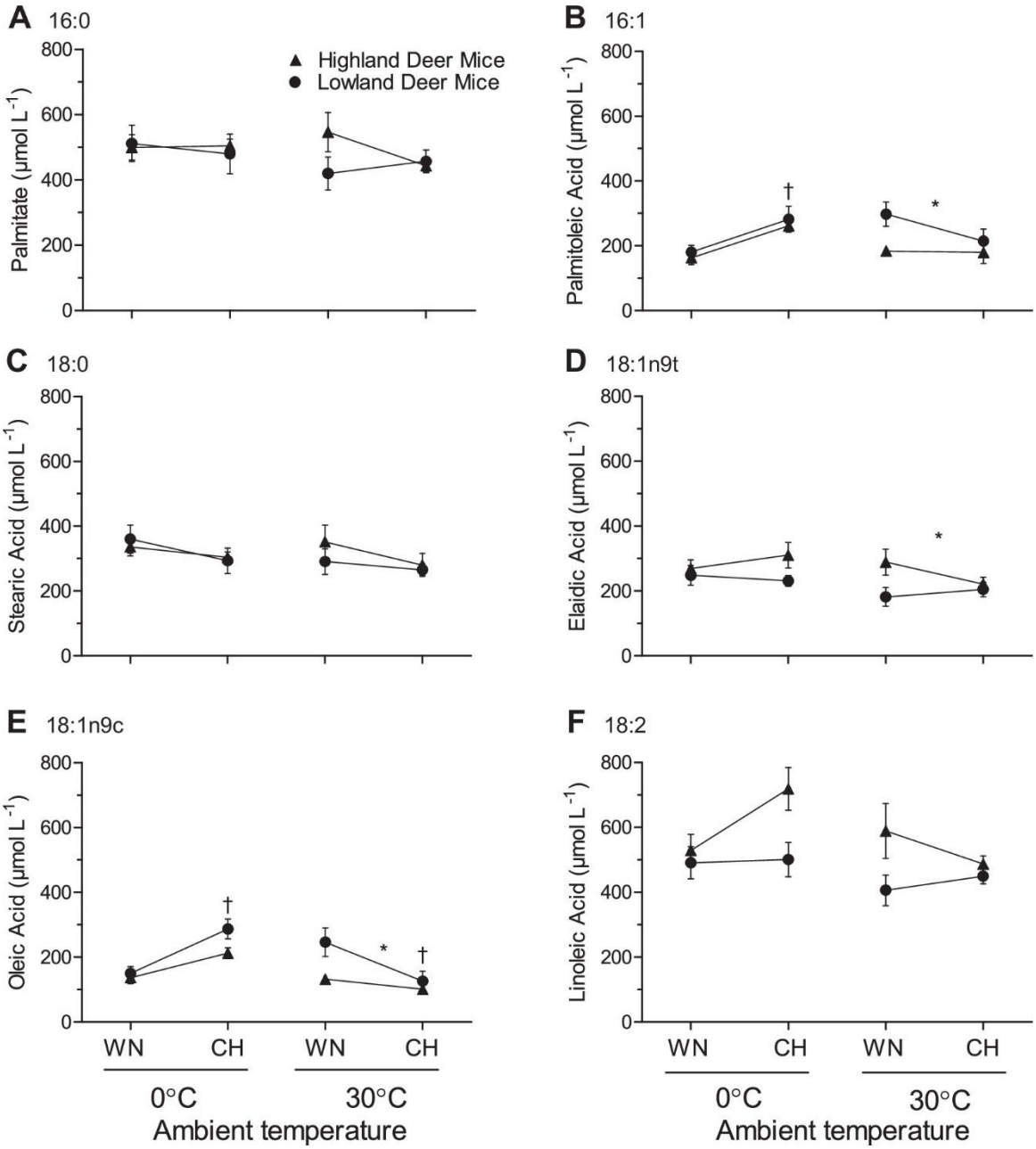
A 16:0
B 16:1
C 18:0
D 18:1n9t
E 18:1n9c
F 18:2
Highland Deer Mice
Lowland Deer Mice
Palmitate (µmol L-1)
Palmitoleic Acid (µmol L-1)
Stearic Acid (µmol L-1)
Elaidic Acid (µmol L-1)
Oleic Acid (µmol L-1)
Linoleic Acid (µmol L-1)
0
200
400
600
800
†
*
WN
CH
0°C
30°C
Ambient temperature

Figure 2.3. Concentrations of individual plasma fatty acids (in µmol L^{-1}) of first-generation laboratory born and raised highland and lowland deer mice (*Peromyscus maniculatus*), acclimated to control warm normoxia (23ºC, 21 kPa O_2; WN) or cold hypoxia (5ºC, 12 kPa O_2; CH), acutely exposed to ambient temperatures of 30ºC and 0ºC. Palmitic acid (16:0) (A); Palmitoleic acid (16:1) (B); at 0ºC there was a significant acclimation effect ($F_{1,23}$ = 12.99, P=0.001) while at 30ºC there was a significant population effect ($F_{1,23}$ = 6.70, P=0.015). Stearic acid (18:0) (C); Elaidic acid (18:1n9t) (D); at 30ºC there was a significant population effect ($F_{1,23}$ = 4.96, P=0.036). Oleic acid (18:1n9c) (E); at 0ºC there was a significant acclimation effect ($F_{1,23}$ = 19.66, P<0.001) while at 30ºC there was a significant population effect ($F_{1,23}$ = 5.77, P=0.025) and acclimation effect ($F_{1,23}$ = 4.91, P=0.037). Linoleic acid (18:2) (F). Symbols representing significant differences result from Holm Sidak post hoc tests (p<0.05). *Main population effect within a given test temperature. †Main acclimation effect within a given test temperature. N=8-9 for WN and 5 for CH lowland deer mice, respectively; N = 9-10 and 4 for WN and CH highland deer mice, respectively. Data are presented as mean ± SEM.

Figure 2.4

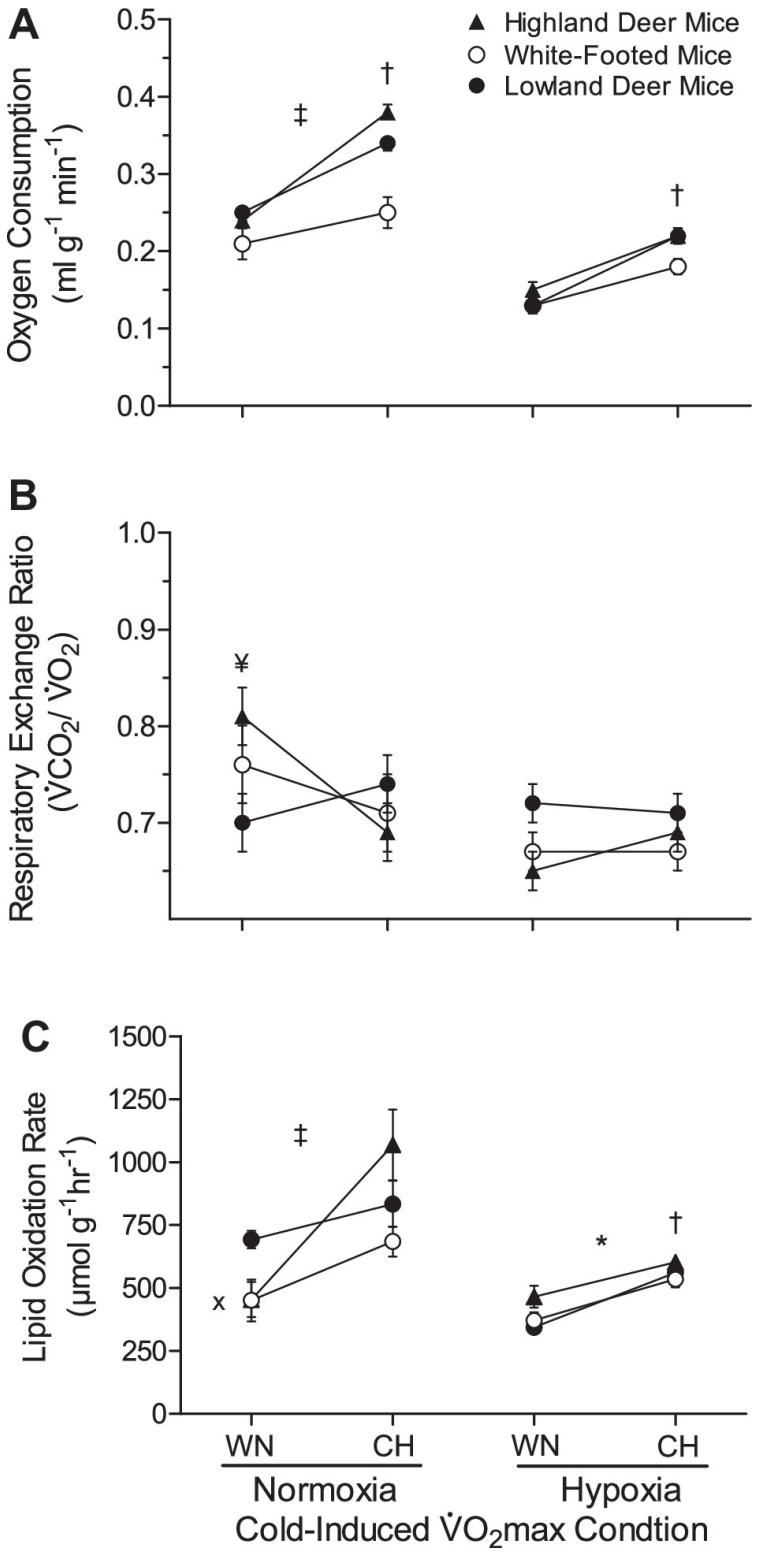
A
B
C
Highland Deer Mice
White-Footed Mice
Lowland Deer Mice
Oxygen Consumption (ml g-1 min-1)
Respiratory Exchange Ratio (V̇CO2/ V̇O2)
Lipid Oxidation Rate (µmol g-1hr-1)
0.5
0.4
0.3
0.2
0.1
0.0
1.0
0.9
0.8
0.7
1500
1250
1000
750
500
250
0
‡
†
¥
x
*
WN
CH
WN
CH
Normoxia
Hypoxia
Cold-Induced V̇O2max Condtion

Figure 2.4. Cold-induced maximal oxygen consumption ($\dot{V}O_2$) (in ml g^{-1} min^{-1}) (A) with the corresponding Respiratory Exchange Ratios (RER= $\dot{V}CO_2/\dot{V}O_2$) (B) whole-animal lipid oxidation rates (in µmol g^{-1} hr^{-1}) (C) of first-generation laboratory born and raised highland and lowland *Peromyscus* mice, acclimated to control warm normoxia (23ºC, 21 kPa O_2;WN) or cold hypoxia (5ºC, 12 kPa O_2; CH), acutely exposed to normoxia (21% O_2) or hypoxia (12% O_2). A) There was a significant effect of condition on cold-induced $\dot{V}O_2$max ($F_{1,135}$ = 353.22, P<0.001) while controlling for the effects of body mass ($F_{1,135}$ = 16.93, P<0.001). White-footed mice weighed significantly more than both highland and lowland deer mice, regardless of acclimation environment (p<0.05). There was a significant effect of acclimation on cold-induced $\dot{V}O_2$max in normoxic ($F_{1,39}$ = 48.85, P<0.001) and hypoxic ($F_{1,95}$ = 170.33, P<0.001) conditions. B) Under normoxic conditions, there was a significant population × acclimation interaction in RER ($F_{2,40}$ = 4.10, P=0.024). C) Lipid oxidation rates showed a significant effect of $\dot{V}O_2$max condition ($F_{1,135}$ = 43.74, P<0.001) and acclimation ($F_{1,135}$ = 55.00, P<0.001). There was a significant interaction between population, acclimation and $\dot{V}O_2$max condition ($F_{1,135}$ =6.93, P=0.001). All factors had mass as a covariate ($F_{1,135}$ = 6.33, P=0.013). In normoxia, there was a significant interaction between population and acclimation ($F_{2,39}$ = 4.62, P=0.016) while controlling for mass ($F_{1,39}$ = 0.202, P=0.656). In hypoxia, there was a significant effect of population ($F_{2,95}$ = 3.16, P=0.047) and acclimation ($F_{1,95}$ = 44.06, P<0.001) whilst controlling for differences in body mass ($F_{1,95}$ = 16.68, P<0.001). Symbols representing significant differences result from Holm Sidak post hoc tests (p<0.05). ‡Significant difference between cold-induced $\dot{V}O_2$max conditions. *Highlanders significantly differ from lowland deer mice within hypoxic cold-induced $\dot{V}O_2$max conditions. †Main acclimation effect within a given cold-induced $\dot{V}O_2$max condition. ¥ WN highland deer mice significantly differ from CH highland and WN lowland deer mice, within the normoxic $\dot{V}O_2$max condition. ^{X}WN highlanders and WN white-footed mice significantly differ from CH highlanders within the normoxic $\dot{V}O_2$max condition. N=5-15 for WN white-footed mice (mass (in g) = 24.8 ± 1.7 and 26.5 ± 1.0 for normoxia and hypoxia, respectively) and CH white-footed mice (mass (in g) = 27.6 ± 1.7 and 26.7 ± 1.0 for normoxia and hypoxia, respectively). N = 9-19 for WN lowland deer mice (mass (in g) = 20.8 ±1.2 and 20.7 ±1.0 for normoxia and hypoxia, respectively) and CH lowland deer mice (mass (in g) = 17.9 ± 1.3 and 20.2 ± 0.9 for normoxia and hypoxia, respectively). N= 8-21 for WN highland deer mice (mass (in g) = 22.0 ± 1.3 and 20.3 ± 0.8 for normoxia and hypoxia, respectively) and CH highland deer mice (mass (in g) = 19.5 ± 1.3 and 21.5 ± 0.9 for normoxia and hypoxia, respectively). Data are presented as mean ± SEM. Mass and $\dot{V}O_2$max in hypoxia data from Tate et al., 2020.

Figure 2.5

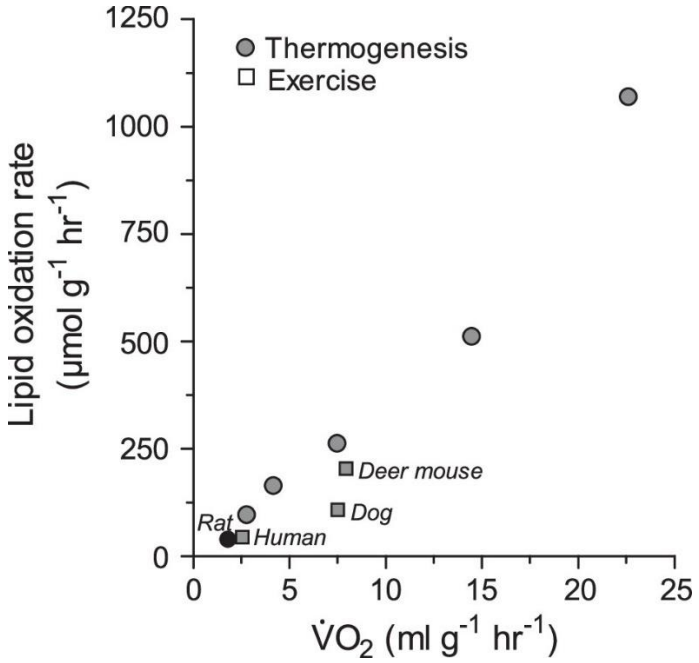
Thermogenesis
Exercise
Lipid oxidation rate (µmol g-1 hr-1)
1250
1000
750
500
250
0
0
5
10
15
20
25
V̇O2 (ml g-1 hr-1)
Deer mouse
Dog
Rat
Human

Figure 2.5. Mass-specific lipid oxidation rates as a function of metabolic rate at 30°C, 15°C, 0°C and normoxic cold-induced $\dot{V}O_2max$ in warm normoxia (23°C, 21 kPa O_2) and cold hypoxia (5°C, 12 kPa O_2) acclimated high-altitude deer mice (this study) compared to those during submaximal aerobic exercise in running humans (1), dogs (49) and deer mice (33) and with moderate shivering thermogenesis in rats (dark circle represents lipid oxidation but only during shivering thermogenesis) (61).

2.9 REFERENCES

1. **Achten J**, **Venables MC**, **Jeukendrup AE**. Fat oxidation rates are higher during running compared with cycling over a wide range of intensities. *Metabolism* 52: 747–752, 2003. doi: 10.1016/S0026-0495(03)00068-4.

2. **Armstrong RB, Essen-Gustavsson B, Hoppeler H, Jones JH, Kayar SR, Laughlin MH, Lindholm A, Longworth KE, Taylor CR, Weibel ER.** O_2 delivery at VO_2max and oxidative capacity in muscles of standardbred horses. *J Appl Physiol* 73(6): 2274-2282, 1992.

3. **Bates D**, **Mächler M**, **Bolker BM**, **Walker SC**. Fitting linear mixed-effects models using lme4. *J Stat Softw* 67, 2015. doi: 10.18637/jss.v067.i01.

4. **Båvenholm PN**, **Pigon J**, **Saha AK**, **Ruderman NB**, **Efendic S**. Fatty acid oxidation and the regulation of malonyl-CoA in human muscle. *Diabetes* 49: 1078-1083, 2000. doi: 10.2337/diabetes.49.7.1078

5. **Beaudry JL**, **McClelland GB**. Thermogenesis in CD-1 mice after combined chronic hypoxia and cold acclimation. *Comp Biochem Physiol - B Biochem Mol Biol* 157: 301–309, 2010. doi: 10.1016/j.cbpb.2010.07.004.

6. **Blondin DP**, **Frisch F**, **Phoenix S**, **Guérin B**, **Turcotte ÉE**, **Haman F**, **Richard D**, **Carpentier AC**. Inhibition of Intracellular Triglyceride Lipolysis Suppresses Cold-Induced Brown Adipose Tissue Metabolism and Increases Shivering in Humans. *Cell Metab* 25: 438–447, 2017. doi: 10.1016/j.cmet.2016.12.005.

7. **Blondin DP**, **Labbé SM**, **Noll C**, **Kunach M**, **Phoenix S**, **Guérin B**, **Turcotte ÉE**, **Haman F**, **Richard D**, **Carpentier AC**. Selective impairment of glucose but not fatty acid or oxidative metabolism in brown adipose tissue of subjects with type 2 diabetes. *Diabetes* 64: 2388–2397, 2015. doi: 10.2337/db14-1651.

8. **Blondin DP**, **Labbé SM**, **Phoenix S**, **Guérin B**, **Turcotte ÉE**, **Richard D**, **Carpentier AC**, **Haman F**. Contributions of white and brown adipose tissues and skeletal muscles to acute cold-induced metabolic responses in healthy men. *J Physiol* 593: 701–714, 2015. doi: 10.1113/jphysiol.2014.283598.

9. **Brand MD**. The stoichiometry of proton pumping and synthesis in mitochondria. *Biochem (Lond)* 16: 20–24, 1994.

10. **Brooks GA, Mercier J.** Balance of carbohydrate and lipid utilization during exercise: the "crossover" concept. *J Appl Physiol* 76(6): 2253-2261, 1994.

11. **Bulow J**. *Lipid mobilization and utilization. In Principles of Exercise Biochemistry*. J.R. Poort. Basel: Karger, 1988.

12. **Cannon B**, **Nedergaard J**. Brown Adipose Tissue: Function and Physiological Significance. *Physiol Rev* 84: 277–359, 2004. doi: 10.1152/physrev.00015.2003.

13. **Casey TM, Withers PC, Casey KK.** Metabolic and respiratory responses of arctic

mammals to ambient temprature during the summer. Comparative Biochemistry and Physiology--Part A: *Physiology* 64(3): 331-341, 1979.

14. **Chappell MA**. Effects of ambient temperature and altitude on ventilation and gas exchange in deer mice (Peromyscus maniculatus). *J Comp Physiol B* 155: 751–758, 1985. doi: 10.1007/BF00694590.

15. **Chappell MA**, **Hammond KA**. Maximal aerobic performance of deer mice in combined cold and exercise challenges. *J Comp Physiol B Biochem Syst Environ Physiol* 174: 41–48, 2004. doi: 10.1007/s00360-003-0387-z.

16. **Chappell MA**, **Holsclaw DS**. Effects of wind on thermoregulation and energy balance in deer mice (Peromyscus maniculatus). *J Comp Physiol B* 154: 619–625, 1984. doi: 10.1007/BF00684416.

17. **Chappell MA**, **Rezende EL**, **Hammond KA**. Age and aerobic performance in deer mice. *J Exp Biol* 206: 1221–1231, 2003. doi: 10.1242/jeb.00255.

18. **Cheviron ZA**, **Bachman GC**, **Connaty AD**, **McClelland GB**, **Storz JF**. Regulatory changes contribute to the adaptive enhancement of thermogenic capacity in high-altitude deer mice. *Proc Natl Acad Sci* 109: 8635–8640, 2012. doi: 10.1073/pnas.1120523109.

19. **Cheviron ZA**, **Connaty AD**, **Mcclelland GB**, **Storz JF**. Functional genomics of adaptation to hypoxic cold-stress in high-altitude deer mice: Transcriptomic plasticity and thermogenic performance. *Evolution (N Y)* 68: 48–62, 2014. doi: 10.1111/evo.12257.

20. **Dick MF**, **Alcantara-Tangonan A**, **Oghli YS**, **Welch KC**. Metabolic partitioning of sucrose and seasonal changes in fat turnover rate in ruby-throated hummingbirds (Archilochus colubris). *J Exp Biol* 223, 2020. doi: 10.1242/jeb.212696.

21. **Foster DO**, **Frydman ML**. Tissue distribution of cold-induced thermogenesis in conscious warm- or cold-acclimated rats reevaluated from changes in tissue blood flow: The dominant role of brown adipose tissue in the replacement of shivering by nonshivering thermogenesis. *Can J Physiol Pharmacol* 57: 257–270, 1979. doi: 10.1139/y79-039.

22. **Frayn KN**. Calculation of substrate oxidation rates in vivo from gaseous exchange. *J Appl Physiol* 55(2):628-634, 1983.

23. **Fristoe TS**, **Burger JR**, **Balk MA**, **Khaliq I**, **Hof C**, **Brown JH**. Metabolic heat production and thermal conductance are mass-independent adaptations to thermal environment in birds and mammals. *Proc Natl Acad Sci U S A* 112: 15934–15939, 2015. doi: 10.1073/pnas.1521662112.

24. **Gessaman JA**, **Nagy K.** Energy metabolism: errors in gas-exchange conversion factors. *Physiol Zool* 61, 1988.

25. **Haman F**, **Legault SR**, **Weber JM**. Fuel selection during intense shivering in humans: EMG pattern reflects carbohydrate oxidation. *J Physiol* 556: 305–313, 2004. doi: 10.1113/jphysiol.2003.055152.

26. **Hargreaves M**, **Kiens B**, **Richter EA**. Effect of increased plasma free fatty acid concentration on muscle metabolism in exercising men. *J Appl Physiol* 70: 194–201, 1991. doi: 10.1152/jappl.1991.70.1.194.

27. **Hayes AJP**, **Chappell MA**,**Hayes JP**, **Chappell MA**. Individual Consistency of Maximal Oxygen Consumption in Deer Mice *Funct Ecol* 4: 495–503, 1990.

28. **Hayes JP**. Altitudinal and seasonal effects on aerobic metabolism of deer mice. *J Comp Physiol B* 159: 453–459, 1989. doi: 10.1007/BF00692417.

29. **Hayes JP**, **O'Connor CS**. Natural Selection on Thermogenic Capacity of High-Altitude Deer Mice. *Evolution (N Y)* 53: 1280, 1999. doi: 10.2307/2640830.

30. **Hothorn T**, **Bretz F**, **Westfall P**. Simultaneous inference in general parametric models. *Biom J* 50: 346–363, 2008.

31. **Khaliq I**, **Fritz SA**, **Prinzinger R**, **Pfenninger M**, **Böhning-Gaese K**, **Hof C**. Global variation in thermal physiology of birds and mammals: Evidence for phylogenetic niche conservatism only in the tropics. *J Biogeogr* 42: 2187–2196, 2015. doi: 10.1111/jbi.12573.

32. **Labbé SM**, **Caron A**, **Bakan I**, **Laplante M**, **Carpentier AC**, **Lecomte R**, **Richard D**. In vivo measurement of energy substrate contribution to cold-induced brown adipose tissue thermogenesis. *FASEB J* 29: 2046–2058, 2015. doi: 10.1096/fj.14-266247.

33. **Lau DS**, **Connaty AD**, **Mahalingam S**, **Wall N**, **Cheviron ZA**, **Storz JF**, **Scott GR**, **McClelland GB**. Acclimation to hypoxia increases carbohydrate use during exercise in high-altitude deer mice. *Am J Physiol - Regul Integr Comp Physiol* 312: R400–R411, 2017. doi: 10.1152/ajpregu.00365.2016.

34. **Lui MA**, **Mahalingam S**, **Patel P**, **Connaty AD**, **Ivy CM**, **Cheviron ZA**, **Storz JF**, **McClelland GB**, **Scott GR**. High-altitude ancestry and hypoxia acclimation have distinct effects on exercise capacity and muscle phenotype in deer mice. *Am J Physiol - Regul Integr Comp Physiol* 308: R779–R791, 2015. doi: 10.1152/ajpregu.00362.2014.

35. **McClelland GB**, **Hochachka PW**, **Weber J-M**. Carbohydrate utilization during exercise after high-altitude acclimation: A new perspective. *Proc Natl Acad Sci U S A* 95: 10288–10293, 1998. doi: 10.1073/pnas.95.17.10288.

36. **McClelland GB**, **Hochachka PW**, **Weber JM**. Effect of high-altitude acclimation on NEFA turnover and lipid utilization during exercise in rats. *Am J Physiol* 277: E1095-102, 1999.

37. **McClelland GB**, **Lyons SA**, **Robertson CE**. Fuel use in mammals: Conserved patterns and evolved strategies for aerobic locomotion and thermogenesis. *Integr Comp Biol* 57: 231–239, 2017. doi: 10.1093/icb/icx075.

38. **McClelland GB**, **Scott GR**. Evolved Mechanisms of Aerobic Performance and Hypoxia Resistance in High-Altitude Natives. *Annu Rev Physiol* 81: 561–583, 2019. doi: 10.1146/annurev-physiol-021317-121527.

39. **McCue MD**, **Albach A**, **Salazar G**. Previous repeated exposure to food limitation enables rats to spare lipid stores during prolonged starvation. *Physiol Biochem Zool* 90: 63–74, 2017. doi: 10.1086/689323.

40. **McCue MD**, **McWilliams SR**, **Pinshow B**. Ontogeny and nutritional status influence oxidative kinetics of nutrients and whole-animal bioenergetics in zebra finches, Taeniopygia guttata: New applications for 13C breath testing. *Physiol Biochem Zool* 84: 32–42, 2011. doi: 10.1086/657285.

41. **McCue MD**, **Pollock ED**. Measurements of substrate oxidation using 13CO2-breath testing reveals shifts in fuel mix during starvation. *J Comp Physiol B Biochem Syst Environ Physiol* 183: 1039–1052, 2013. doi: 10.1007/s00360-013-0774-z.

42. **Mccue MD**, **Voigt CC**, **Jefimow M**, **Wojciechowski MS**. Thermal acclimation and nutritional history affect the oxidation of different classes of exogenous nutrients in Siberian hamsters, Phodopus sungorus. *J Exp Zool Part A Ecol Genet Physiol* 321: 503–514, 2014. doi: 10.1002/jez.1882.

43. **McCue MD**, **Welch KC**. 13C-Breath testing in animals: theory, applications, and future directions. *J Comp Physiol B* 186(3): 265-285, 2016.

44. **Moriya K**, **Leblanc J**, **Arnold J**. Effects of Exercise and Intermittent Cold Exposure on Shivering and Nonshivering Thermogenesis in Rats. *Jpn J Physiol* 37: 715–727, 1987.

45. **Nespolo RF**, **Opazo JC**, **Rosenmann M**, **Bozinovic F**. Thermal acclimation, maximum metabolic rate, and nonshivering thermogenesis of Phyllotis xanthopygus (Rodentia) in the Andes mountains. *J Mammal* 80: 742–748, 1999. doi: 10.2307/1383243.

46. **Newstead CG**. The relationship between ventilation and oxygen consumption in man is the same during both moderate exercise and shivering. *J Physiol* 383: 455–459, 1987. doi: 10.1113/jphysiol.1987.sp016420.

47. **Price ER**, **Armstrong C**, **Guglielmo CG**, **Staples JF**. Selective Mobilization of Saturated Fatty Acids in Isolated Adipocytes of Hibernating 13-Lined Ground Squirrels *Ictidomys tridecemlineatus*. *Physiol Biochem Zool* 86: 205–212, 2013. doi: 10.1086/668892.

48. **Rezende EL**. Cold-acclimation in Peromyscus: temporal effects and individual

variation in maximum metabolism and ventilatory traits. *J Exp Biol* 207(2): 295-305, 2004.

49. **Roberts TJ**, **Weber JM**, **Hoppeler H**, **Weibel ER**, **Taylor CR**. Design of the oxygen and substrate pathways. II. Defining the upper limits of carbohydrate and fat oxidation. *J Exp Biol* 199: 1651–1658, 1996.

50. **Robertson CE**, **McClelland GB**. Developmental delay in shivering limits thermogenic capacity in juvenile high-altitude deer mice (Peromyscus maniculatus). *J Exp Biol* 222, 2019. doi: 10.1242/jeb.210963.

51. **Rosenmann MS**, **Morrison PR**. Maximum oxygen consumption and heat loss facilitation in small homeotherms by He-O2. *Amer J Phsyiol* 226: 490–495, 1974.

52. **Schippers MP**, **LeMoine CMR**, **McClelland GB**. Patterns of fuel use during locomotion in mammals revisited: The importance of aerobic scope. *J Exp Biol* 217: 3193–3196, 2014. doi: 10.1242/jeb.099432.

53. **Schippers MP**, **Ramirez O**, **Arana M**, **Pinedo-Bernal P**, **McClelland GB**. Increase in carbohydrate utilization in high-altitude andean mice. *Curr Biol* 22: 2350–2354, 2012. doi: 10.1016/j.cub.2012.10.043.

54. **Scholander PF, Hock R, Walters V, Irving L.** Adaptation to cold in arctic and tropical mammals and birds in relation to body temperature, insulation, and basal metabolic rate. *Biol Bull* 99(2): 259-271, 1950.

55. **Sokolović M**, **Wehkamp D**, **Sokolović A**, **Vermeulen J**, **Gilhuijs-Pederson LA**, **van Haaften RIM**, **Nikolsky Y**, **Evelo CTA**, **van Kampen AHC**, **Hakvoort TBM**, **Lamers WH**. Fasting induces a biphasic adaptive metabolic response in murine small intestine. *BMC Genomics* 8: 1–18, 2007. doi: 10.1186/1471-2164-8-361.

56. **Stephens FB**. Does skeletal muscle carnitine availability influence fuel selection during exercise? *Proc Nutr Soc* 77: 11–19, 2018. doi: 10.1017/S0029665117003937.

57. **Tate KB**, **Ivy CM**, **Velotta JP**, **Storz JF**, **McClelland GB**, **Cheviron ZA**, **Scott GR**. Circulatory mechanisms underlying adaptive increases in thermogenic capacity in high-altitude deer mice. *J Exp Biol* 220(20): 3616-3620, 2017.

58. **Tate KB**, **Wearing OH**, **Ivy CM**, **Cheviron ZA**, **Storz JF**, **McClelland GB**, **Scott GR**. Coordinated changes across the O2 transport pathway underlie adaptive increases in thermogenic capacity in high-altitude deer mice. *P Biol Sci* 287: 20192750, 2020. doi: 10.1098/rspb.2019.2750.

59. **Team RC**. R: a language and environment for statistical computing [Online]. Wienna, Austria: R Foundation for Statistical Computing. http://www.r-project.org [2013].

60. **Templeman NM**, **Schutz H**, **Garland T**, **McClelland GB**. Do mice bred selectively for high locomotor activity have a greater reliance on lipids to power submaximal aerobic exercise? *AJP Regul Integr Comp Physiol* 303: R101–R111, 2012. doi: 10.1152/ajpregu.00511.2011.

61. **Vaillancourt E**, **Haman F**, **Weber JM**. Fuel selection in Wistar rats exposed to cold: Shivering thermogenesis diverts fatty acids from re-esterification to oxidation. *J Physiol* 587: 4349–4359, 2009. doi: 10.1113/jphysiol.2009.175331.

62. **Van Sant MJ**, **Hammond KA**. Contribution of Shivering and Nonshivering Thermogenesis to Thermogenic Capacity for the Deer Mouse (*Peromyscus maniculatus*). *Physiol Biochem Zool* 81: 605–611, 2008. doi: 10.1086/588175.

63. **Weber JM**. Metabolic fuels: Regulating fluxes to select mix. *J Exp Biol* 214: 286–294, 2011. doi: 10.1242/jeb.047050.

64. **Weber JM**, **Brichon G**, **Zwingelstein G**, **Mcclelland G**, **Saucedo C**, **Weibel ER**, **Taylor CR**. Design of the oxygen and substrate pathways. IV. Partitioning energy provision from fatty acids. *J Exp Biol* 199: 1667–1674, 1996.

65. **Weber JM**, **Haman F**. Oxidative fuel selection: adjusting mix and flux to stay alive. *Int Congr Ser* 1275: 22–31, 2004. doi: 10.1016/j.ics.2004.09.043.

66. **Weibel ER**, **Taylor CR**, **Weber JM**, **Vock R**, **Roberts TJ**, **Hoppeler H**. Design of the oxygen and substrate pathways. VII. Different structural limits for oxygen and substrate supply to muscle mitochondria. *J Exp Biol* 199: 1699–1709, 1996.

67. **White CR**, **Portugal SJ**, **Martin GR**, **Butler PJ**. Respirometry: Anhydrous drierite equilibrates with carbon dioxide and increases washout times. *Physiol Biochem Zool* 79: 977–980, 2006. doi: 10.1086/505994.

68. **Withers PC**. Measurement of VO2, VCO2, and evaporative water loss with a flow-through mask. *J Appl Phyiol* 42(1):120-123, 1977.

69. **Withers PC**, **Casey TM**, **Casey KK**. Allometry of respiratory and haematological parameters of arctic mammal. *Comp Biochem Phyiol A* 64(3): 343-350, 1979.

70. **Yu CCW**, **McManus AM**, **Li AM**, **Sung RYT**, **Armstrong N**. Cardiopulmonary exercise testing in children. *Hong Kong J Paediatr* 15: 35–47, 2010. doi: 10.1378/chest.120.1.81.

CHAPTER 3: THERMOGENESIS IS SUPPORTED BY HIGH RATES OF CIRCULATORY FATTY ACID AND TRIGLYCERIDE DELIVERY IN HIGHLAND DEER MICE

Modified and reproduced with permission from Lyons, S.A., and McClelland G.B. (2022). *J Exp Biol* 225, 2022. doi: 10.1242/jeb.244080.

3.1 ABSTRACT

Highland native deer mice (*Peromyscus maniculatus*) have greater rates of lipid oxidation during maximal cold challenge in hypoxia (hypoxic cold-induced $\dot{V}O_2max$) compared to their lowland conspecifics. Lipid oxidation is also increased in deer mice acclimated to simulated high altitude (cold hypoxia), regardless of altitude ancestry. The underlying lipid metabolic pathway traits responsible for sustaining maximal thermogenic demand in deer mice is currently unknown. The objective of this study was to characterize key steps in the lipid oxidation pathway in highland and lowland deer mice acclimated to control (23^{o}C, 21kPa O_2) or cold hypoxic (5^{o}C, 12kPa O_2) conditions. We hypothesized that capacities for lipid delivery and tissue uptake will be greater in highlanders and further increase with cold hypoxia acclimation. With the transition from rest to hypoxic cold-induced $\dot{V}O_2max$, both highland and lowland deer mice showed increased plasma glycerol concentrations and fatty acid availability. Interestingly, acclimation to cold hypoxia led to increased plasma triglyceride concentrations at cold-induced $\dot{V}O_2max$, but only in highlanders. Highlanders also had significantly greater delivery rates of circulatory free fatty acids and triglycerides due to higher plasma flow rates at cold-induced $\dot{V}O_2max$. We found no population or acclimation differences in fatty acid translocase (FAT/CD36) abundance in the gastrocnemius or brown adipose tissue, suggesting that fatty acid uptake across membranes is not limiting during

thermogenesis. Our data indicate that circulatory lipid delivery plays a major role in supporting the high thermogenic rates observed in highland versus lowland deer mice.

3.2 INTRODUCTION

The constant cold of high altitude places a high demand for aerobic heat production on mammals living in these environments. Small highland native endotherms must also contend with the high rates of heat loss due to their unfavorably large surface area to volume ratios compared to larger species. To counteract the rapid heat loss to the cold high alpine conditions and remain active, these small endotherms must elevate heat production in the face of low environmental oxygen levels. Indeed, field metabolic rates determined for wild highland deer mice (*Peromyscus maniculatus*; Wagner 1845) were higher than those living at low altitude, even during the summer months (Hayes, 1989).

An elevated cold-induced maximal oxygen consumption in hypoxia (hypoxic cold-induced $\dot{V}O_2max$, thermogenic capacity) has been associated with increased survival in deer mice living at high altitude (Hayes and O'Connor, 1999). This likely explains why highland deer mice have higher hypoxic cold-induced $\dot{V}O_2max$ than lowland deer mice (Cheviron *et al.*, 2012). The higher thermogenic capacity observed in highland deer mice is supported by an increased capacity for O_2 delivery to thermo-effector tissues (Tate *et al.*, 2017; Tate *et al.*, 2020). These higher rates of O_2 delivery support higher rates of substrate oxidation, with lipids being the principal fuel for thermogenesis in these mice (Cheviron *et al.*, 2012; Lyons *et al.*, 2021). Indeed, the rates of lipid oxidation during peak thermogenesis in highland deer mice are higher than during exercise (Lau *et al.*, 2017) and the highest observed for mammals (Lyons *et al.*, 2021). However, the

underlying mechanisms that allow for these high rates of lipid oxidation to support heat production are currently unclear.

In eutherian mammals such as deer mice, facultative thermogenesis occurs by two main metabolic processes, shivering thermogenesis and non-shivering thermogenesis (NST). Higher hypoxic cold-induced $\dot{V}O_2max$ in highland versus lowland deer mice are the result of higher rates of both shivering and NST (Robertson and McClelland, 2019; Coulson *et al.,* 2021) and increases in thermogenic capacity are accompanied by increases in lipid oxidation (Lyons *et al.,* 2021). Moreover, only highlanders demonstrate higher rates of NST in response to the chronic cold hypoxia experienced at high altitude (Velotta *et al.,* 2016; Coulson et al., 2021), suggesting that the capacity for substrate oxidation is also affected by chronic cold hypoxia. The prolonged need for heat production can be maintained using the relative large lipid stores in mammals (Weber, 2011), and highland mice tend to have higher body fat compared to lowlanders (Robertson and McClelland, 2021). Indeed, the more limited carbohydrate stores would likely be depleted in only ~15 - 20min, even at metabolic rates for moderate thermogenesis (McClelland *et al.,* 2017). Interestingly, despite their abundance, lipid use is limited during locomotion and rates of fatty acid oxidation plateau at moderate intensities of aerobic exercise in mammals (Schippers *et al.,* 2014; Lau *et al.,* 2017). Therefore, the high rates of lipid use for thermogenesis compared to exercise would require deer mice to further increase lipid availability to thermo-effector tissues for oxidation.

The pathway for lipid use is a complex multistep process that can be regulated at many pathway steps, from mobilization from storage depots to oxidation in working

tissues. Thermo-effector tissues can rely on lipids delivered by the circulation from extracellular supplies, mainly stored as triglycerides in white adipose tissue (WAT) and circulating triglycerides (TGs), or these tissues can use their intracellular supplies, stored as triglyceride-rich lipid droplets in skeletal muscle and brown adipose tissue (BAT). Circulatory delivery of non-esterified fatty acids (NEFAs) depends on plasma NEFA concentration and the rate of plasma flow to working tissues (plasma flow = $cardiac\ output\ \times\ (1 - hematocrit)$) (McClelland *et al.*, 1994). Uptake into working muscle and BAT is facilitated by membrane transport through the fatty acid translocase (FAT/ CD36), and then through the cytosol by fatty acid binding proteins (FABP) (reviewed in McClelland, 2004). Indeed, the capacity for circulatory and membrane transport has been shown to correlate with organismal and/or tissue oxidative capacity in mice and other mammals (McClelland *et al.*, 1994; Bonen *et al.*, 2000; Bradley *et al.*, 2012; Templeman *et al.*, 2012). Tissue capacity for oxidation of delivered NEFA depends on mitochondrial volume density and the capacity of mitochondria for ß-oxidation of fatty acids. In muscle, fatty acids are transported into mitochondria to provide ATP to power shivering, while in BAT, fatty acids activate uncoupling protein 1 (UCP-1) and provide substrate for powering the futile cycling mechanisms involved with non-shivering thermogenesis. Some, or all, of these steps may be a target of selection for increased lipid use to support enhanced rates of thermogenesis in highland deer mice. Different steps may also respond to cold hypoxia acclimation to alter pathway flux at high altitude.

The objective of this study was to examine key steps of the lipid metabolic pathway that may contribute to the higher thermogenic capacity in hypoxia of highland deer mice

compared to their lowland counterparts. We compared first generation laboratory born and raised highland and lowland deer mice acclimated to warm normoxic conditions or to cold hypoxic conditions simulating high altitude. We hypothesize that the differences in lipid oxidation rates during hypoxic cold-induced $\dot{V}O_2max$ between highland and lowland deer mice are due, in part, to differences in the capacity for mobilization, circulatory delivery and uptake of fatty acids into thermo-effector tissues. We further hypothesize that acclimation to cold hypoxic conditions increases the capacity of the lipid pathway to deliver, uptake and oxidize fatty acids in thermo-effector tissues in highland deer mice.

3.3 METHODS

Animals and acclimation groups

Wild-caught highland native (HA) deer mice (*Peromyscus maniculatus rufinus*) were trapped at high altitude at the summit of Mount Evans CO (4,350m a.s.l.) while lowland native (LA) deer mice (*Peromyscus maniculatus nebracensis*) were trapped at low altitude in Nine-mile Prairie, NE, USA (320m a.s.l.). Wild mice were transferred to McMaster University (90m a.s.l.) and housed in common laboratory conditions at ~23^{o}C, a 12:12h light:dark cycle, with food and water *ad libitum*. Mice were bred within their respective population to produce first generation laboratory-born and raised mice. Mice used in this study were a mix of both males and females of at least 6 months of age and highland and lowland individuals were randomly assigned to one of two acclimation groups, warm normoxia (WN, 23^{o}C and 760mmHg) or cold hypoxia (CH, 5^{o}C and 480mmHg), using hypobaric chambers (McClelland *et al.*, 1998; Lyons *et al.*, 2021) in a

climate-controlled room, simulating an altitude of ~4300m. For acclimation to CH, deer mice were first housed at 5^{o}C for 24 hours at normobaria before being placed in hypobaric chambers. Mice in cold hypoxia were returned to normobaria in cold for a brief period (less than 1 hour per week) for cage cleaning and replenishing food and water. All procedures were approved by the McMaster University Animal Research Ethics Board in accordance with guidelines set by the Canadian Council on Animal Care.

Mouse Tissue Sampling

Tissues were sampled under one of two conditions: at rest or immediately after mice had reached hypoxic cold-induced $\dot{V}O_2max$. To sample in resting conditions, deer mice were placed into a ~600 ml respirometry chamber at their acclimation temperature and allowed to settle for ~30 minutes undisturbed as outside air was pushed into the chamber at 600 ml min^{-1} using a mass-flow controller (Sable Systems, Las Vegas, NV, USA). After this adjustment period, 5% isoflurane was flowed into the chamber at 600 ml min^{-1} until the mouse was unconscious, then removed from the chamber for cervical dislocation and decapitation. Mice were also sampled immediately after an hypoxic cold-induced $\dot{V}O_2max$ trial (conditions described in Lyons *et al.*, 2021), In brief, hypoxic cold-induced $\dot{V}O_2max$ was determined by pushing heliox (12% O_2, 88% He) at 1000 ml min^{-1} using mass flow meters and controllers (Sierra Instruments, Monterey, CA; MFC-4, Sable Systems, NV) through copper coils housed inside a temperature control cabinet and into a respirometry chamber (~500 ml) cooled to -10^{o}C. Mice were exposed for ~15 min until it was determined $\dot{V}O_2max$ was achieved as previously described (Lyons *et al.*, 2021)

before being euthanized by introducing 5% isoflurane into the chamber, followed by cervical dislocation and decapitation for blood and tissue collection.

Blood samples were centrifuged at 10,000 × g to separate plasma from erythrocytes and other blood cells. Plasma was quickly frozen in liquid nitrogen and then stored at -80^{o}C until analysis. Other tissues were sampled within 5 minutes of euthanasia in the following order, right gastrocnemius, right soleus, interscapular BAT (iBAT), right inguinal white adipose tissue (ingWAT), left ingWAT, and left gastrocnemius. The right gastrocnemius, right soleus and right ingWAT of mice sampled at rest were set aside for experiments described below. The rest of the tissues were quickly frozen between two aluminum plates cooled in liquid nitrogen and then stored at -80^{o}C until future measurements.

White Adipose Tissue Lipolytic Capacity

Lipolytic rate of WAT was assessed *in vitro* using methods reported previously (Price *et al.,* 2008; Price *et al.,* 2013) with some modifications. Briefly, fresh ingWAT was divided in two equal pieces, both were individually weighed, and then added to separate beakers containing 20 µl mg^{-1} of Krebs Ringer buffer (in mM: 119.78 NaCl, 15 $NaHCO_3$, 9.99 D-glucose, 4.56 KCl, 2.5 $CaCl_2$ dihydrate, 1.5 sodium phosphate monobasic, 0.70 sodium phosphate dibasic, 0.49 $MgCl_2$, and 4% w/v bovine serum albumin, pH 7.4) kept at 37^{o}C. The tissue was minced with scissors and then the contents of each beaker was transferred to a separate 20 ml glass vial. In one vial norepinephrine (Millipore Sigma, St. Louis, MO) was added to a final concentration of 1 µM (Raclot and

Groscolas, 1993), the other vial received no norepinephrine and acted as an unstimulated control. Both control and norepinephrine treated vials were incubated at 37^{o}C in a shaking water bath for 90min. At the end of the incubation, the solutions were passed through glass microfibre filters (VWR, West Chester, PA, USA) and the filtrate was stored at -80^{o}C for later determination of glycerol concentration. Glycerol concentration was measured using a serum triglyceride determination kit (Sigma-Aldrich, St. Louis) according to the instructions provided by the company. Briefly, 10µl of each filtrate was mixed with 250µl of glycerol free reagent and absorbance was determined at 540nm using a Spectromax Plus 384, 96-well microplate reader (Molecular Devices, Sunnyvale, CA).

Plasma Glycerol, Triglycerides and Fatty Acids

Concentrations of plasma glycerol and triglycerides were assessed using a triglyceride quantification assay kit (Sigma-Aldrich). Non-esterified fatty acid concentrations were determined by gas chromatography as previously described for deer mice (Lyons et al., 2021).

Sample Preparation for Western Blotting and ELISA

The protein expression of FAT/CD36 and FABP were determined using gastrocnemius muscle cytosolic and sarcolemmal fractions prepared as previously described (Templeman et al., 2012) with some minor modifications. Frozen tissue

samples were powdered using a liquid N_2 cooled mortar and pestle and ~70 mg of tissue was homogenized using a glass-on-glass homogenizer in buffer (5µl mg^{-1} tissue) containing (in mM): 30 HEPES, 210 sucrose, 2 EGTA, 40 NaCl, and protease inhibitor cocktail (0.75 × volume). The homogenate was then centrifuged at 600 × g for 10 min at 4°C, and the resulting supernatant was centrifuged at 10 000 × g for 20 min at 4°C. The resultant supernatant was diluted (0.75 × volume) with a buffer containing 1.167 M KCl and 58.3 mM Na_4PPi at pH 7.4 and centrifuged at 230,000 × g for 2 hours at 4°C. The supernatant was collected as the cytosolic fraction and stored at -80°C, while the resulting pellet was resuspended in a buffer containing 10 mM Tris-HCl and 1 mM EDTA, at pH 7.4. This suspension was combined with 16% SDS (0.33 × volume) and centrifuged at 1100 × g for 20 min at room temperature, with the resulting supernatant collected as the sarcolemmal fraction and stored at -80°C.

Tissue expression of FAT/CD36

Western blotting was used to measure protein abundance of FAT/CD36 in whole tissue homogenates of gastrocnemius muscle and iBAT, as well as the sarcolemmal fraction of the gastrocnemius from deer mice sampled immediately after hypoxic cold-induced $\dot{V}O_2max$. In brief, frozen gastrocnemius and BAT samples were powdered under liquid N_2 as described above and homogenized in ice-cold RIPA buffer (in mM: 150 NaCl, 50 Tris-HCl, 1% Triton X-100, 0.5% deoxycholic acid, 0.1% SDS, pH 8.0). Total homogenate protein concentrations were quantified using Bradford assay (Bio-Rad Laboratories Ltd, Mississauga, ON). To avoid interference of SDS in protein

quantification, sarcolemmal fraction protein was quantified using BCA assay (Thermo Fisher Scientific, Waltham, MA, USA). A total of 40 μg for gastrocnemius, 20 μg for BAT protein and 30 μg for gastrocnemius sarcolemmal fraction proteins were denatured by heating to 95^{o}C for 5 minutes in Laemmli sample buffer (Bio-Rad) with β-mercaptoethanol. Proteins were separated on 12% SDS PAGE gels and then transferred to a PVDF membrane using the Transblot Turbo Transfer System (Bio-Rad). Membranes were incubated overnight at 4^{o}C with 5% skimmed milk in 1× phosphate buffered saline, 0.1% Tween. On the following day, membranes were probed with primary antibody against FAT/CD36 (CD36 Polyclonal Antibody, Invitrogen, PA-16813) at a dilution of 1:500 for 1 hour at room temperature, followed by an incubation with HRP-conjugated secondary antibody (goat anti-rabbit, Invitrogen, cat. # 31466) at dilution of 1:5000 for 1 hour at room temperature. Band densities were detected by chemiluminescence and normalized to total lane protein determined using Coomassie blue. Images were taken and analyzed using a ChemiDoc MP Imaging System (Bio-Rad) and the Image Lab software package (Bio-Rad), respectively (Lui et al., 2015).

Fatty Acid Binding Protein

Concentration of H-FABP in the cytosolic fractions of gastrocnemius muscles was quantified using an enzyme-linked immunosorbent assay (ELIZA), similar to methods described in Templeman et al., (2012). Equal concentrations of total cytosolic protein (0.015μg) were assayed for each sample, using a commercial H-FABP ELIZA kit for

mice (HK413; Hycult Biotech, Uden, Netherlands). H-FABP protein levels are expressed relative to total cytosolic protein content.

Intramuscular triglycerides

Intramuscular triglyceride (IMTG) concentration was determined in the gastrocnemius muscle as described previously (McClelland et al., 1999). Briefly, ~25-50 mg of powdered frozen muscle was weighed and placed in a glass tube containing 30 µL mg^{-1} of Folch (1:1 chloroform: methanol; Folch et al., 1957) and homogenized using a power homogenizer. Tubes were then shaken for 20 min, followed by a centrifugation at 1811 × g for 10 min at room temperature. The resulting supernatant was then transferred to a new glass tube, while the pellet was washed with 1 mL of Folch and centrifuged again at 1811 × g. The supernatants were then combined, followed by the addition of chloroform (0.5 × volume), bringing the ratio to 2:1 chloroform: methanol. Next, 26.8 mM KCl was added (0.25 × volume) and the mixture was centrifuged at 2500 rpm for 10 min at room temperature. The aqueous phase (top layer) was discarded, and 2 ml of ethanol was added to the organic phase (bottom layer). The mixture was then evaporated completely under N_2 gas at 40^{o}C and resuspended in 250 µl of isopropanol. IMTG concentration was then assessed using the triglyceride quantification assay kit (Sigma-Aldrich).

Enzyme apparent Vmax

We measured the apparent maximal activities (Vmax) of β-hydroxyacyl-CoA dehydrogenase (HOAD), citrate synthase (CS) and cytochrome c oxidase (COX) in the gastrocnemius. Activities of HOAD and COX were measured on fresh homogenates, while CS activity was measured after homogenates had been frozen and thawed three times. Approximately 30 mg of powdered tissue was homogenized on ice using a glass-on-glass homogenizer in 20 volumes of homogenizing buffer containing 100mM potassium phosphate (pH 7.2), 5 mM EDTA, and 0.1% Triton X-100. Assays were performed at 37^{o}C in triplicate, and controls for background activities were determined for each assay by omitting substrate. Assay conditions were as follows: *COX:* 0.1 mM of reduced cytochrome c (omitted in control) in 100 mM K_2HPO_4 (pH 7.0) at an absorbance of 550 nm. *HOAD:* 0.1 mM acetoacetyl-CoA (omitted in control), and 0.28 mM NADH in 100 mM triethanolamine·HCl (pH 7.0) at an absorbance of 340 nm. *CS*: 0.5 mM oxaloacetate (omitted in control), 0.22 mM acetyl-CoA, and 0.1 mM dithiobisnitrobenzoic acid (DTNB) in 40 mM Tris-HCl (pH 8.0) at an absorbance of 412 nm.

The Vmax of carnitine palmitoyltransferase (CPT) was measured on isolated mitochondria from freshly dissected gastrocnemius. Isolation of mitochondria from deer mouse muscle has been previously described in Mahalingam et al., (2020). Protein content was measured using a standard Bradford Assay (BioRad). Total CPT activity was measured at 412nm in the following assay conditions: 5 mM L-carnitine (omitted in control), 2 mM palmitoyl-CoA, and 0.2m DTNB in 100 mM K_2PO_4 (pH 7.2).

In vitro soleus fatty acid oxidation

The rate of fatty acid oxidation was measured in soleus muscle by tracking the metabolic fate of a radiolabelled fatty acid (Steinberg and Dyck, 2000). In brief, 309.5 mM of $NaHCO_3$ was gassed for 1 hour with 100% CO_2 and was then diluted (5.25 × volume) with modified Krebs Henseleit buffer (in mM: 148 NaCl, 5.94 KCl, 3.17 $CaCl_2$ • $2H_20$, 1.49 KH_2PO_4, and 1.49 $MgSO_4.7\ H_20$, containing 4% w/v fatty acid-free bovine serum albumin (Sigma), 2mM pyruvate and 0.5 mM palmitate, pH 7.4) and gassed (95% O_2, 5% CO_2) at 30ºC for 1 hour, creating the incubation buffer. The right soleus was removed fresh, weighed, and placed in a 20 ml vial containing 2 ml of incubation buffer for 20 min. The soleus was then transferred to second vial containing 2 ml of incubation buffer for another 20 min incubation. After the second preincubation, the soleus was transferred to a vial consisting of 0.4 µCi of [1-^{14}C]-palmitic acid (Amersham Biosciences, Baie d'Urfé, Quebec), and an open 0.8 ml microcentrifuge tube filled with 400 µl of benzethonium hydroxide was placed in the same vial, which was then sealed for 60 min. The soleus was then removed, followed by the addition of 1 ml of 1 M acetic acid to the vial and immediately capped. The acetic acid added to the vial released $^{14}CO_2$ from the buffer solution, which was collected in the benzethonium hydroxide of the microcentrifuge tube for 60 minutes. The benzethonium hydroxide was then transferred to a clean scintillation vial with 5 mL of scintillation fluid and the counts per minute (CPM) of ^{14}C were measured for 5 min using a Tricarb 2900 TR liquid scintillation analyzer using QuantaSmart 1.31 (Packard Instrument) analysis software.

Statistics

Statistics were performed using the lme4 package in R v.4.0.0 (https://www.r-project.org/). We used a 2-way analysis of variance (ANOVA) to assess the main effects of deer mouse population and acclimation environment, and to assess the main effects of population and condition (rest versus $\dot{V}O_2max$). We also used a 3-way ANOVA to assess the interactions between deer mouse populations, acclimations, and activity condition, where appropriate. Pairwise Holm-Sidak *post hoc* tests were performed to assess significant interactions. All data are presented as means ± s.e.m. A statistical significance value was set at $P<0.05$.

3.4 RESULTS

Fat lipolytic capacity and storage

Fat stores were assessed by quantifying the mass of ingWAT relative to body mass. Highland deer mice were heavier (body mass, $F_{1,27} = 15.10$, $P <0.001$) and had greater absolute amounts of ingWAT ($F_{1,27} = 8.90$, $P =0.01$) compared to lowland deer mice. When expressed relative to body mass, highlanders had 1.8-fold greater ingWAT per g body mass compared to lowland deer mice ($F_{1,27} = 8.28$, $P <0.01$). Cold hypoxia acclimation had no effect on body mass ($F_{1,27} = 2.67$, $P = 0.11$), ingWAT mass ($F_{1,27} = 1.28$, $P = 0.27$) or relative ingWAT abundance ($F_{1,27} = 0.51$, $P = 0.56$) in either population (Table 3.1).

The capacity for WAT to mobilize fatty acids was assessed by measuring the rate of glycerol release of ingWAT *in vitro*. When lipolysis was maximally stimulated by the addition of norepinephrine, there were no significant effects of either population ($F_{1,33}$ = 1.02, P=0.32) or acclimation ($F_{1,33}$ = 0.08, P = 0.78) on ingWAT lipolytic capacity (Fig. 3.1).

Lipid concentrations and circulatory transport rates

Plasma glycerol concentrations were determined as an index of whole-body lipolysis *in vivo*. Plasma glycerol concentrations were approximately 3-fold greater in deer mice after a maximal thermogenic challenge compared with levels in mice at rest ($F_{1,73}$ = 178.35, P<0.001), independent of acclimation condition ($F_{1,73}$ = 3.35, P=0.07). Furthermore, lowland deer mice had significantly greater plasma glycerol concentrations compared to highland deer mice in warm normoxia acclimation conditions (significant population effect; $F_{1,39}$ = 14.68, P<0.001). Cold hypoxia acclimation led to an increase in resting plasma glycerol concentrations in both populations ($F_{1,46}$ = 16.01, P<0.001) and in plasma glycerol concentrations at $\dot{V}O_2max$ ($F_{1,46}$ = 10.03, P=0.004), but no significant population differences were observed ($F_{1,34}$ = 0.35, P=0.56) (Fig. 3.2A).

To calculate rates of circulatory transport of plasma lipids we determined the concentrations of plasma NEFA and TGs at rest and immediately after hypoxic cold-induced $\dot{V}O_2max$. Overall, we found that plasma NEFA concentrations doubled from rest to cold-induced $\dot{V}O_2max$ ($F_{1,55}$ = 158.04, P<0.001). This occurred in both populations and regardless of acclimation conditions (Fig. 3.2B). This increase in total plasma NEFA was

the result of significant increases in all the individual fatty acids measured ($p<0.05$), apart from oleic acid, which did not show a significant increase from resting levels ($F_{1,55}$ = 3.62, P=0.062) (Table 3.2). In general, highlanders displayed higher concentrations of total NEFA compared to lowlanders ($F_{1,55}$ = 9.26, P=0.004) and there was a tendency for NEFAs to increase after cold hypoxia acclimation that approached statistical significance ($F_{1,55}$ = 3.77, P=0.057).

We also found that plasma TG concentrations were significantly higher in highland compared to lowland deer mice ($F_{1,74}$ = 12.70, P<0.001). Cold hypoxia acclimation increased circulating TG concentrations in both populations ($F_{1,74}$ = 4.08, P=0.047). Interestingly, lowland deer mice showed no change in plasma TG with the transition from rest to cold-induced $\dot{V}O_2$max, but cold hypoxia highland deer mice showed a doubling in plasma TG as energy demand increased (significant population × condition interaction; $F_{1,32}$ = 6.06, P=0.02) (Fig. 3.2C).

The rate of circulatory substrate delivery is the product of their concentration and rate of plasma flow (McClelland *et al.*, 1994). Thus, we determined rates of NEFA and TG circulatory delivery by calculating rates of plasma flow using published data for cardiac output and hematocrit during hypoxic cold-induced $\dot{V}O_2$max for deer mice in the same acclimation conditions (Tate *et al.*, 2020). Highland deer mice had significantly greater plasma flow rates compared to lowlanders ($F_{1,13}$ = 13.60, P=0.003) and cold hypoxia acclimation significantly increased plasma flow rates ($F_{1,13}$ = 13.14, P=0.003) during hypoxic cold-induced $\dot{V}O_2$max (Fig. 3.3A). This led to significantly greater rates of NEFA ($F_{1,13}$ = 17.53, P=0.001) and TG delivery ($F_{1,13}$ = 20.23, P <0.001) in highland deer

mice compared to lowlanders. Similar to the effect of acclimation on plasma flow, cold hypoxia significantly increased NEFA and TG delivery rates ($F_{1,13}$ = 14.21, P=0.002, $F_{1,13}$ = 40.49, P<0.001) during hypoxic cold-induced $\dot{V}O_2max$ (Fig. 3.3B & 3C). There was also a significant population × acclimation interaction, where cold hypoxia acclimation led to a doubling of NEFA delivery rates and tripling of TG delivery rates in highlanders but not lowlanders ($F_{1,13}$ = 5.54, P=0.035; $F_{1,13}$ = 18.00, P<0.001, respectively) (Fig. 3.3B & 3.3C).

Intramuscular triglycerides

The concentrations of IMTG in gastrocnemius muscle were not significantly different between populations ($F_{1,65}$ = 0.27, P=0.61) and did not change with acclimation ($F_{1,65}$ = 0.91, P=0.34). Interestingly, there were also no decline in gastrocnemius triglyceride content between rest and cold-induced $\dot{V}O_2max$ ($F_{1,65}$ = 2.53, P=0.12) (Fig. 3.4).

Fatty acid transport proteins

The capacity of thermo-effector tissue for fatty acid uptake was assessed by quantifying the total protein abundance of FAT/CD36 in both iBAT and the gastrocnemius. We found no significant effect of population ($F_{1,16}$ = 0.12, P=0.734) or acclimation ($F_{1,16}$ = 0.022, P=0.885) on the abundance of FAT/CD36 in iBAT (Fig. 3.5).

We also found FAT/CD36 expression in whole tissue homogenates of the gastrocnemius did not show any significant effect of population ($F_{1,19}$ = 0.042, P=0.841).

However, cold hypoxia acclimation led to a significant increased FAT/CD36 protein abundance ($F_{1,19}$ = 5.674, P=0.028) (Fig. 3.6A). When sarcolemmal-specific expression of this transporter was assessed in the gastrocnemius at $\dot{V}O_2max$, we found no significant effect of population ($F_{1,16}$ = 0.446, P=0.514) or acclimation ($F_{1,16}$ = 1.162, P=0.297) (Fig. 3.6B). Furthermore, there were no significant effects of population ($F_{1,17}$ = 1.18, P=0.29) or acclimation ($F_{1,17}$ = 0.001, P=0.97) on the abundance of the cytosolic H-FABP in gastrocnemius muscle (Fig. 3.6C).

Skeletal Muscle Enzyme Activity

To assess any differences in the capacity for aerobic metabolism and for fatty acid oxidation, we determined the apparent Vmax of specific enzymes in the gastrocnemius. CPT activity was measured as a marker for fatty acid uptake from the cytosol into the mitochondria. Total CPT activity did not differ between deer mouse populations ($F_{1,28}$ = 2.47, P=0.13) or with acclimation environments ($F_{1,28}$ = 1.05, P=0.32) (Fig. 3.7A). The activity of HOAD, a marker of β-oxidation, showed no differences between deer mouse populations ($F_{1,30}$ =0.57, P=0.46) or acclimation groups ($F_{1,30}$ =0.05, P=0.83) (Fig. 3.7B). In contrast, CS activity, a marker for mitochondrial volume, was significantly higher in highland deer mice compared to lowlanders ($F_{1,28}$ =5.66, P=0.02). However, acclimation had little effect on CS activity ($F_{1,28}$ =0.60, P=0.45) (Fig. 3.7C). COX activity, commonly used to assess mitochondrial quality, was significantly higher in cold hypoxia acclimated deer mice ($F_{1,30}$ =7.14, P=0.01); however, there were no significant population differences ($F_{1,30}$ =0.25, P=0.62) (Fig. 3.7D).

Results: Exogenous lipid oxidation

Intact solei were used to measure the rate of exogenous ^{14}C-palmitic acid oxidation. We observed no significant differences between population ($F_{1,29}$ =2.63, P=0.12) or acclimations ($F_{1,29}$ =0.57, P=0.46) (Fig. 3.S1).

3.5 DISCUSSION

The main objective of this study was to determine if capacities at key steps in the lipid metabolic pathway might explain population differences in maximal lipid oxidation observed at peak thermogenesis in highland and lowland deer mice. Moreover, we assessed whether these steps are modified with acclimation to cold hypoxia simulating the high-altitude environment. Rates of lipid oxidation increased when mice moved from resting to hypoxic cold-induced $\dot{V}O_2$max conditions. Both highland and lowland deer mice showed an increase in plasma glycerol and NEFA concentrations after hypoxic cold-induced $\dot{V}O_2$max, suggesting a significant stimulation of lipolysis and circulatory NEFA availability. Plasma NEFA concentrations were greater in highlanders than lowlanders at both rest and at hypoxic cold-induced $\dot{V}$O2max. These population differences may be supported by the greater mass-specific ingWAT depots in highlanders. However, in vitro lipolytic capacity of adipocytes from this depot were equivalent in both populations. Furthermore, plasma TGs were also greater in highlanders compared to lowlanders, both at rest and at $\dot{V}O_2$max, and regardless of acclimation condition. As a result, greater plasma flow rates in highlanders at $\dot{V}O_2$max resulted in circulatory NEFA and TG

delivery rates that were 3.1 and 7.3-fold greater than in lowlanders, respectively. In contrast, protein abundance of FAT/CD36 in both the gastrocnemius and iBAT did not differ between populations or with acclimation. These data suggest that higher circulatory delivery rates of NEFA and TG to the thermo-effector tissues are primarily responsible for the high rates of lipid oxidation necessary to support the superior hypoxic cold-induced $\dot{V}O_2max$ observed in highlanders.

Circulatory NEFA and TG availability is dependent on effective convective transport by the cardiovascular system. Circulatory transport of NEFAs is the product of their concentration and plasma flow (McClelland et al., 1994). Highland deer mice have higher plasma flow rates during hypoxic $\dot{V}O_2max$ than lowlanders (Fig. 3.3A) as the result of greater cardiac output and a blunted increase in hematocrit in response to cold hypoxia (Tate *et al.*, 2020). During thermogenic $\dot{V}O_2max$, most of the blood flow is likely directed to BAT and shivering muscle. This high plasma flow would allow highland deer mice to increase NEFA delivery to these thermo-effector tissues. It is possible that acclimation to cold hypoxia changes the relative proportions of blood flow to these tissues. Indeed, when warm acclimated rats are subjected to an acute cold challenge most blood is directed to muscle (Foster and Frydman, 1979), but after cold acclimation there is a redirection of blood flow to BAT (Foster and Frydman, 1979). It is unclear whether the same redistribution of blood flow would occur after cold hypoxia acclimation or with an acute hypoxic cold challenge.

Highland deer mice have larger mass-specific ingWAT depots than lowlanders (Table 3.1). Given the high energy density of lipids, greater fat stores may be

advantageous for sustained periods of heat production (Weber, 2011) and provide additional insulation (Wronska and Kmiec, 2012). However, we have previously found that highland and lowland deer mice have equivalent thermal conductance (Lyons *et al*, 2021), suggesting that population differences in ingWAT reflect altered energy storage and not insulation. The population differences in WAT depot size were also maintained after cold hypoxia acclimation, suggesting both populations matched food intake to the higher thermogenic demand of the acclimation conditions (Barnett, 1965). This is not the case when cold hypoxia occurred over the early development period, with lowlanders showing a large reduction in fat mass at weaning, while highland pups were able to maintain body composition in these conditions (Robertson and McClelland, 2021). These data suggest that developmental plasticity may have an important influence on the available lipid stores for adult deer mice and may affect thermogenic capacity and/or thermogenic endurance.

Although the size of lipid stores differed between populations, the tissue itself appeared to be phenotypically similar. When the lipolytic capacity of WAT was assessed *in vitro,* we found no differences in the maximal rates of glycerol release in response to norepinephrine stimulation (Fig. 3.1). However, *in vivo* conditions that stimulate WAT lipolysis and the appearance of NEFAs in the blood may differ between the populations. For example, the release of NEFAs into circulation from WAT is reliant on tissue blood flow and the availability of albumin binding sites (Scow and Chernick, 1970), which may differ between highland and lowland mice. We used circulatory glycerol as a marker for whole-body lipolysis, as glycerol liberated during lipolysis in WAT and skeletal muscle

generally appears in the circulation (Weber, 2011), since these tissues lack significant activity of glycerol kinase (Newsholme and Taylor, 1969). Indeed, plasma glycerol showed dynamic changes with the transition from rest to $\dot{V}O_2max$, which may indicate large increases in lipolysis when maximal aerobic heat production was stimulated (Fig. 3.2A). However, the highest plasma glycerol concentrations that we measured were similar between highland and lowland deer mice despite significant differences in whole-animal lipid oxidation (Lyons *et al.*, 2021). It is important to note that glycerol turnover and lipid oxidation are not always correlated in mammals (Weber *et al.*, 1993); however, we found that increases in plasma glycerol were associated with increases in plasma NEFAs in deer mice at $\dot{V}O_2max$, suggesting that the availability of circulatory NEFAs tracks changes in whole-animal lipid oxidation (Fig. 3.2A & 3.2B).

Changes in total plasma NEFA concentrations were likely not the result of differential kinetics in most of the individual fatty acids (Table 3.2), consistent with results reported for rats undergoing shivering thermogenesis (Vaillancourt et al., 2009). The exception was circulating levels of oleic acid, which remained unchanged as metabolic rate increased (Table 3.2). This suggests that either mobilization of oleic acid was not induced or release from WAT was matched with an equivalent uptake into heat producing tissues. Oleic acid is also predominately found in the sn-2 (middle) position in TG and is associated with re-esterification. (Karupaiah & Sundram, 2007). Our results may suggest a targeted re-esterification of oleic acid during increased cold exposure in deer mice. An increased availability of NEFA can occur through alterations in the NEFA-TG cycle, where NEFAs are preferentially directed towards oxidation rather than re-

esterification (McClelland *et al.,* 2001). This cycle has been observed to change during shivering in rats, where fatty acid re-esterification decreased from 79% to 35% with cold exposure to support the necessary increase in fatty acid oxidation (Vaillancourt *et al.,* 2009). In contrast, hypoxia acclimation has been found to increase the NEFA-TG cycle in lab rats at rest (McClelland *et al.,* 2001), and this accelerated cycling can contribute to thermogenesis by increasing the metabolic rate (Reidy and Weber, 2002). More work needs to be done to better understand how thermogenic demand and oxygen availability influence NEFA-TG cycling in heat production at high altitude.

Along with plasma NEFA, circulating TGs represent an additional large and often overlooked energy reserve available to support tissue metabolism (Moyes and West, 1995; Magnoni and Weber, 2007; Bartelt *et al.,* 2011). It is possible that circulating NEFAs are not sufficient to sustain the prolonged high rates of lipid oxidation for heat production in mice. However, delivery of NEFAs in the form of TGs could be used by highland deer mice to ensure rapid substrate supply in times of high energy demand. It has been proposed that circulatory TG may be used by migratory birds to support the extremely high rates of lipid oxidation during prolonged flight (Weber, 2009). The evidence surrounding this phenomenon is currently unclear, with support from research on small migratory passerines (Jenni-Eiermann & Jenni, 1992), but not robins (Gerson & Guglielmo, 2013). Nonetheless, our findings may suggest the high rates of TG circulatory delivery observed in highland deer mice at $\dot{V}O_2max$ (Fig. 3.2C, 3.3A & 3.3C) are used to help support the higher rates of lipid oxidation during thermogenesis compared to lowland deer mice (Lyons et al., 2021). The use of this energy reserve for heat production

has been shown to occur in thermoregulating mice where circulatory TG are cleared by both BAT (Bartelt *et al.,* 2011) and skeletal muscle (Jensen *et al.,* 2008). Mice with elevated lipoprotein lipase show an increase in thermal tolerance during a cold challenge, presumably because of an increased capacity for fat oxidation (Jensen *et al.,* 2008; Bartelt *et al.,* 2011). It is unknown whether lipoprotein lipase abundance or activity is greater in highlanders, enabling them to effectively utilize circulating TG to assist with fuelling thermogenesis.

We quantified the abundance of FAT/CD36 to determine if capacity for membrane NEFA transport could explain population differences in lipid oxidation at $\dot{V}O_2max$ (Lyons *et al.,* 2021). While gastrocnemius FAT/CD36 abundance did increase after cold hypoxia acclimation in both populations, there were no differences in FAT/CD36 abundance between the populations (Fig. 3.6A & 3.6B). Furthermore, gastrocnemius FABP content was also the same between highland and lowland deer mice (Fig. 3.6C). In another hindlimb muscle, the soleus also demonstrated no differences in exogenous lipid oxidation between populations or acclimations (Fig. 3.S1). These results suggest that the capacity for NEFA uptake in shivering muscle may not significantly contribute to population differences observed in whole-animal lipid oxidation during hypoxic cold-induced $\dot{V}O_2max$ (Lyons *et al.,* 2021). Additionally, we found that IMTG in the gastrocnemius did not change from rest to cold-induced $\dot{V}O_2max$ (Fig. 3.4). These data suggest that in deer mice the gastrocnemius primarily relies on circulatory NEFA to support oxidation during shivering thermogenesis. This higher lipid delivery and greater muscle capillarization (Lui *et al.,* 2015) may be sufficient to support shivering-induced

rates of lipid oxidation in the more aerobic gastrocnemii of highland deer mice (Lui *et al.*, 2015; Mahalingam *et al.*, 2017; 2020; Fig. 3.7C).

At $\dot{V}O_2max$, NST in BAT has been shown to account for over 50% of total $\dot{V}O_2$ in deer mice (Van Sant and Hammond, 2008). Highland deer mice have been observed to increase NST capacity after cold hypoxia acclimation compared to lowlanders (Coulson *et al.*, 2021). Interestingly, BAT size and mitochondrial density did not explain the increases in NST after cold hypoxia acclimation (Coulson *et al.*, 2021). We found that BAT expression of FAT/CD36 was not affected by cold hypoxia acclimation (Fig. 3.5), suggesting that BAT capacity for NEFA uptake from the circulation is not part of the plasticity response in NST. However, increased circulatory delivery rates of NEFAs and TGs to BAT may contribute to the increased lipid oxidation observed at the whole animal level. Additionally, use of intracellular TG in BAT may increase the upon cold challenge as previously observed in studies in both mice and humans (Blondin *et al.*, 2015; Labbé *et al.*, 2015; Blondin *et al.*, 2017).

3.6 CONCLUSIONS

The current study helps shed light on how the lipid metabolic pathway contributes to the elevated whole-animal lipid oxidation rates observed in highland deer mice during hypoxic cold-induced $\dot{V}O_2max$. Our results show that highland deer mice have much higher rates of NEFA and TG circulatory delivery compared to lowlanders, and cold hypoxia acclimation further increases these lipid delivery rates. Past work on humans has shown that at high exercise intensities, an increase in circulatory fat availability does not lead to increased muscle fat use (Hargreaves *et al.*, 1991). Although it is unclear if the

same is true for exercising deer mice, our data suggests that the limitations of muscle lipid uptake during exercise are circumvented during thermogenesis. This difference in fuel use between these two energetically taxing but distinct activities is probably due to differential recruitment of the metabolically active tissues involved. During thermogenesis BAT accounts for ~50% of total energy use, but skeletal muscle lipid use remains higher than those observed in deer mice during submaximal exercise (Lau *et al.*, 2017). This suggests that a larger muscle mass may be recruited during shivering compared to locomotion. Collectively, the muscles recruited for shivering use lipids at a high rate, but individually each shivering muscle may be operating at a metabolic rate that can be supported by circulating lipids, which may explain the high lipid oxidation rates observed in thermoregulating highland deer mice. In the future, determining the destination and uptake rate of circulating NEFA and TG into thermo-effector tissues during thermogenesis will help further elucidate how lipids are used during thermogenesis.

3.7 ACKNOWLEDGEMENTS

The authors would like to thank S. Coulson for technical assistance with enzyme assays, Dr. C. Robertson with western blots and dissections, C. West and O. Wearing with post summit tissue sampling, and Dr. E. Leonard with scintillation counting.

3.8 FIGURES AND TABLES

Table 3.1

Table 1. Body mass and inguinal white adipose tissue (ingWAT) mass of highland and lowland deer mice (*Peromyscus maniculatus*), acclimated to control warm normoxia (23°C, 21 kPa O_2) or cold hypoxia (5°C, 12 kPa O_2) conditions

	Highland		Lowland	
	Warm normoxia	Cold hypoxia	Warm normoxia	Cold hypoxia
Body mass (g)	22.6±1.1*	20.5±1.0*	20.5±2.8	16.2±0.7
IngWAT mass (mg)	245.1±52.0*	194.0±19.1*	113.4±14.6	67.7±8.0
IngWAT g^{-1} body mass ($\times 10^3$)	10.1±1.7*	9.6±0.9*	6.7±1.2	4.3±0.6

Values are presented as means±s.e.m. Respective sample sizes for warm normoxia and cold hypoxia were *N*=12 and *N*=9 for highlanders, and *N*=4 and *N*=6 for lowlanders. *Significant differences (P<0.05) resulting from Holm–Šídák *post hoc* tests compared with lowland deer mice within an acclimation condition.

Figure 3.1

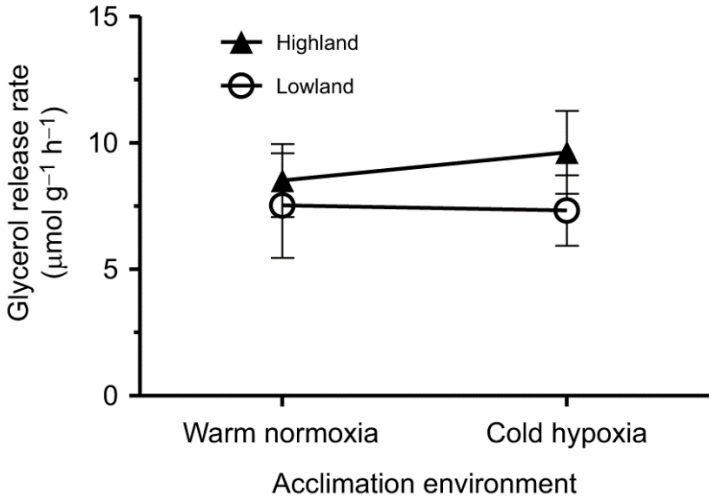
15
10
5
0
Highland
Lowland
Glycerol release rate
(μmol g⁻¹ h⁻¹)
Warm normoxia
Cold hypoxia
Acclimation environment

Figure 3.1. Rate of glycerol release from inguinal white adipose tissue (ingWAT) in first-generation laboratory born and raised highland and lowland deer mice (*Peromyscus maniculatus*). Deer mice were acclimated to control warm normoxia (23°C, 21 kPa O_2) or cold hypoxia (5°C, 12 kPa O_2) conditions. Excised ingWAT was stimulated with 1µM of norepinephrine and the rate of lipolysis was determined *in vitro* by measuring the rate of glycerol appearance into incubation medium (µmol g^{-1} hr^{-1}). Sample sizes for warm normoxia and cold hypoxia were *N*=9 and *N*=9 for highlanders, and *N*=9 and *N*=10 for lowlanders, respectively. Data are reported as means ± s.e.m.

Figure 3.2

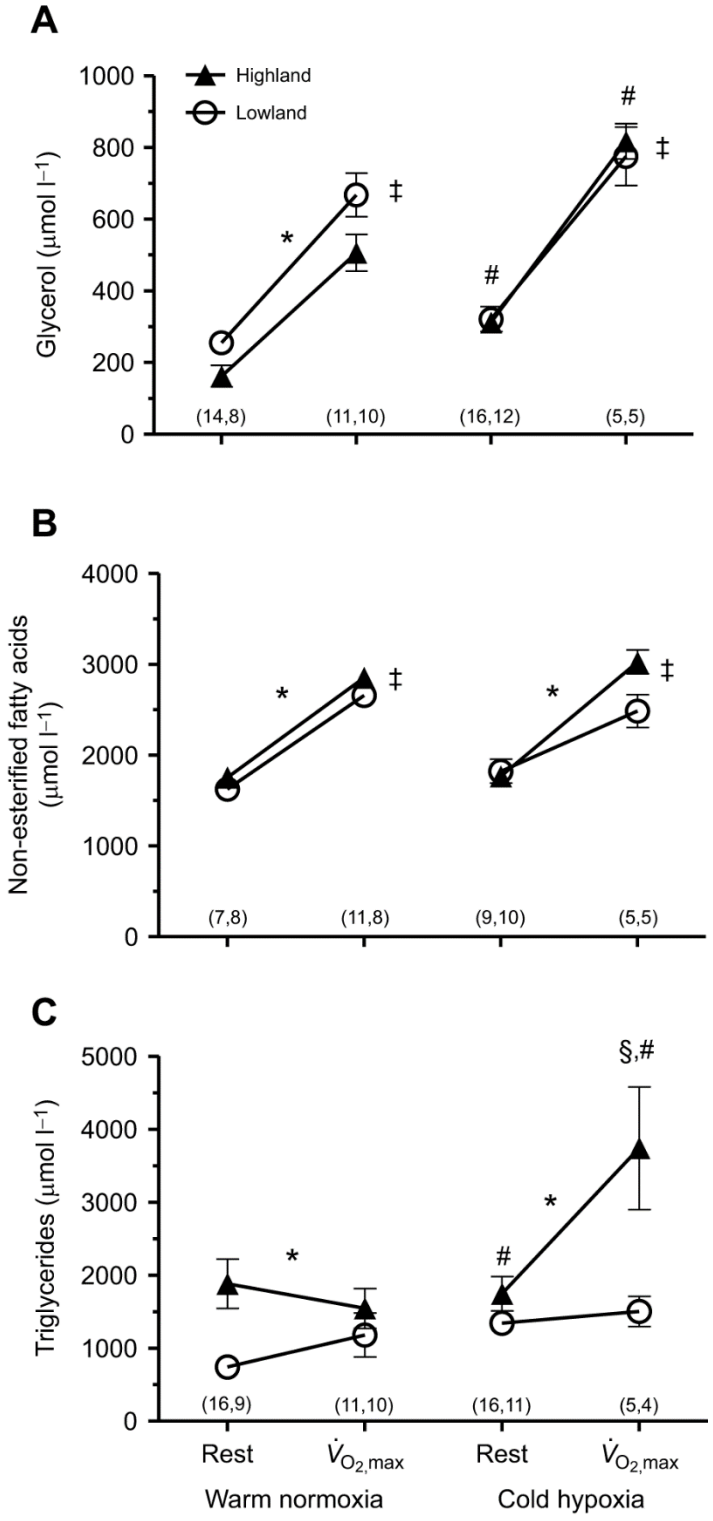
A
Highland
Lowland
Glycerol (μmol l–1)
1000
800
600
400
200
0
*
‡
#
#
‡
(14,8)
(11,10)
(16,12)
(5,5)
B
Non-esterified fatty acids (μmol l–1)
4000
3000
2000
1000
0
*
‡
*
‡
(7,8)
(11,8)
(9,10)
(5,5)
C
Triglycerides (μmol l–1)
5000
4000
3000
2000
1000
0
*
§,#
*
#
(16,9)
(11,10)
(16,11)
(5,4)
Rest
V̇O2,max
Rest
V̇O2,max
Warm normoxia
Cold hypoxia

Figure 3.2. Plasma concentrations of glycerol and lipids in highland and lowland deer mice. Concentration of glycerol (A), non-esterified fatty acids (NEFAs) (B) and triglycerides (TGs) (C) in first-generation laboratory born and raised highland and lowland deer mice (Peromyscus maniculatus), acclimated to control warm normoxia or cold hypoxia conditions, sampled at rest or at cold-induced $\dot{V}O_2max$. Symbols represent significant differences resulting from Holm–Sidak *post hoc* tests ($P<0.05$). ‡Significant difference between rest and cold-induced $\dot{V}O_2max$. *Significant difference between populations. #Significant difference between acclimations. §Cold hypoxia acclimated highland deer mice are significantly different from all other groups. Sample sizes of both deer mouse populations are shown in parentheses underneath symbols within a testing condition (highland, lowland). Data are reported as means ±s.e.m.

Table 3.2

Table 2. Concentrations of individual free fatty acids (μmol l^{-1}) of lowland deer mice (*P. maniculatus*), acclimated to control warm normoxia or cold hypoxia conditions, during rest and cold-induced $\dot{V}_{O_2,max}$

	Highland				Lowland			
	Warm normoxia		Cold hypoxia		Warm normoxia		Cold hypoxia	
	Rest	$\dot{V}_{O_2,max}$	Rest	$\dot{V}_{O_2,max}$	Rest	$\dot{V}_{O_2,max}$	Rest	$\dot{V}_{O_2,max}$
Palmitic acid (16:0)	459±20*	700±31‡,*	474±26	760.3±37.9‡	419±20	611±32‡	465±35	604±39‡
	(26.2±1.1%)	(24.6±1.1%)	(26.8±1.5%)	(25.1±1.3%)	(25.8±1.2%)	(23.0±1.2%)	(25.5±1.9%)	(24.3±1.6%)
Palmitoleic acid (16:1)	135±23*	178±20‡,*	150±22	191±28	181±33	253±30‡	172±24	196±23
	(7.7±1.3%)	(6.3±0.7%)	(8.5±1.2%)	(6.3±0.9%)	(11.1±2.0%)	(9.5±1.1%)	(9.4±1.3%)	(7.9±0.9%)
Stearic acid (18:0)	284±8*	475±19‡,*	283±10	447±22‡	266±13	384±21‡	277±20	392±27‡
	(16.2±0.5%)	(16.7±0.7%)	(16.0±0.6%)	(14.8±0.7%)	(16.4±0.8%)	(14.4±0.8%)	(15.2±1.1%)	(15.8±1.1%)
Elaidic acid (18:1n9t)	223±29*	351±19‡,*	195±16	401±24‡	171±21	331±24‡	218±22	287±33‡
	(12.7±1.7%)	(12.3±0.7%)	(11.0±0.9%)	(13.3±0.8%)	(10.5±1.3%)	(12.4±0.9%)	(11.9±1.2%)	(11.6±1.3%)
Oleic acid (18:1n9c)	110±11	106±7	121±9	110±15	148±28	117±17	148±22	98±13
	(6.3±0.6%)	(3.7±0.3%)	(6.9±0.5%)	(3.6±0.5%)	(9.1±1.7%)	(4.4±0.6%)	(8.1±1.2%)	(3.9±0.5%)
Linoleic acid (18:2)	542±23*	1041±56‡,*	545±31	1118±34‡	440±25	963±46‡	542±57	908±70‡
	(30.9±1.3%)	(36.5±2.0%)	(30.8±1.8%)	(36.9±1.1%)	(27.1±1.5%)	(36.2±1.7%)	(29.7±3.1%)	(36.5±2.8%)

Values (μmol l^{-1}) are presented as means±s.e.m. Percentage (%) of specific fatty acid to total NEFA is shown in parentheses underneath. In warm normoxia acclimation, sample sizes for rest and $\dot{V}_{O_2,max}$ were respectively *N*=7 and *N*=11 for highland deer mice, and *N*=8 and *N*=8 for lowland deer mice, while in cold hypoxia acclimation, sample sizes for rest and $\dot{V}_{O_2,max}$ were respectively *N*=9 and *N*=5 for highland deer mice, and *N*=10 and *N*=5 for lowland deer mice. Symbols representing significant differences result from Holm–Šídák *post hoc* tests ($P<0.05$).

‡Significantly different ($P<0.05$) from resting conditions, within acclimation.

*Significantly different ($P<0.05$) from lowland deer mice, within acclimation.

Figure 3.3

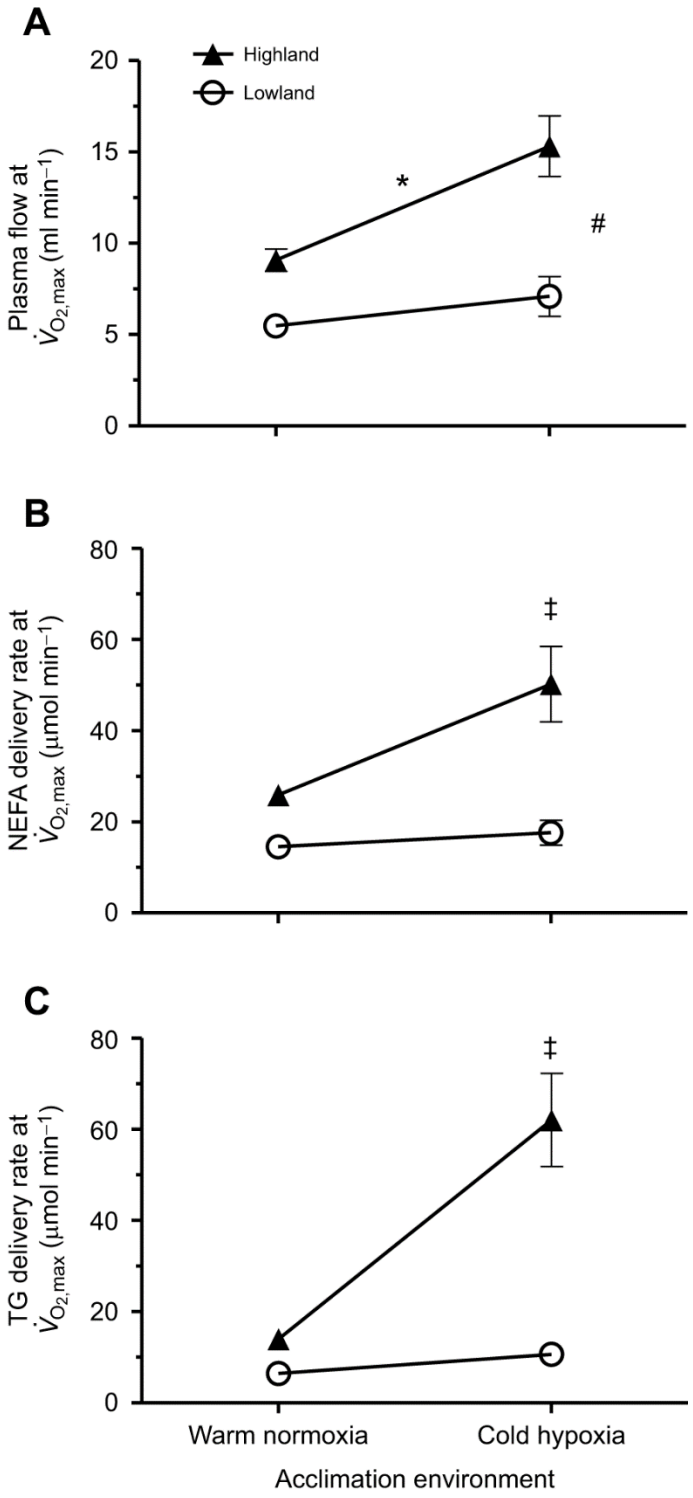
A
Highland
Lowland
Plasma flow at $\dot{V}_{O_2,max}$ (ml min^{-1})
20
15
10
5
0
*
#
B
NEFA delivery rate at $\dot{V}_{O_2,max}$ (µmol min^{-1})
80
60
40
20
0
‡
C
TG delivery rate at $\dot{V}_{O_2,max}$ (µmol min^{-1})
80
60
40
20
0
‡
Warm normoxia
Cold hypoxia
Acclimation environment

Figure 3.3. Plasma flow rate and delivery rate of fatty acids and triglycerides at cold-induced $\dot{V}O_2$max in hypoxia. Plasma flow rate (A), non-esterified fatty acid (NEFA) delivery rate (B) and triglyceride (TG) delivery rate (C) in highland and lowland deer mice acclimated to control warm normoxia or cold hypoxia conditions, sampled at cold-induced $\dot{V}O_2$max. Sample sizes for warm normoxia and cold hypoxia were *N*=7 and *N*=4 for highlanders, and *N*=3 and *N*=3 for lowlanders. Symbols represent significant differences resulting from Holm-Sidak *post hoc* tests (P <0.05). *Significant difference between populations. #Significant difference between acclimations. ‡Cold hypoxia acclimated highlanders are significantly different from all other treatment groups. Data are reported as means ± s.e.m. Plasma flow rates were calculated as $cadiac\ output \times (1 - hematocrit)$, using previously reported cardiac output and hematocrit for deer mice exposed to the same acclimation conditions (Tate *et al.*, 2017).

Figure 3.4

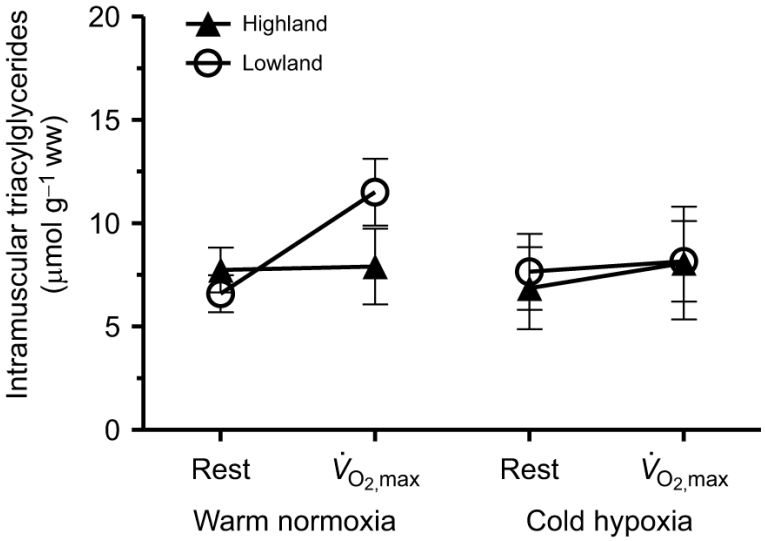
Highland
Lowland
Intramuscular triacylglycerides
(μmol g−1 ww)
20
15
10
5
0
Rest
V̇O2,max
Rest
V̇O2,max
Warm normoxia
Cold hypoxia

Figure 3.4. Intramuscular triglyceride concentration during rest and immediately after cold-induced $\dot{V}O_2max$. First-generation laboratory born and raised highland and lowland deer mice (*Peromyscus maniculatus*), acclimated to control warm normoxia (23°C, 21 kPa O_2) or cold hypoxia (5°C, 12 kPa O_2) conditions, sampled at rest or immediately after cold-induced $\dot{V}O_2max$. In warm normoxia acclimation, sample sizes for rest and $\dot{V}O_2max$ were respectively *N*=16 and *N*=10 for highlanders, and *N*=9 and *N*=9 for lowlanders, while in cold hypoxia acclimation, sample sizes for rest and $\dot{V}O_2max$ were respectively *N*=9 and *N*=5 for highlanders, and *N*=10 and *N*=5 for lowlanders. Values are presented as μmol of TG g^{-1} of gastrocnemius wet weight (w.w). Data are reported as means ± s.e.m.

Figure 3.5

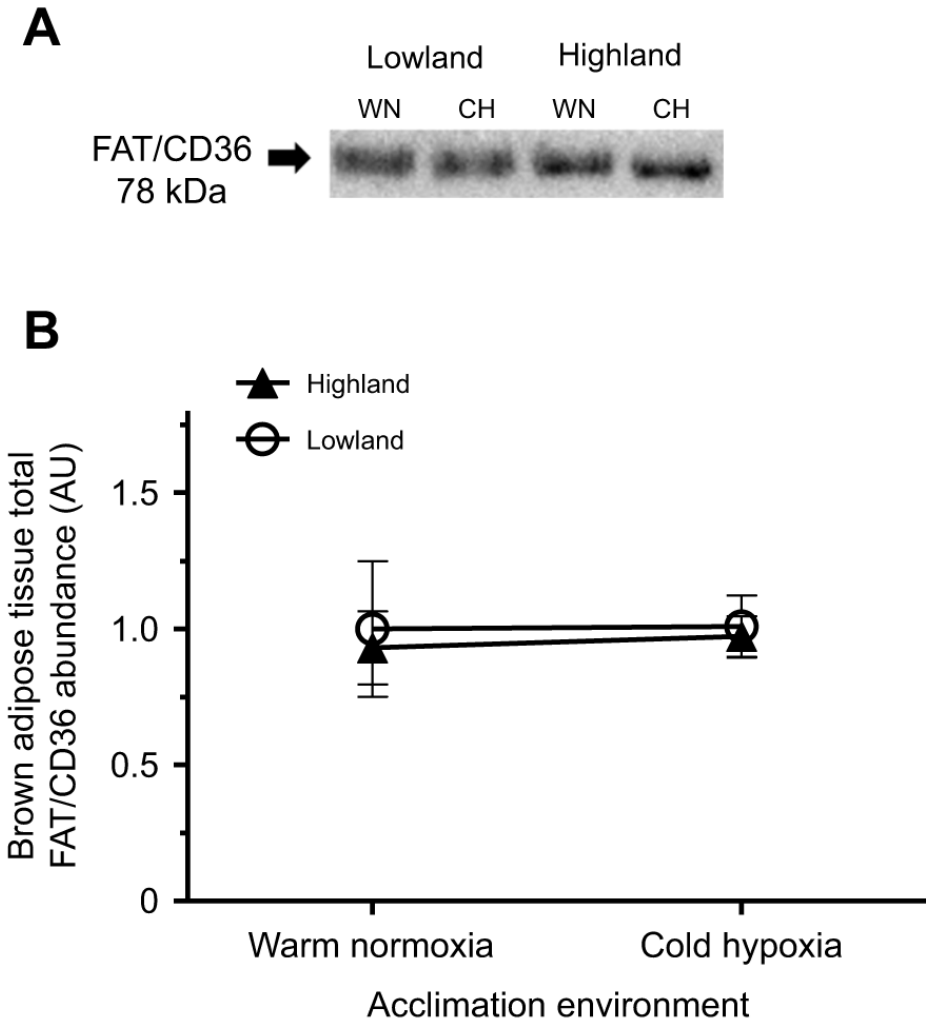
A
Lowland
Highland
WN
CH
WN
CH
FAT/CD36
78 kDa
B
Highland
Lowland
Brown adipose tissue total
FAT/CD36 abundance (AU)
1.5
1.0
0.5
0
Warm normoxia
Cold hypoxia
Acclimation environment

Figure 3.5. Relative protein abundance of fatty acid translocase (FAT/CD36) in brown adipose tissue. Representative western blot (A) and plotted protein abundance (B) of FAT/CD36. Sample sizes for warm normoxia (WN) and cold hypoxia (CH) were *N*=5 and *N*=4 for highlanders, and *N*=5 and *N*=6 for lowlanders. Data are reported as means ± s.e.m.

Figure 3.6

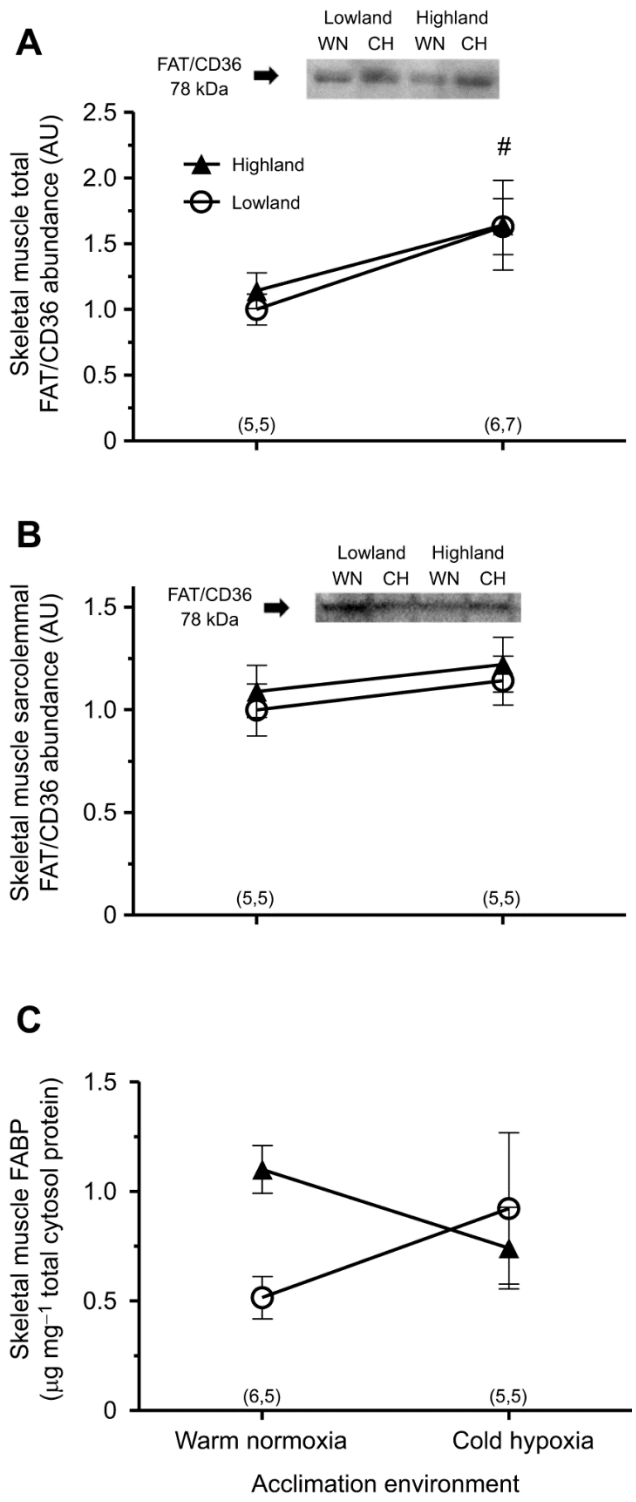
A
Lowland
Highland
WN CH WN CH
FAT/CD36
78 kDa
Skeletal muscle total
FAT/CD36 abundance (AU)
Highland
Lowland
#
2.5
2.0
1.5
1.0
0.5
0
(5,5)
(6,7)
B
Lowland
Highland
WN CH WN CH
FAT/CD36
78 kDa
Skeletal muscle sarcolemmal
FAT/CD36 abundance (AU)
1.5
1.0
0.5
0
(5,5)
(5,5)
C
Skeletal muscle FABP
(μg mg−1 total cytosol protein)
1.5
1.0
0.5
0
(6,5)
(5,5)
Warm normoxia
Cold hypoxia
Acclimation environment

Figure 3.6. FAT/CD36 and fatty acid binding protein (FABP) concentrations in skeletal muscle. (A) FAT/CD36 protein expression in skeletal muscle, (B) sarcolemmal fraction FAT/CD36 protein expression and (C) FABP concentration in the gastrocnemius of highland and lowland deer mice (*Peromyscus maniculatus*), acclimated to control warm normoxia (WN) or cold hypoxia (CH) conditions. Representative western blots are shown (A, B). Symbols represent significant differences resulting from Holm-Sidak *post hoc* tests ($P < 0.05$). #Significant difference between acclimations. Sample sizes of both deer mouse populations are shown in parentheses underneath symbols within an acclimation (highland, lowland). Data are reported as means ± s.e.m.

Figure 3.7

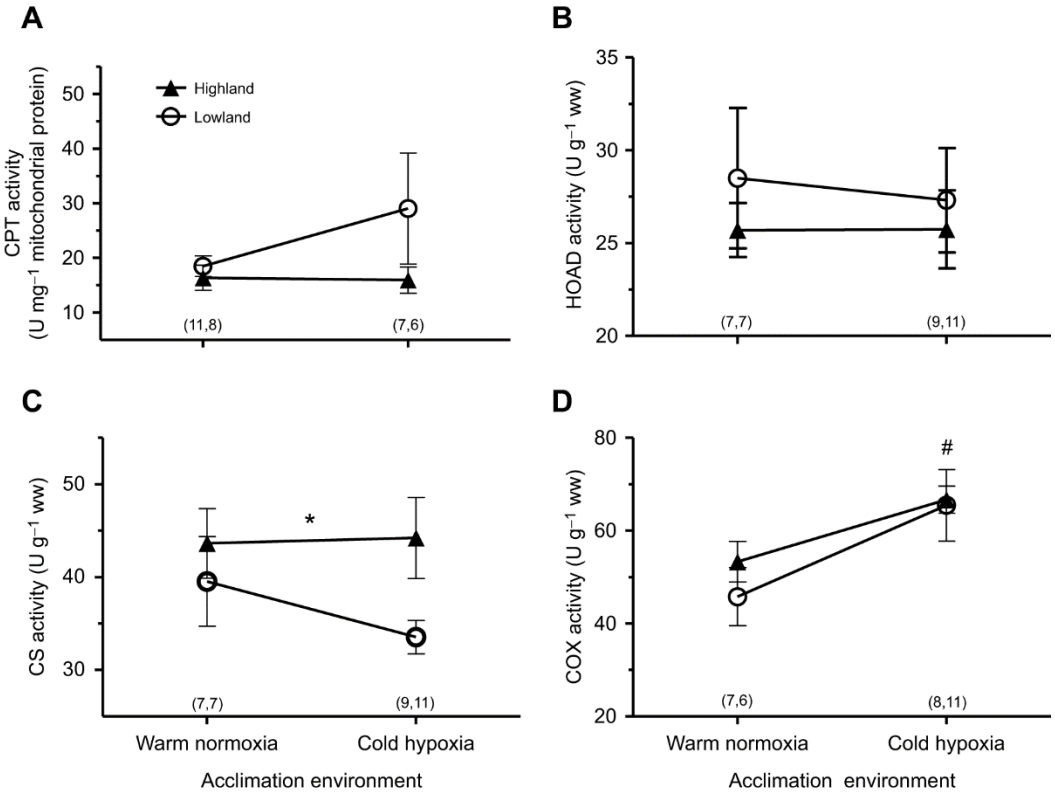
A
B
C
D
Highland
Lowland
CPT activity
(U mg−1 mitochondrial protein)
HOAD activity (U g−1 ww)
CS activity (U g−1 ww)
COX activity (U g−1 ww)
(11,8)
(7,6)
(7,7)
(9,11)
(8,11)
*
#
Warm normoxia
Cold hypoxia
Acclimation environment

Figure 3.7. Apparent maximal enzyme activities (Vmax) in isolated muscle mitochondria and in the gastrocnemius. Vmax of carnitine palmitoyl transferase (CPT) in isolated muscle mitochondria (A), and β-hydroxyacyl-CoA dehydrogenase (HOAD) (B), citrate synthase (CS) (C) and cytochrome c oxidase (COX) (D) in the gastrocnemius. CPT activity was standardized to mitochondrial protein, and HOAD, CS and COX activities were standardized to g^{-1} wet weight (ww). Symbols represent significant differences resulting from Holm–Sidak *post hoc* tests ($P<0.05$). *Significant difference between populations. #Significant difference between acclimations. Sample sizes of both deer mouse populations are shown in parentheses underneath symbols within an acclimation (highland, lowland). Data are reported as means ±s.e.m.

3.9 REFERENCES

Barnett, S. A. (1965). Adaptation of Mice To Cold. *Biol. Rev. Camb. Philos.* **40**, 5–51. doi: 10.1111/j.1469-185X.1965.tb00794.x.

Bartelt, A., Bruns, O.T., Reimer, R., Hohenberg, H., Ittrich, H., Peldschus, K., Kaul, M.G., Tromsdorf, U.I., Weller, H., Waurisch, C. and Eychmüller, A. (2011). Brown adipose tissue activity controls triglyceride clearance. *Nat. Med.* **17(2)**, 200–206. doi: 10.1038/nm.2297.

Blondin, D.P., Labbé, S.M., Noll, C., Kunach, M., Phoenix, S., Guérin, B., Turcotte, É.E., Haman, F., Richard, D. and Carpentier, A.C. (2015). Selective impairment of glucose but not fatty acid or oxidative metabolism in brown adipose tissue of subjects with type 2 diabetes. *Diabetes*, **64(7)**, 2388–2397. doi: 10.2337/db14-1651.

Blondin, D.P., Frisch, F., Phoenix, S., Guérin, B., Turcotte, É.E., Haman, F., Richard, D. and Carpentier, A.C. (2017). Inhibition of Intracellular Triglyceride Lipolysis Suppresses Cold-Induced Brown Adipose Tissue Metabolism and Increases Shivering in Humans. *Cell Metab.* **25(2)**, 438–447. doi: 10.1016/j.cmet.2016.12.005.

Bonen, A., Luiken, J. J., Arumugam, Y., Glatz, J. F., & Tandon, N. N. (2000). Acute regulation of fatty acid uptake involves the cellular redistribution of fatty acid translocase. *J. Biol. Chem.* **275(19)**, 14501-14508. doi: 10.1074/jbc.275.19.14501.

Bradley, N. S., Snook, L. A., Jain, S. S., Heigenhauser, G. J., Bonen, A., & Spriet, L. L. (2012). Acute endurance exercise increases plasma membrane fatty acid transport proteins in rat and human skeletal muscle. *Am. J. Physiol.-Endoc. M.* **302(2)**, E183–E189. doi: 10.1152/ajpendo.00254.2011.

Cheviron, Z. A., Bachman, G. C., Connaty, A. D., McClelland, G. B., & Storz, J. F. (2012). Regulatory changes contribute to the adaptive enhancement of thermogenic capacity in high-altitude deer mice. *P. Natl. A. Sci.* **109(22)**, 8635–8640. doi: 10.1073/pnas.1120523109.

Coulson, S. Z., Robertson, C. E., Mahalingam, S., & McClelland, G. B. (2021). Plasticity of non-shivering thermogenesis and brown adipose tissue in high-altitude deer mice. *J. Exp. Biol.* **224(10)**. doi: 10.1242/jeb.242279.

Folch, J., Lees, M. and Sloane Stanley, G. H. (1957). A simple method for the isolation and purification of total lipides from animal tissues. *J. Biol. Chem.* **226(1)**, 497–509. doi: 10.1016/s0021-9258(18)64849-5.

Foster, D. O. and Frydman, M. L. (1979). Tissue distribution of cold-induced thermogenesis in conscious warm- or cold-acclimated rats reevaluated from changes in tissue blood flow: The dominant role of brown adipose tissue in the replacement of shivering by nonshivering thermogenesis. *Can. J. Physiol. Pharm.* **57(3)**, 257–270. doi: 10.1139/y79-039.

Gerson, A. R., & Guglielmo, C. G. (2013). Energetics and metabolite profiles during early flight in American robins (*Turdus Migratorius*). *J. Comp. Physiol. B.* **183(7)**, 983-991. doi: 10.1007/s00360-013-0767-y.

Hargreaves, M., Kiens, B. and Richter, E. A. (1991). Effect of increased plasma free fatty acid concentration on muscle metabolism in exercising men. *J. Appl. Physiol.* **70(1)**, 194–201. doi: 10.1152/jappl.1991.70.1.194.

Hayes, J. P. (1989). Altitudinal and seasonal effects on aerobic metabolism of deer mice. *J. Comp. Physiol. B.* **159(4)**, 453–459. doi: 10.1007/BF00692417.

Hayes, J. P. and O'Connor C. S. (1999). Natural selection on thermogenic capacity of high-altitude deer mice. *Evolution*, **53**, 1280-1287. doi:10.2307/2640830

Jenni-Eiermann, S., & Jenni, L. (1992). High plasma triglyceride levels in small birds during migratory flight: a new pathway for fuel supply during endurance locomotion at very high mass-specific metabolic rates?. *Physiol. Zool.* **65(1)**, 112-123. doi: 10.1086/physzool.65.1.30158242

Jensen, D. R., Knaub, L. A., Konhilas, J. P., Leinwand, L. A., MacLean, P. S., & Eckel, R. H. (2008). Increased thermoregulation in cold-exposed transgenic mice overexpressing lipoprotein lipase in skeletal muscle: an avian phenotype?. *J. Lipid Res.* **49(4)**, 870–879. doi: 10.1194/jlr.M700519-JLR200.

Karupaiah, T., & Sundram, K. (2007). Effects of stereospecific positioning of fatty acids in triacylglycerol structures in native and randomized fats: a review of their nutritional implications. *Nutr. Metab.* **4(1)**, 1-17. https://doi.org/10.1186/1743-7075-4-16

Labbé, S. M., Caron, A., Bakan, I., Laplante, M., Carpentier, A. C., Lecomte, R., & Richard, D. (2015). In vivo measurement of energy substrate contribution to cold-induced brown adipose tissue thermogenesis. *FASEB J.* **29(5)**, 2046–2058. doi: 10.1096/fj.14-266247.

Lau, D.S., Connaty, A.D., Mahalingam, S., Wall, N., Cheviron, Z.A., Storz, J.F., Scott, G.R. and McClelland, G.B. (2017). Acclimation to hypoxia increases carbohydrate use during exercise in high-altitude deer mice. *Am. J. Physiol.-Reg. I.* **312(3)**, R400–R411. doi: 10.1152/ajpregu.00365.2016.

Lui, M. A., Mahalingam, S., Patel, P., Connaty, A. D., Ivy, C. M., Cheviron, Z. A., Storz, J. F., McClelland, G. B., & Scott, G. R. (2015). High-altitude ancestry and hypoxia acclimation have distinct effects on exercise capacity and muscle phenotype in deer mice. *Am. J. Physiol.-Reg. I.* **308(9)**, R779–R791. https://doi.org/10.1152/ajpregu.00362.2014

Lyons, S. A., Tate, K. B., Welch Jr, K. C., & McClelland, G. B. (2021). Lipid oxidation during thermogenesis in high-altitude deer mice (*Peromyscus maniculatus*). *Am. J. Physiol.-Reg. I.* **320(5)**, R735–R746. doi:

10.1152/ajpregu.00266.2020.

Magnoni, L. and Weber, J.-M. (2007). Endurance swimming activates trout lipoprotein lipase: plasma lipids as a fuel for muscle. *J. Exp. Biol.* **210(22)**, 4016–4023. doi: 10.1242/jeb.007708.

Mahalingam, S., Cheviron, Z. A., Storz, J. F., McClelland, G. B., & Scott, G. R. (2020). Chronic cold exposure induces mitochondrial plasticity in deer mice native to high altitudes. The *J. Physiol.* **598(23)**, 5411-5426.

Mahalingam, S., McClelland, G. B., & Scott, G. R. (2017). Evolved changes in the intracellular distribution and physiology of muscle mitochondria in high-altitude native deer mice. *J. Physiol.* **595(14)**, 4785-4801.

McClelland, G., Zwingelstein, G., Taylor, C.R., and Weber, J.M. (1994). Increased capacity for circulatory fatty acid transport in a highly aerobic mammal. *Am. J. Physiol.-Reg. I.* **266**, R1280-6. doi: 10.1152/ajpregu.1994.266.4.r1280.

McClelland, G. B. (2004). Fat to the fire: the regulation of lipid oxidation with exercise and environmental stress. *Comp. Biochem. Physiol. B.* **139**, 443-460. doi:10.1016/j.cbpc.2004.07.003

McClelland, G. B., Hochachka, P. W., Reidy, S. and Weber, J.-M. (2001). High altitude acclimation increases the triacylglycerol/fatty acid cycle at rest and during exercise. *Am. J. Physiol.-Endoc. M.* **281**, E537-E544. doi:10.1152/ajpendo.2001.281.3.E537

McClelland, G. B., Hochachka, P. W. and Weber, J.-M. (1998). Carbohydrate utilization during exercise after high-altitude acclimation: a new perspective. *Proc. Natl. Acad. Sci. USA* **95**, 10288-10293. doi:10.1073/pnas.95.17.10288

McClelland, G. B., Hochachka, P. W. and Weber, J. M. (1999). Effect of high-altitude acclimation on NEFA turnover and lipid utilization during exercise in rats. *Am. J. Physiol.* **277,** E1095-102. Available at: http://www.ncbi.nlm.nih.gov/pubmed/10600800.

McClelland, G. B., Lyons, S. A. and Robertson, C. E. (2017). Fuel use in mammals: Conserved patterns and evolved strategies for aerobic locomotion and thermogenesis. *Integr. Comp. Biol.* **57(2)**, 231–239. doi: 10.1093/icb/icx075.

Moyes, C. D. and West, T. G. (1995). *Exercise metabolism of fish*. In Metabolic Biochemistry, vol. 4, eds. P. W. Hochachka and T. P. Mommsen, pp. 368-392. Amsterdam: Elsevier Science.

Newsholme, E. A. and Taylor, K. (1969). Glycerol kinase activities in muscles from vertebrates and invertebrates. *Biochem. J.* **112(4)**, 465–474. doi: 10.1042/bj1120465.

Price, E.R., Armstrong, C., Guglielmo, C.G. and Staples, J.F. (2013). Selective

Mobilization of Saturated Fatty Acids in Isolated Adipocytes of Hibernating 13-Lined Ground Squirrels *Ictidomys tridecemlineatus. Physiol. Biochem. Zool.* **86(2)**, 205–212. doi: 10.1086/668892.

Price, E. R., Krokfors, A. and Guglielmo, C. G. (2008). Selective mobilization of fatty acids from adipose tissue in migratory birds. *J. Exp. Biol.* **211(1)**, 29–34. doi: 10.1242/jeb.009340.

Raclot, T. and Groscolas, R. (1993). Differential mobilization of white adipose tissue fatty acids according to chain length, unsaturation, and positional isomerism. *J. Lipid Res.* **34(9)**, pp. 1515–1526.

Reidy, S. P. and Weber, J. M. (2002). Accelerated substrate cycling: A new energy-wasting role for leptin in vivo. *Am. J. Physiol.- Endoc. M.* **282,** 312–317. doi: 10.1152/ajpendo.00037.2001.

Robertson, C. E. and McClelland, G. B. (2019). Developmental delay in shivering limits thermogenic capacity in juvenile high-altitude deer mice (*Peromyscus maniculatus*). *J. Exp. Biol.* **222(21)**. doi: 10.1242/jeb.210963.

Robertson, C. E. and McClelland, G. B. (2021). Ancestral and developmental cold alter brown adipose tissue function and adult thermal acclimation in Peromyscus. *J. Comp. Physiol. B.* **191(3)**, 589–601. doi: 10.1007/s00360-021-01355-z.

Van Sant, M. J. and Hammond, K. A. (2008). Contribution of Shivering and Nonshivering Thermogenesis to Thermogenic Capacity for the Deer Mouse (*Peromyscus maniculatus*). *Physiol. Biochem. Zool.* **81(5)**, 605–611. doi: 10.1086/588175.

Schippers, M. P., LeMoine, C. M. R. and McClelland, G. B. (2014). Patterns of fuel use during locomotion in mammals revisited: The importance of aerobic scope. *J. Exp. Biol.* **217(18)**, 3193–3196. doi: 10.1242/jeb.099432.

Scow, R. O., & Chernik, S. S. (1970). *Mobilization, transport and utilization of free fatty acids*. ln: *Comprehensive Biochemistry* (ed. M. Florkin and E. H. Stotz, pp.20-49. New York: Elsevier.

Steinberg, G. R. and Dyck, D. J. (2000). Development of leptin resistance in rat soleus muscle in response to high-fat diets. *Am. J. Physiol.- Endo. M.* **279,** 1374–1382. doi: 10.1152/ajpendo.2000.279.6.e1374.

Tate, K. B., Ivy, C. M., Velotta, J. P., Storz, J. F., McClelland, G. B., Cheviron, Z. A. and Scott, G. R. (2017). Circulatory mechanisms underlying adaptive increases in thermogenic capacity in high-altitude deer mice. *J. Exp. Biol.* **220**, 3616-3620. doi:10.1242/jeb.164491

Tate, K. B., Wearing, O. H., Ivy, C. M., Cheviron, Z. A., Storz, J. F., McClelland, G. B. and Scott, G. R. (2020). Coordinated changes across the O2 transport pathway

underlie adaptive increases in thermogenic capacity in high-altitude deer mice. *Proc. R. Soc. B.* **287**, 20192750. doi:10.1098/rspb.2019.2750

Templeman, N. M., Schutz, H., Garland Jr, T., & McClelland, G. B. (2012). Do mice bred selectively for high locomotor activity have a greater reliance on lipids to power submaximal aerobic exercise? *Am. J. Physiol. - Reg. I.* **303(1)**, R101–R111. doi: 10.1152/ajpregu.00511.2011.

Vaillancourt, E., Haman, F. and Weber, J. M. (2009). Fuel selection in Wistar rats exposed to cold: shivering thermogenesis diverts fatty acids from re-esterification to oxidation. *J. Physiol.* **587**, 4349-4359. doi:10.1113/jphysiol. 2009.175331

Velotta, J. P., Jones, J., Wolf, C. J., & Cheviron, Z. A. (2016). Transcriptomic plasticity in brown adipose tissue contributes to an enhanced capacity for nonshivering thermogenesis in deer mice. *Mol. Ecol.* **25(12)**, 2870–2886. doi: 10.1111/mec.13661.

Weber, J. M. (2009). The physiology of long-distance migration: Extending the limits of endurance metabolism. *J. Exp. Biol.* **212(5)**, 593–597. doi: 10.1242/jeb.015024.

Weber, J. M. (2011). Metabolic fuels: Regulating fluxes to select mix. *J. Exp. Biol.* **214(2)**, 286–294. doi: 10.1242/jeb.047050.

Weber, J. M., Roberts, T. J. and Taylor, C. R. (1993). Mismatch between lipid mobilization and oxidation: Glycerol kinetics in running African goats. *Am. J. Physiol. - Reg. I.* **264**, pp. 0–6. doi: 10.1152/ajpregu.1993.264.4.r797.

Wronska, A. and Kmiec, Z. (2012). Structural and biochemical characteristics of various white adipose tissue depots. *Acta Physiol.* **205(2)**, 194–208. doi: 10.1111/j.1748-1716.2012.02409.x.

CHAPTER 4: HIGHLAND DEER MICE REDIRECT TISSUE FATTY ACID UPTAKE TO SUPPORT THERMOGENESIS AFTER COLD HYPOXIA ACCLIMATION

4.1 ABSTRACT

During maximal cold challenge in hypoxia (hypoxic cold-induced $\dot{V}O_2max$), highland deer mice (*Peromyscus maniculatus*) have high rates of circulatory fatty acid delivery compared to lowland deer mice. Fatty acid delivery also increases in deer mice acclimated to conditions simulating montane environments. These high circulatory fatty acid delivery rates have been suggested to play a major role in supporting the high rates of thermogenesis observed in highland deer mice. However, the distribution of these fatty acids to the tissues involved in thermogenesis remains unknown. The goal of this study was to use [1-^{14}C]2-bromopalmitic acid to examine the uptake of circulating fatty acids into 24 different tissues during hypoxic cold-induced $\dot{V}O_2max$ in highland and lowland deer mice acclimated to thermoneutral (30°C, 21 kPa O_2) or cold hypoxic (5°C, 12 kPa O_2) conditions. We found that in highlanders, acclimation to cold hypoxia increased the relative uptake of fatty acids in brown adipose tissue (BAT), while decreasing fat uptake into skeletal muscle. Cold hypoxia acclimation increased BAT FAT/CD36 abundance in both deer mouse populations, but no differences were observed in muscle. Highland BAT also showed evidence of higher mitochondrial densities and capacities for beta-oxidation compared to lowlanders, particularly following cold hypoxia acclimation. Additionally, total muscle contributed to over 50% of the fatty acids taken up during maximal thermogenesis. This study provides insight on the tissues involved with the uptake of

circulating fatty acids during hypoxic cold-induced $\dot{V}O_2max$ and deepens our understanding on how high rates of lipid oxidation are supported in highland deer mice.

4.2 INTRODUCTION

Lipids are known to be the primary substrate for fuelling relatively low intense activities, such as moderate exercise, in humans and other mammals (26). Lipids are also the primary substrate used for thermogenesis in rodents, at both submaximal and peak rates of heat production (18, 31). The primary consumer of oxygen and substrates during exercise are the skeletal muscles (1), and as work intensities increase, their recruitment pattern tracks changes in substrate use from lipids to carbohydrates, at least for humans and some other mammals (15, 26). The situation is somewhat different during thermogenesis, as small eutherian mammals recruit both brown adipose tissue (BAT) and skeletal muscle for non-shivering (NST) and shivering (ST) forms of heat production. These thermo-effector tissues contribute to maximal cold-induced oxygen consumption ($\dot{V}O_2max$), supported by lipids as the principal substrate (18). In rodents, however, it is unclear which skeletal muscles participate in shivering and how substrates are partitioned between muscles and BAT during thermogenesis. It is also unclear if variation in substrate uptake by thermo-effector tissues, 1) exists between animals living in different thermal environments, or 2) occurs because of environmentally induced plasticity.

Deer mice (*Peromyscus maniculatus*) native to high-altitude environments have evolved a variety of mechanisms to overcome low temperatures and low partial pressures of oxygen. For example, highland native deer mice are capable of elevated rates of lipid oxidation to support high rates of heat production in hypoxia (18). These elevated rates of

lipid oxidation in highlanders have been attributed to higher rates of NST and a greater capacity for lipid transport (7, 17). Indeed, rates of circulatory delivery of free fatty acids was found to be approximately 3-fold greater in highland versus lowland deer mice during cold-induced $\dot{V}O_2max$ in hypoxia (17). However, it is unclear which tissues are taking up these fatty acids and how uptake is distributed among skeletal muscles and BAT. Previous work in rats has provided some insight elucidating tissue recruitment during thermogenesis. Increases in blood flow to skeletal muscle occurs in warm acclimated rats during an acute cold exposure, but after cold acclimation, blood flow gets shunted away from skeletal muscle and redirected towards BAT (8). An increase in blood flow to these tissues during cold exposure would highlight their increased metabolic activity, and presumably, the potential tissues for uptake of circulating fatty acids.

The contribution of individual tissues to thermogenesis can be estimated by determining the uptake of circulating fatty acids. This uptake reflects both tissue blood flow and metabolic rate and can give a more comprehensive picture of thermo-effector recruitment. The objective of this study was to quantify tissue uptake of circulatory free fatty acids to determine which tissues contribute to whole-animal lipid oxidation during peak thermogenesis in deer mice. We compared highland and lowland deer mice acclimated to either normoxic thermoneutral or cold hypoxia simulating high-altitude conditions. Tissue uptake of circulatory free fatty acids was determined using [1-^{14}C]2-bromopalmitic acid for 24 tissues, including central organs (liver, heart, and diaphragm), white adipose tissue (inguinal and gonadal), BAT (interscapular and auxiliary) and skeletal muscles of the forelimb, hindlimb and trunk. In certain tissues, fatty acid uptake

was compared to the protein abundance of membrane transporters and activities of metabolic enzymes. We hypothesized that in deer mice, variation in whole-animal lipid oxidation rates during thermogenesis is associated with the high rates of fatty acid uptake by thermo-effector tissues. As highland deer mice are known to increase NST with cold hypoxia acclimation (7), we predict a redistribution of fatty acid uptake from muscle to BAT after cold hypoxia acclimation while lowlanders will not show this change.

4.3 METHODS

Common Garden Experiment

All procedures were approved by the McMaster University Animal Research Ethics Board in accordance with guidelines set by the Canadian Council on Animal Care. Mice used in this study were part of an established breeding colony of highland (*P.m. rufinus*) and lowland (*P.m. nebracensis*) deer mice at McMaster University as previously described (16). Briefly, wild highland deer mice were trapped in Mount Evans, CO (4,350m a.s.l.) and lowland deer mice were trapped in Kearney, NE, USA (656m a.s.l.). Wild mice were transferred to McMaster University (90m a.s.l.) and housed in common laboratory conditions at ~23^{o}C, on a 12:12h light:dark cycle, with unlimited access to food and water. Mice were bred within their respective populations to produce second generation laboratory-born and raised mice. Mice in this study were at least 6 months of age, and a mix of both males and females. Highland and lowland deer mice were randomly assigned to one of two acclimation groups, thermoneutral (TN, 30^{o}C and 21kPa) using a temperature controlled rodent incubator (Powers Scientific Inc., PA) or cold hypoxia (CH, 5^{o}C and 12kPa, using hypobaric chambers (18, 20) in a climate-

controlled room, simulating high altitude (~4300m). Deer mice acclimated to CH were first housed at 5^{o}C for 24 hours at normobaria before being placed in hypobaric chambers. For routine cage cleaning and replenishment of food and water, CH deer mice were only returned to normobaria for less than 1 hour per week. All mice were kept in their respective acclimation conditions for six to eight weeks.

^{14}C-Bromopalmitic acid infusate preparation

Preparation of bromopalmitic acid infusate was modified from previous methods (Oakes *et al.*, 2006; Schönke *et al.*, 2018). On the day of the experiment, 10^7 DPM of [1-^{14}C]2-bromopalmitic acid organic stock solution (0.0045mCi, or 45ul of bromopalmitic acid stock, MC 451, Moravek Inc., CA) was dried under N_2 at room temperature in a glass test tube and reconstituted in 100ul of unlabeled infusate (saline containing 1.2% bovine serum albumin (Millipore Sigma, St Louis, MO, USA) and 0.15 mM palmitic acid (Sigma Alderich). The labelled infusate was then gently mixed in a 37^{o}C water bath for 1h.

^{14}C-Bromopalmitic acid injection and maximal cold challenge

To facilitate tail vein injection, tails of the deer mice were cleaned of hair 48h prior to trial. Mice were weighed and then were placed in a tail veiner restraint (Braintree Scientific, Inc., MA). Using a 27-gauge needle, 100ul of ^{14}C-bromopalmitate infusate (4.5µCi) was injected via the tail vein. Mice were then immediately exposed to maximal

cold challenge conditions for 12 minutes to determine cold-induced $\dot{V}O_2max$, as described in Lyons et al., (2021). In brief, hypoxic cold-induced $\dot{V}O_2max$ was determined by pushing heliox (12% O_2, 88% He) at 1000 ml min^{-1} through copper coils housed inside a temperature control cabinet and into a respirometry chamber (volume ~500 ml) cooled to -10^oC using mass flow meters and controllers (Sierra Instruments, Monterey, CA; MFC-4, Sable Systems, NV). Cold-induced $\dot{V}O_2max$ was determined as the highest 10 seconds of $\dot{V}O_2$ over the course of the entire trial. After 12 minutes in these conditions, mice were anesthetized using an isoflurane-soaked cotton ball. At exactly 15 min since the time of injection, mice were decapitated, blood and tissue were collected, flash frozen in liquid N_2, and stored at -80^oC until future processing. Tissues were dissected in the following order: soleus, red gastrocnemius, white gastrocnemius, tibialis anterior, extensor digitorum longus, rectus femoris, vastus lateralis, vastus medialis, semitendinosus, biceps femoris, gluteus, interscapular brown adipose tissue, erector spinae, trapezius, auxiliary brown adipose tissue, biceps, triceps, masseter, inguinal white adipose tissue, gonadal white adipose tissue, liver, diaphragm, right ventricle, and left ventricle.

Tissue Processing and Analysis

The processing of tissue for ^{14}C-activity was modified from methods used by Schonke et al., (2018). Frozen tissues were weighed and placed in a vial containing 1M NaOH (30µl mg^{-1} tissue), and briefly minced. The vial was then sealed and placed in a rotating water bath at 50^oC for 1.5 hours. After the tissue dissolved, an equivalent volume

of 1M HCl was added to the vial to neutralize the solution. Then, 200 µl of the dissolved tissue was placed in a glass scintillation vial containing 2 ml of scintillation fluid (Ecoscint A, National Diagnostics, GA). Counts per minute (CPM) of ^{14}C were measured for 5 min using a Tricarb 2900 TR liquid scintillation analyzer using QuantaSmart 1.31 (Packard Instrument) analysis software.

Enzyme apparent Vmax

We measured the apparent maximal activities (Vmax) of β-hydroxyacyl-CoA dehydrogenase (HOAD), citrate synthase (CS) and cytochrome c oxidase (COX) in the red gastrocnemius, white gastrocnemius, tibialis anterior, rectus femoris, erector spinae, and interscapular brown adipose tissue as described previously for deer mice (17). Activities of HOAD and COX were measured on fresh homogenates, while CS activity was measured after homogenates had been frozen and thawed two times. Approximately 30 mg of powdered tissue was homogenized on ice using a glass-on-glass homogenizer in buffer (20 µl mg^{-1} tissue) containing 100mM potassium phosphate (pH 7.2), 5 mM EDTA, and 0.1% Triton X-100. Assays were performed at 37^{o}C in triplicate, and controls for background activities were determined for each assay by omitting substrate. Assay conditions were the following: *COX:* 0.1 mM of reduced cytochrome c (omitted in control) in 100 mM K_2HPO_4 (pH 7.0) at an absorbance of 550 nm. *HOAD:* 0.1 mM acetoacetyl-CoA (omitted in control), and 0.28 mM NADH in 100 mM triethanolamine·HCl (pH 7.0) at an absorbance of 340 nm. *CS*: 0.5 mM oxaloacetate

(omitted in control), 0.22 mM acetyl-CoA, and 0.1 mM dithiobisnitrobenzoic acid (DTNB) in 40 mM Tris (pH 8.0) at an absorbance of 412 nm.

Western Blotting FAT/CD36

Fatty acid translocase CD36 (FAT/CD36) protein abundance in whole tissue homogenates of interscapular BAT (iBAT), erector spinae, red gastrocnemius and white gastrocnemius was determined using western blot analysis as previously described (17). Powdered tissue samples were homogenized using a motorized homogenizer in 25 volumes of ice-cold RIPA buffer (150 mM NaCl, 50 mM Tris·HCl, 1.0% Triton X-100, 0.5% deoxycholic acid, and 0.1% SDS, at pH 8.0). Total homogenate protein concentrations were quantified using Bradford assay (Bio-Rad Laboratories Ltd, Mississauga, ON). The protein isolates were diluted 1:1 in 2X Laemmli buffer (65.8 mM Tris-HCl, pH 6.8, 2.1% SDS, 26.3% (w/v) glycerol, 0.01% bromophenol blue, and 10% β-mercaptoethanol) and were denatured for 5 min at 95^{o}C. Denatured protein (20 μg for BAT and 40 μg for muscles) were separated on precast 12% sodium dodecyl sulfate-polyacrylamide gels (Bio-Rad) for 30 min at 100 V and then 45 min at 150V in a Mini-Protein Tetra System (Bio-Rad). Separated proteins were then transferred to polyvinylidene difluoride membranes (Bio-Rad) using the Transblot Turbo Transfer System (Bio-Rad) at 25 V for 7 min. Membranes were incubated overnight at 4°C with blocking buffer (5% skimmed milk in 1× phosphate buffered saline, 0.1% Tween). The following day, membranes were incubated with primary antibody against FAT/CD36 (CD36 polyclonal antibody, Invitrogen, PA-16813) at a dilution of 1:500 in blocking

buffer for 1 h at room temperature, followed by an incubation with HRP-conjugated secondary antibody (goat anti-rabbit, Invitrogen, cat. #31466) at dilution of 1:5000 in blocking buffer for 1 h at room temperature. Band densities were detected by chemiluminescence and normalized to total lane protein determined using Coomassie Blue. Images were taken and analyzed using a ChemiDoc MP Imaging System (Bio-Rad) and the Image Lab software package (Bio-Rad), respectively (16, 17).

Statistical analysis

We employed a 2-way analysis of variance (ANOVA) to assess the main effects of deer mouse population, acclimation condition, and their interaction. Pairwise Holm-Šídák *post hoc* tests were performed to evaluate significant interactions and we set the value for statistical significance to $P < 0.05$. Statistical analyses were performed using the lme4 package (https://CRAN.Rproject.org/package=lme4) in R v.4.2.0 (https://www.r-project.org/) and Prism software (version 5.01; GraphPad Software, San Diego, CA). All data are presented as means ± s.e.m.

4.4 RESULTS

Respiration at Thermogenic Capacity

Hypoxic cold-induced $\dot{V}O_2max$ was used to assess thermogenic capacity in lowland and highland deer mice acclimated to TN or CH conditions. Overall, we found that thermogenic capacity was 4-13% greater in highland deer mice compared to lowlanders (Figure 4.1A; significant effect of population, $F_{1,87} = 5.49$; $P = 0.02$), while CH

acclimation led to an increase in $\dot{V}O_2max$ of roughly 1.6-fold (significant effect of acclimation, $F_{1,87} = 153.0$; $P < 0.0001$). To help understand the possible population differences in substrate use at $\dot{V}O_2max$ and the influence of CH acclimation, we compared respiratory exchange ratios (RER). We found that RER at $\dot{V}O_2max$ ranged from 0.75-0.85, suggesting both populations relied principally on lipids as the main metabolic substrate. We found no significant differences between populations ($F_{1,85} = 1.52$; $P = 0.22$) or between acclimations ($F_{1,85} = 2.99$; $P = 0.09$). However, absolute whole-animal lipid oxidation rates showed a significant population × acclimation interaction ($F_{1,85} = 7.79$; $P = 0.007$), where only highlanders increased lipid oxidation rates by 2.7-fold following CH acclimation ($P < 0.05$). Furthermore, highlanders had lipid oxidation rates that were approximately 1.6-fold greater than lowlanders after CH acclimation ($P < 0.05$). In contrast, TN acclimated lowlanders and highlanders showed no differences in lipid oxidation rate ($P > 0.05$).

Fatty Acid Tissue Uptake during Thermogenesis

We used a radiolabelled tracer fatty acid (^{14}C-2-bromopalmitic acid) to determine fatty acid tissue uptake during a maximal cold challenge in deer mice. We determined tissue specific ^{14}C activity (CPM per mg tissue), total tissue ^{14}C activity (total CPM per g body weight), and relative ^{14}C uptake (% total activity of all sampled tissues) (Table 4.1 & 4.2, Figure 4.2). We found that specific ^{14}C activity significantly increased for both auxiliary and interscapular BAT depots and gonadal WAT following CH acclimation ($P < 0.05$), while those of the right and left ventricles, liver and diaphragm decreased

following CH acclimation in both deer mouse populations ($P < 0.05$). For the skeletal muscles, we found that in the soleus, specific activity was greater in lowlanders compared to highlanders ($P < 0.05$). White gastrocnemius specific activity in lowlanders was greater than highlanders, but only in TN acclimation conditions ($P < 0.05$). In CH conditions, white gastrocnemius specific activity was greater compared to TN conditions, but only for highland deer mice ($P < 0.05$). Specific activity of the tibialis anterior showed a unique interaction, where in TN conditions, lowlanders were greater than highlanders, but the opposite was observed in CH conditions ($P < 0.05$). Thus, in the tibialis anterior, specific activity increased with CH acclimation compared to TN for highlanders but decreased for lowlanders ($P < 0.05$). Specific activity of the masseter was observed to decrease with CH acclimation, but only in lowland deer mice ($P < 0.05$). No other skeletal muscles or tissues demonstrated an effect of population or acclimation for tissue specific activity ($P > 0.05$). In general, total ^{14}C tissue activity was greater in both BAT depots and the erector spinae of lowlanders compared to highlanders ($P < 0.05$). Furthermore, total ^{14}C tissue activity decreased with CH acclimation in erector spinae, tibialis anterior and the white gastrocnemius in both populations of deer mice ($P < 0.05$).

^{14}C-2-bromopalmitic acid uptake was expressed for each tissue as both an absolute and percentage of total uptake by all sampled tissues (omitting liver, diaphragm, and left and right ventricles due to their much higher uptake) (Table 4.1 & 4.2, Figure 4.2). The total activity for skeletal muscles, WAT and BAT were summed and presented as the absolute and percent uptake of ^{14}C-2-bromopalmitic acid for all sampled muscles, WAT and BAT (Figure 4.3). While there were no significant population ($F_{1,18} = 0.01$; $P = 0.91$)

or acclimation ($F_{1,18}$ = 0.38; P = 0.54) effects for the absolute uptake of fatty acids into skeletal muscle (Figure 4.3A), the proportion of total fatty acid uptake attributed to skeletal muscle was greater in TN acclimated highlanders (~75%) than TN acclimated lowlanders (~57%; P < 0.05) (Figure 4.3B). This population difference appeared to be driven by higher uptake in the following TN acclimated highlander skeletal muscles: the biceps brachii, the rectus femoris, the red gastrocnemius, the tibialis anterior and the triceps (P < 0.05; Figure 4.2). Interestingly, only highlanders showed a decrease in the percent uptake of radiolabelled fatty acid into skeletal muscles following CH acclimation, with a decline from ~75% to 56% of total measured uptake (population × acclimation interaction: $F_{1,18}$ = 8.22; P = 0.01). This acclimation response in highlanders was associated with decreases in the percent uptake of fatty acids in the biceps femoris, erector spinae, masseter, rectus femoris, tibialis anterior and the white gastrocnemius following CH acclimation (P < 0.05; Figure 4.2). The findings for BAT mirror the results for muscles. There was a significant population × acclimation interaction for the absolute uptake of fatty acids into BAT (Figure 4.3A; $F_{1,18}$ = 5.21; P = 0.01), and percentage of fatty acid taken up by BAT (Figure 4.3B; $F_{1,18}$ = 9.25; P < 0.01), where fatty acid uptake in BAT was lower in TN acclimated highlanders (~16%) compared to TN lowlanders (~37%; P < 0.05); however, only in highlanders did BAT increase fatty acid uptake (by ~36%) following CH acclimation, predominately driven by changes in uptake by the interscapular BAT depot (P < 0.05; Figure 4.2). Total WAT contributed ~8% of total radiolabelled fatty acid uptake, but did not differ between populations ($F_{1,18}$ < 0.01; P = 0.94) or with acclimation ($F_{1,18}$ = 1.43; P = 0.25) (Figure 4.2 & 4.3, Table 4.1).

Tissue Enzyme Activity

To assess the capacity for aerobic metabolism and fatty acid oxidation, we determined the apparent Vmax for marker enzymes CS, HOAD, and COX in six tissues of interest (BAT and 5 skeletal muscles) (Figure 4.4). These tissues were assessed because they demonstrated population differences, and/or showed plasticity with CH acclimation, on their capacities to uptake fatty acids based on tracer fatty acid results mentioned previously.

The apparent Vmax for CS (Figure 4.4A), a marker for mitochondrial volume, was greater in three of the five muscles in highlanders and increased with CH acclimated deer mice, compared to lowlanders and TN acclimated mice, respectively. The rectus femoris (population: $F_{1,25} = 4.44$, $P = 0.04$; acclimation: $F_{1,25} = 5.10$, $P = 0.04$), red gastrocnemius (population: $F_{1,25} = 4.34$, $P = 0.05$; acclimation: $F_{1,25} = 4.26$, $P = 0.05$), white gastrocnemius (population: $F_{1,26} = 11.27$, $P < 0.01$; acclimation: $F_{1,26} = 6.66$, $P = 0.02$) showed significant effects of both population and acclimation. The erector spinae displayed a significant effect of acclimation for CS activity, which was higher following CH acclimation in both populations ($F_{1,26} = 8.11$, $P < 0.01$). The tibialis anterior displayed no significant effects of population ($P > 0.05$) nor acclimation ($P > 0.05$) (Figure 4.4A). iBAT displayed a significant population × acclimation interaction ($F_{1,26} = 11.95$, $P < 0.01$), where CS activity in TN acclimated lowlanders was 73% greater than in TN acclimated highlanders ($P < 0.05$). Additionally, only highlanders showed an increase in iBAT CS activity by three-fold upon CH acclimation ($P < 0.05$).

The activity of HOAD was measured as a marker for β-oxidation capacity (Figure 4.4B). In highlanders, HOAD was ~23% higher in the erector spinae ($F_{1,26}$ = 4.29, P = 0.05) and ~57% higher in the white gastrocnemii ($F_{1,26}$ = 15.10, P < 0.01) compared to lowland deer mice. No other muscles displayed any significant population effects (P > 0.05). The activity of HOAD in iBAT showed a significant population × acclimation interaction ($F_{1,26}$ = 8.47, P < 0.01), where CH increased HOAD activity by 3.5-fold in highlanders (P < 0.05). All other tissues measured showed no effect of CH acclimation on HOAD activity (P > 0.05).

Maximal COX activity was used as a marker to assess mitochondrial quality and function, as COX is the primary site of cellular oxygen consumption and is important for the production of ATP (Figure 4.4C). There were no significant differences in cytochrome c oxidase activities between populations (P > 0.05) or acclimations (P > 0.05) among the measured tissues.

Fatty acid translocase CD36

The capacity for fatty acid uptake in iBAT, erector spinae, and both red and white gastrocnemii was evaluated by quantifying the total protein abundance of FAT/CD36 in whole tissue homogenates. CH acclimation led to a significant increase in FAT/CD36 protein abundance in iBAT ($F_{1,15}$ = 12.14, P < 0.05). Abundance of FAT/CD36 trended to be higher in the iBAT of highlanders compared to lowlanders but failed to reach statistical significance (effects of population, $F_{1,15}$ = 4.25, P = 0.06) (Figure 4.5A). For the erector spinae, we found no significant effects of population ($F_{1,16}$ = 1.93, P = 0.18) or

acclimation ($F_{1,16}$ = 0.84, P = 0.37) on FAT/CD36 protein abundance (Figure 4.5B). Similarly, both red and white gastrocnemii displayed no differences in FAT/CD36 abundance between populations ($F_{1,15}$ = 0.11, P = 0.75 and $F_{1,16}$ = 0.04, P = 0.85, respectively) or with acclimation ($F_{1,15}$ = 0.33, P = 0.57 and $F_{1,16}$ = 3.82, P = 0.07, respectively) (Figure 4.5C & 4.5D).

4.5 DISCUSSION

The main objective of this study was to assess uptake of circulating fatty acids into a variety of tissues during maximal cold challenge and evaluate variation in tissue uptake between highland and lowland deer mice acclimated to either TN or simulated high-altitude conditions. Additionally, we assessed the metabolic properties of tissues demonstrating variation in fatty acid uptake between populations or with acclimation, to better understand their putative contribution to thermogenesis. We found circulatory fatty acid uptake at cold-induced $\dot{V}O_2$max could be divided into tissues with high (liver, heart, diaphragm, iBAT), moderate (auxiliary BAT, erector spinae, masseter, thigh muscles, and hamstring muscles) and low (WAT depots and small skeletal muscles located on the extremities of the forelimb and hindlimb) uptake when standardized to body mass. When skeletal muscle fatty acid uptake was combined and compared to that of BAT, we found that CH acclimation caused a shift towards greater BAT uptake, but only in highland deer mice. This was consistent with increases in whole animal lipid oxidation (Figure 4.1C) and previous data showing NST increases with CH in highlanders (7). Greater fatty acid uptake in BAT could be due to higher membrane uptake, as CH acclimation increase total BAT FAT/CD36 abundance in both populations. Interestingly, highlanders had higher

activities of CS and HOAD in BAT, which further increased with CH acclimation. Perhaps a greater sink for lipid oxidation results in increased capacity for BAT fatty acid uptake from the circulation. In three of the five skeletal muscles we examined, highlanders showed higher CS activity compared to lowlanders. With CH acclimation, there was an increase in CS in these same muscles, suggesting greater mitochondrial densities compared to TN acclimation. Two muscles in highland deer mice, the erector spinae and white gastrocnemius, also demonstrated increases in HOAD. Interestingly, these differences in muscle phenotype did not match the variation in fatty acid uptake. These results show that tissue uptake of circulatory fatty acids varies during peak thermogenesis, both between lowland and highland populations of deer mice, but also with CH acclimation simulating altitude conditions of 4300m. Using a comprehensive sampling of tissues, we were able to demonstrate a coordinated redistribution of fatty acid uptake from skeletal muscles to BAT in highland deer mice exposed to conditions found in their natural environment.

Thermogenic capacity is a trait used to assess the ability for heat production and the ability to maintain high and stable body temperature during maximal cold challenge. Here, we confirmed findings of our previous work demonstrating that during hypoxic cold-induced $\dot{V}O_2max$, thermogenic capacity is greater in highland deer mice (18). A significant increase in cold-induced $\dot{V}O_2max$ with CH acclimation led to significantly greater thermogenic capacity in highlanders compared to lowland deer mice (Figure 4.1A). In contrast to this previous work, where animals were kept at standard holding conditions (23^{o}C, 21 kPa), we used a TN acclimation (30^{o}C, 21 kPa) to ensure mice were

within their thermoneutral zone (11). When both populations were acclimated to TN conditions, post-tests revealed no significant differences in cold-induced $\dot{V}O_2max$ between populations. However, $\dot{V}O_2max$ values were lower than previously reported for these populations (18), demonstrating that common holding conditions used previously represent a mild cold acclimation (22). Similarly, we found that lipid oxidation rates were lower in TN deer mice than previously reported for deer mice kept in common holding conditions (18). CH highland deer mice showed a significant increase in lipid oxidation (Figure 4.1C) associated with the increase in $\dot{V}O_2max$ and decline in RER with acclimation (Figure 4.1B). This decline in RER is consistent with the response in highlanders to cold acclimation (11), and suggests the addition of hypoxia did not antagonize this effect.

High rates of lipid oxidation in highland deer mice during hypoxic cold-induced $\dot{V}O_2max$ are possible due to the elevated circulatory delivery of fatty acids to active tissues (17). While previous work on rats has examined fatty acid uptake of 9 tissues following cold exposure, including liver, BAT, heart, kidney, diaphragm, and a few skeletal muscles (10), it has been unclear which tissues take up fatty acids during maximal rates of heat production and if this differs with altitude ancestry or CH acclimation. Therefore, we determined the fate of circulating fatty acids in thermoregulating deer mice to provide insight on the tissues contributing to total heat production. The use of a radiolabelled 2-bromopalmitic acid has been employed by many studies tracing fatty acid uptake into tissues of interest (9, 10, 12, 23, 24, 27). It is important to note that while using this non-oxidizable tracer fatty acid provides

information for fatty acid tissue localization, it does not indicate its fate once trapped inside the cell (intracellular storage or mitochondrial oxidation). Despite this, there is clear evidence to suggest that with cold acclimation and cold exposure, increased fatty acid uptake directly correlates with increased fatty acid oxidation, especially in thermo-active tissue, such as BAT (10, 30). While it is possible that ^{14}C-bromopalmitate taken up by tissues may have been destined for intracellular storage, deer mice in this study were exposed to maximal cold challenges. Thus, it could be expected that the fate of ^{14}C-bromopalmitate would predominately be used in tissue mitochondrial oxidation for powering thermogenesis.

We found that large proportions of fatty acids were delivered to central tissues (liver, heart, and diaphragm) and to BAT. In addition, individual muscles that are larger and closer to the core of the animal (i.e., erector spinae, rectus femoris, bicep femoris) take up more fatty acids than smaller muscles located near the extremities (i.e., biceps brachii, soleus, tibialis anterior) (Table 4.1). We also observed a redistribution of tissue fatty acid uptake with CH acclimation. CH acclimated highland deer mice showed a decline in muscle uptake and an increase in BAT uptake of fatty acids compared to TN highlanders (Figure 4.2 & 4.3). Previous findings demonstrate that BAT increases both fatty acid uptake and oxidation following cold acclimation, with no changes in other organs or muscle tissue (10). This shift in muscle to BAT fatty acid uptake may be associated with a redirection of blood flow, as observed in cold acclimated rats exposed to an acute cold challenge (8). Lowland deer mice did not show a redistribution of fatty acid uptake in

CH, which may reflect the antagonistic influence of hypoxia on chronic cold acclimation (2).

BAT is crucial for thermogenesis in small eutherian mammals as it is the main site of NST. This tissue becomes highly active during cold exposure, where fatty acids both activate mitochondrial UCP-1 and provide metabolic substrate for sustaining NST (5). It has been speculated that BAT activity can contribute over 50% of the heat produced during thermogenesis (8, 32). In this study, we were interested in determining fatty acid delivery to BAT (interscapular and auxiliary) during a bout of maximal thermogenesis. Only highlanders increased circulating fatty acid uptake into BAT depots from 16% (TN) to 36% (CH) of total measured uptake (Figure 4.3B), which appeared to be driven by the uptake of fatty acids into iBAT (Figure 4.2). This shift led to a corresponding decrease in highlander muscle fatty acid uptake with CH acclimation (75% to 56%), driven by the masseter, erector spinae, bicep femoris, rectus femoris, white gastrocnemius and the tibialis anterior. While the capacity for fatty acid transport into iBAT via FAT/CD36 increased for deer mice after CH acclimation, there were no differences between populations in FAT/CD36 expression (Figure 4.5A), confirming previous findings (17). However, CH acclimated highlanders had elevated CS and HOAD activities in iBAT (Figure 4.4A & 4.4B), suggesting an increased mitochondrial density and β-oxidation capacity compared to lowland iBAT. These findings closely correspond to the unique acclimation response highlanders demonstrate to CH, where norepinephrine-induced NST, iBAT mitochondrial UCP-1 expression, and iBAT mitochondrial respiration all increase after acclimation to CH (7). Altogether, these findings at the BAT level may

explain the unique CH acclimated increase in whole-animal lipid oxidation rates observed in thermoregulating highland deer mice (Figure 4.1C; (18).

Muscle recruitment for ST primarily occurs upon acute cold exposure or intense cold challenges and increases rates of fatty acid oxidation in muscle (3). Interestingly, rodents acclimated to warm conditions exposed to acute cold challenges have minimal BAT activity and rely predominately on ST for heat production (31). In this study, we used a TN acclimation to minimize BAT activity, supported by the reduced CS and HOAD activities in iBAT (Figure 4.4), to gain more insight on muscle's role for fatty acid uptake during thermogenesis. We found that TN acclimated highlanders had a higher total uptake of ^{14}C-bromopalmitic acid into skeletal muscles (~75%) compared to TN acclimated lowlanders (~57%, Figure 4.3), despite no population differences in whole-animal lipid oxidation rates during hypoxic cold-induced $\dot{V}O_2$max for TN acclimated deer mice. These findings suggest that the rates of fat use by shivering muscle is greater for highland deer mice, at least during TN acclimation, compared to lowlanders. While the muscle's capacity for fatty acid uptake may not be limited by protein abundances of FAT/CD36 (Figure 4.5B-D, (17), perhaps TN acclimated highlanders can increase blood flow to shivering muscle more effectively than lowlanders during cold-induced $\dot{V}O_2$max. An increased cardiac output of highlanders (29), in combination with an increased capillarity of highland muscle tissue (16, 21), and increased rate of fatty acid delivery in highlanders (17) may account for these observations. Furthermore, the elevated oxidative phenotype of highlander muscle would allow for increased capacities for lipid oxidation (Figure 4.4, (6, 14, 16, 17).

Highland deer mice have evolved mechanisms to overcome two major limitations associated with thermogenesis: 1) the inhibitory effect chronic hypoxia has on BAT activity (2, 7), and 2) the limitation of O_2 and substrate transport to thermo-effector tissue (21). Whole-animal lipid oxidation rates during cold-induced $\dot{V}O_2max$ in hypoxia were not affected by CH acclimation in lowland deer mice (Figure 4.1C), consistent with previous work demonstrating no changes in NST after CH acclimation (7). Unlike highlanders, there were no shifts in fatty acid uptake from muscle to BAT following CH acclimation (Figure 4.3) and no changes in iBAT CS activity with CH in lowlanders (Figure 4.4). These findings suggest that acclimation to hypoxic conditions may be hindering lowlanders' ability to transport O_2 and metabolic substrate to thermo-effector tissue during heat production, limiting the rate lipids can be metabolised (2, 21). However, highlanders show a full acclimation response regardless of the hypoxic conditions, most likely attributed to their evolved capacities for O_2 and substrate transport (21). Therefore, the blunted BAT activity and the impeded O_2 delivery associated with hypoxia during acclimation to simulated high-altitude conditions may be the reason lowlanders have lower thermogenic lipid oxidation rates compared to highlanders.

4.6 PERSPECTIVES AND SIGNIFICANCE

Highland deer mice have evolved amazing thermoregulatory capacities to ensure survival in the challenging environments of high altitude. Altogether, our findings suggest that highland deer mice acclimated to simulated high-altitude conditions increase maximal heat production with a corresponding increase in lipid metabolism, consistent with previous studies (18, 29). These findings may be associated with the increased

cardiac output (28, 29), circulatory fat delivery rates (17), oxidative phenotype of muscle (14, 16, 17, 19), and aerobic capacity of BAT (7, 11) of highland deer mice. While there has been emerging evidence for the increased role of circulatory lipids for powering thermogenesis in thermo-effector tissue (17), the specific distribution of these circulatory lipids had yet to be determined in detail.

In this study, we determined fatty acid uptake among 24 tissues during peak thermogenesis in both highland and lowland deer mice acclimated to either TN or CH conditions. Our study emphasizes that in deer mice, larger and more centralized tissues, such as the liver, iBAT, and rectus femoris, uptake more circulatory fatty acids than smaller muscles located near the extremity of the animal, like the soleus and biceps brachii. We show that during cold-induced $\dot{V}O_2max$, CH acclimation increases fatty acid uptake from the circulation into BAT, to a greater extent in highlanders. Our results provide supporting evidence for BAT's essential role in enhancing heat production by increasing NST, while the importance of ST is decreased (3, 13). However, while individual muscles may not be as active as BAT for fatty acid uptake, collectively, total muscle may provide the largest source of circulatory fatty acid clearance during heat production (> 50%, Figure 4.3; (4, 25)). These high clearance rates of fatty acids are presumably for sustaining ST and contribute to the high rates of lipid oxidation observed in deer mice (17, 18). Lastly, we propose the high rates of lipid oxidation observed in thermoregulating highland deer mice are associated with the adaptations allowing them to overcome the hindering effects hypoxia has on O_2 transport (21) and BAT activity (2, 7). Future research should continue to distinguish the contribution of circulating lipids and

intracellular lipids in both BAT and muscles in the context of total heat production in highland native deer mice.

4.7 ACKNOWLEDGEMENTS

The authors would like to thank E. Garrett for technical assistance with enzyme assays.

4.8 FIGURES AND TABLES

Figure 4.1

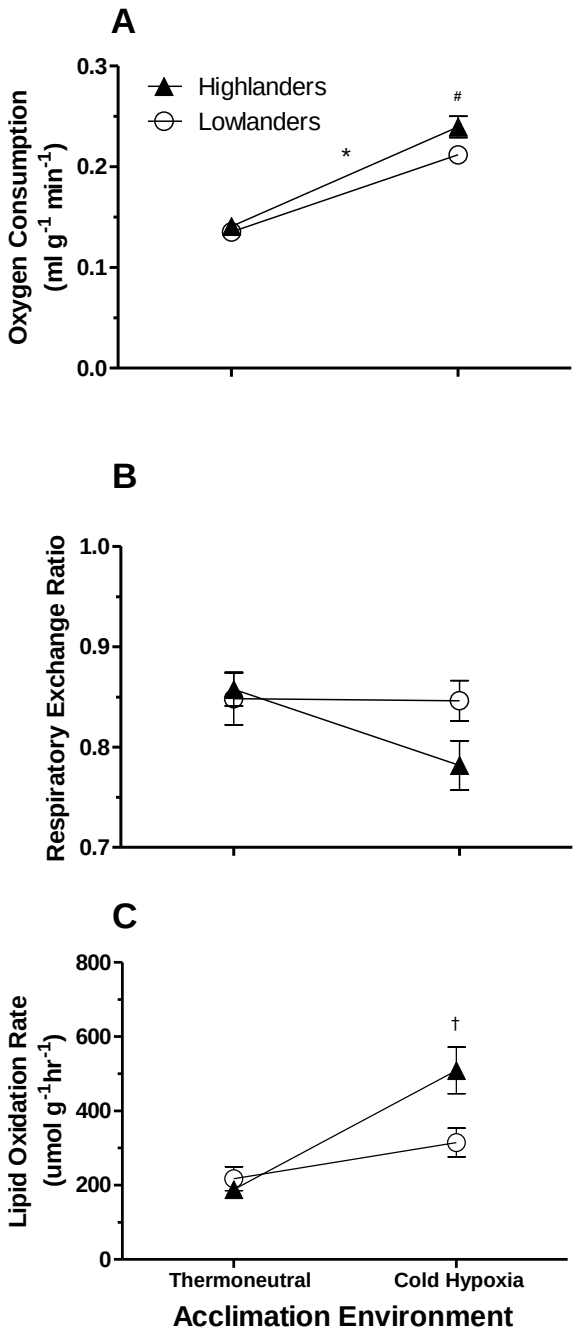

Figure 4.1. Cold-induced maximal oxygen consumption ($\dot{V}O_2max$) (in ml g^{-1} min^{-1}) (A) with the corresponding Respiratory Exchange Ratios (RER= $\dot{V}CO_2/\dot{V}O_2$) (B)

and whole-animal lipid oxidation rates (in µmol g^{-1} hr^{-1}) (C) of second-generation laboratory born and raised highland and lowland deer mice (*Peromyscus maniculatus*), acclimated to thermoneutral (30ºC, 21 kPa O_2;WN) or cold hypoxia (5ºC, 12 kPa O_2; CH) conditions. *Significant difference between populations. #Significant difference between acclimations. †CH highlanders are different than WN highlanders. Sample sizes for thermoneutral and cold hypoxia were *N*=24 and *N*=20 for highlanders, and *N*=25 and *N*=23 for lowlanders, respectively. Data are presented as mean ± s.e.m.

Figure 4.2

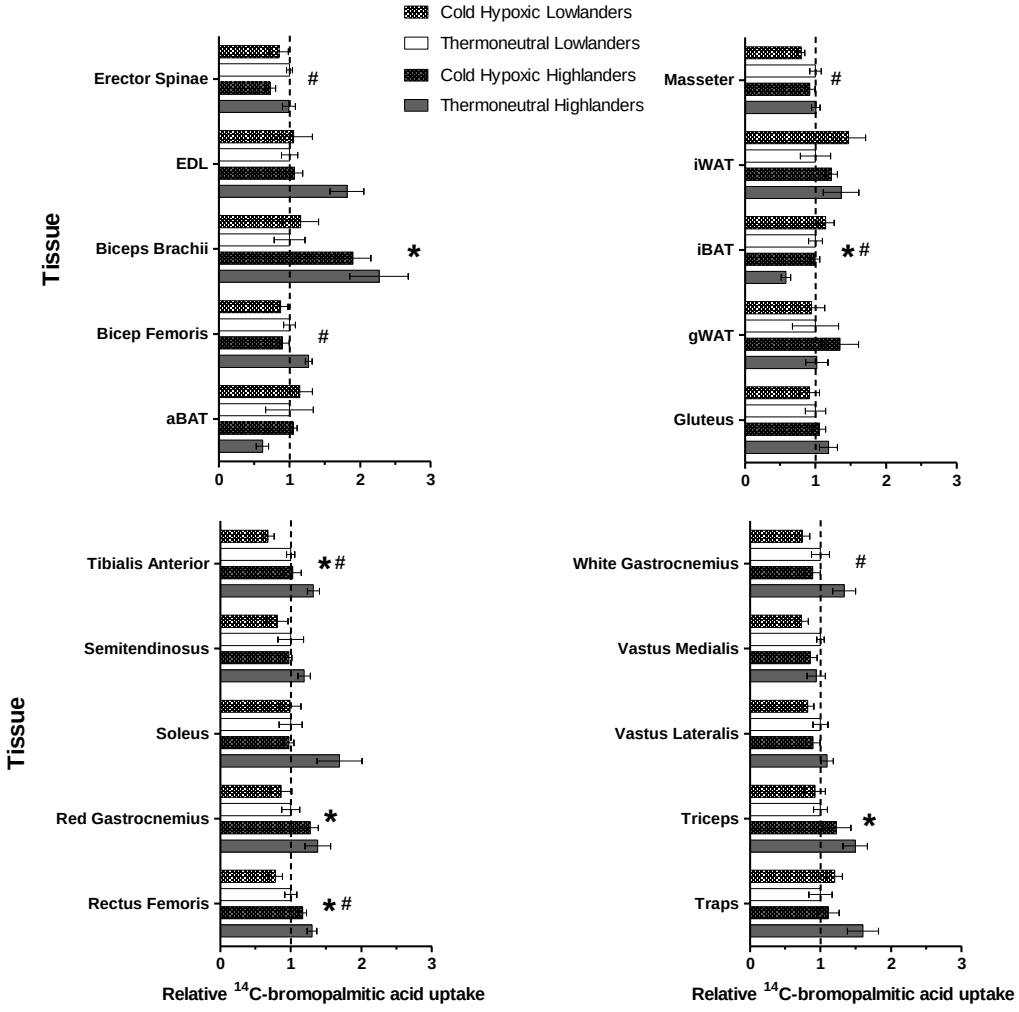
Cold Hypoxic Lowlanders
Thermoneutral Lowlanders
Cold Hypoxic Highlanders
Thermoneutral Highlanders
Tissue
Erector Spinae
EDL
Biceps Brachii
Bicep Femoris
aBAT
Masseter
iWAT
iBAT
gWAT
Gluteus
Tibialis Anterior
Semitendinosus
Soleus
Red Gastrocnemius
Rectus Femoris
White Gastrocnemius
Vastus Medialis
Vastus Lateralis
Triceps
Traps
0
1
2
3
Relative 14C-bromopalmitic acid uptake

Figure 4.2. The relative tissue uptake of ^{14}C-palmitic acid of second-generation highland and lowland deer mice (*Peromyscus maniculatus*) acclimated to thermoneutral conditions (30ºC, 21kPa) or cold hypoxia (5ºC, 12kPa) exposed to a maximal cold challenge in hypoxia. All data are presented as means ± s.e.m., standardized to the relative tissue uptake of thermoneutral lowlanders (represented by the dashed line). See Table 4.1B for non-standardized values and sample sizes. *Significant main population effect ($P < 0.05$). # Significant main acclimation effect ($P < 0.05$).

Table 4.1 Average tissue mass, specific tissue activity (^{14}C-counts per minute (CPM) per mg tissue), total tissue activity (total tissue CPM per g body mass), and relative tissue uptake of ^{14}C-palmitic acid (as % CPM of all tissues) of highland and lowland deer mice acclimated to thermoneutral conditions (30ºC, 21kPa) or cold hypoxia (5ºC, 12kPa) exposed to a maximal cold challenge (cold-induced $\dot{V}O_2max$). Data are presented as means ± s.e.m., with sample sizes in parentheses.

Tissue	**Tissue mass (mg)**				**Specific activity (CPM mg^{-1})**			
	Highlanders		Lowlanders		Highlanders		Lowlanders	
	TNZ	CH	TNZ	CH	TNZ	CH	TNZ	CH
Auxiliary BAT	32.8 ± 3.4 (6)	25.7 ± 4.4 (5)	35.1 ± 6.4 (5)	30.1 ± 5.1 (6)	56.9 ± 16.0 (6)	**109.3 ± 20.3# (4)**	59.1 ± 18.5 (4)	**189.0 ± 44.9# (6)**
Bicep Brachii	**17.2 ± 1.9* (6)**	**16.2 ± 1.0* (5)**	10.0 ± 1.7 (3)	13.3 ± 1.4 (6)	54.3 ± 9.6 (6)	56.3 ± 5.7 (5)	90.3 ± 27.3 (3)	61.0 ± 7.3 (6)
Bicep Femoris	**142.9 ± 9.3† (6)**	**106.5 ± 12.3‡ (5)**	106.1 ± 5.7 (5)	117.3 ± 7.7 (6)	3.8 ± 0.6 (6)	5.8 ± 1.3 (5)	6.5 ± 1.1 (5)	5.3 ± 0.5 (6)
Diaphragm	**50.0 ± 5.0* (6)**	**75.1 ± 5.4*# (5)**	46.6 ± 4.6 (5)	**55.2 ± 5.0# (6)**	59.9 ± 11.2 (6)	**32.2 ± 8.5# (5)**	60.0 ± 8.6 (5)	**38.6 ± 4.3# (6)**
Extensor Digitorum Longus	5.9 ± 0.5 (6)	4.1 ± 0.5 (5)	4.4 ± 0.9 (5)	4.0 ± 0.3 (5)	120.8 ± 23.8 (6)	178.0 ± 40.0 (5)	206.9 ± 41.5 (5)	149.7 ± 21.0 (6)
Erector Spinae	85.3 ± 5.0 (6)	72.3 ± 10.4 (5)	89.9 ± 2.5 (5)	98.0 ± 9.8 (6)	7.8 ± 0.6 (6)	11.4 ± 2.7 (5)	9.2 ± 1.1 (5)	7.8 ± 1.0 (6)
Gluteus	94.1 ± 5.0 (6)	99.9 ± 14.8 (5)	68.8 ± 3.2 (4)	98.3 ± 10.9 (6)	5.8 ± 0.8 (6)	6.5 ± 1.5 (5)	9.3 ± 1.4 (5)	6.2 ± 0.8 (6)
Gonadal WAT	104.9 ± 5.1 (5)	244.7 ± 116.3 (5)	95.6 ± 24.3 (5)	68.6 ± 11.7 (6)	2.3 ± 0.5 (6)	**3.5 ± 1.4# (5)**	2.9 ± 0.7 (4)	**10.5 ± 2.6# (6)**
Interscapular BAT	108.3 ± 13.2 (6)	82.5 ± 9.0 (5)	111.1 ± 19.0 (5)	108.3 ± 13.2 (6)	20.0 ± 9.2 (6)	**49.3 ± 14.3# (5)**	21.3 ± 4.7 (4)	**47.9 ± 9.0# (6)**
Inguinal WAT	112.1 ± 20.0 (5)	163.3 ± 42.2 (5)	84.9 ± 29.9 (4)	89.0 ± 20.1 (6)	3.2 ± 1.2 (6)	1.8 ± 0.8 (4)	2.4 ± 1.0 (4)	13.5 ± 4.9 (6)
Liver	**676.0 ± 69.9* (6)**	**755.7 ± 38.6*# (5)**	469.2 ± 51.0 (5)	**692.6 ± 58.9# (6)**	15.6 ± 2.1 (6)	**10.6 ± 1.1# (5)**	25.7 ± 5.6 (5)	**11.7 ± 1.9# (6)**
Left Ventricle	72.6 ± 2.7 (6)	88.5 ± 2.7 (4)	52.9 ± 3.7 (5)	**104.8 ± 11.7‡ (6)**	66.8 ± 8.2 (6)	**34.0 ± 5.9# (5)**	82.4 ± 7.8 (5)	**28.7 ± 4.7# (6)**
Masseter	75.6 ± 2.7 (6)	80.0 ± 6.2 (5)	66.0 ± 4.1 (5)	**90.9 ± 5.6‡ (6)**	8.2 ± 1.0 (6)	8.2 ± 1.3 (5)	12.8 ± 2.0 (5)	**6.8 ± 1.2‡ (5)**
Rectus Femoris	**77.0 ± 3.9* (6)**	**69.0 ± 7.1* (5)**	58.9 ± 6.6 (5)	64.0 ± 4.5 (6)	8.2 ± 1.5 (6)	12.0 ± 3.0 (5)	14.7 ± 3.8 (5)	10.3 ± 1.7 (6)
Red Gastrocnemius	**37.5 ± 3.4* (6)**	**41.0 ± 2.6* (5)**	31.5 ± 5.2 (5)	28.5 ± 1.3 (5)	26.3 ± 4.1 (6)	24.7 ± 5.4 (5)	41.6 ± 13.9 (5)	32.2 ± 4.0 (6)
Right Ventricle	23.3 ± 2.4 (6)	**35.9 ± 2.7# (5)**	24.6 ± 3.2 (5)	**37.7 ± 4.9# (6)**	206.1 ± 32.7 (6)	**92.3 ± 15.3# (5)**	186.6 ± 45.3 (5)	**78.5 ± 16.3# (6)**
Soleus	5.5 ± 0.4 (6)	4.8 ± 0.8 (5)	3.5 ± 0.2 (3)	4.6 ± 0.5 (6)	**159.3 ± 16.2* (6)**	**192.5 ± 48.5* (5)**	307.9 ± 71.1 (3)	220.7 ± 34.9 (6)
Semitendinosus	128.2 ± 4.9 (6)	106.5 ± 10.5 (5)	95.3 ± 15.4 (5)	105.2 ± 10.4 (6)	3.9 ± 0.63 (6)	6.2 ± 1.6 (5)	6.2 ± 0.6 (4)	5.6 ± 0.5 (6)
Tibialis Anterior	32.1 ± 2.0 (6)	27.4 ± 3.5 (5)	26.0 ± 3.6 (4)	28.7 ± 1.9 (6)	**18.0 ± 2.4† (6)**	**26.2 ± 6.6†‡ (5)**	30.9 ± 8.9 (4)	**16.6 ± 1.3‡ (6)**
Trapezius	69.6 ± 6.1 (6)	49.8 ± 8.3 (5)	55.6 ± 4.8 (5)	68.0 ± 4.1 (6)	14.4 ± 1.8 (6)	31.3 ± 9.5 (5)	18.5 ± 3.7 (5)	17.2 ± 1.7 (6)
Triceps	68.5 ± 3.1 (6)	66.2 ± 8.0 (5)	53.8 ± 4.5 (5)	63.1 ± 5.2 (6)	10.5 ± 1.1 (6)	12.1 ± 2.4 (5)	14.9 ± 1.5 (5)	11.4 ± 1.1 (6)
Vastus Lateralis	62.1 ± 4.0 (6)	54.7 ± 6.4 (5)	59.8 ± 6.3 (5)	61.6 ± 2.6 (6)	9.8 ± 0.4 (6)	15.1 ± 4.8 (5)	10.4 ± 0.5 (4)	11.4 ± 1.4 (6)
Vastus Medialis	13.1 ± 1.6 (6)	11.0 ± 1.4 (5)	13.2 ± 1.2 (5)	11.0 ± 0.9 (6)	54.5 ± 5.6 (6)	92.8 ± 21.7 (5)	80.4 ± 20.7 (4)	88.7 ± 10.2 (6)
White Gastrocnemius	**56.4 ± 4.0† (6)**	42.2 ± 6.1 (5)	37.7 ± 0.7 (4)	42.2 ± 3.4 (6)	**9.3 ± 1.1† (6)**	**15.6 ± 3.8‡ (5)**	17.3 ± 2.4 (5)	13.9 ± 1.4 (6)

Values for liver *total activity* are x10^3. *Significant main population effect (P <0.05). # Significant main acclimation effect (P<0.05). Significant differences in population × acclimation interactions result from Holm Sidak post hoc tests (P < 0.05). †Significantly different than lowlanders, within an acclimation. ‡Significantly different than thermoneutral conditions, within a population.

Table 4.1 ***continued…***

Tissue	Total activity (CPM g^{-1} body weight)				Relative tissue uptake (%)			
	Highlanders		Lowlanders		Highlanders		Lowlanders	
	TNZ	CH	TNZ	CH	TNZ	CH	TNZ	CH
Auxiliary BAT	**814.2 ± 214.2* (6)**	**1237.9 ± 288.2* (5)**	1701.4 ± 512.4 (5)	2117.8 ± 477.0 (6)	5.73 ± 0.82 (6)	9.76 ± 0.50 (4)	9.26 ± 3.13 (5)	10.61 ± 1.64 (6)
Bicep Brachii	220.9 ± 47.8 (6)	210.3 ± 50.1 (5)	150.6 ± 37.9 (3)	155.6 ± 29.6 (6)	**1.72 ± 0.31* (6)**	**1.44 ± 0.19* (5)**	0.76 ± 0.17 (3)	0.88 ± 0.19 (6)
Bicep Femoris	1085.7 ± 168.9 (6)	819.8 ± 155.5 (5)	1250.1 ± 173.8 (5)	1044.3 ± 123.7 (6)	8.15 ± 0.31 (6)	**5.76 ± 0.62# (5)**	6.42 ± 0.53 (5)	**5.60 ± 0.69# (6)**
Diaphragm	2180.0 ± 356.5 (6)	2232.2 ± 392.9 (5)	2174.5 ± 317.2 (5)	1663.9 ± 250.6 (6)	-	-	-	-
Extensor Digitorum Longus	59.4 ± 12.2 (6)	37.4 ± 7.3 (5)	59.4 ± 13.3 (5)	48.7 ± 14.0 (6)	0.44 ± 0.06 (6)	0.26 ± 0.03 (5)	0.24 ± 0.03 (4)	0.26 ± 0.07 (6)
Erector Spinae	**848.0 ± 93.9* (6)**	**574.1 ± 30.8*# (4)**	1288.9 ± 127.7 (5)	**1042.7 ± 133.9# (6)**	6.63 ± 0.61 (6)	**4.88 ± 0.50# (5)**	6.68 ± 0.28 (5)	**5.69 ± 0.89# (6)**
Gluteus	758.0 ± 115.9 (6)	708.1 ± 79.8 (5)	941.1 ± 136.7 (5)	811.5 ± 80.4 (6)	5.82 ± 0.63 (6)	5.19 ± 0.44 (5)	4.91 ± 0.71 (5)	4.48 ± 0.70 (6)
Gonadal WAT	519.7 ± 105.7 (6)	554.9 ± 82.8 (5)	583.6 ± 198.6 (5)	561.9 ± 105.0 (6)	3.19 ± 0.50 (5)	4.22 ± 0.83 (5)	3.13 ± 1.03 (5)	2.96 ± 0.58 (6)
Interscapular BAT	**2225.0 ± 461.5* (6)**	**3780.2 ± 447.4* (5)**	5338.4 ± 683.9 (5)	6381.4 ± 1191.0 (6)	**16.12 ± 1.82* (6)**	**27.45 ± 1.87*# (5)**	27.66 ± 2.75 (5)	**31.59 ± 3.37# (6)**
Inguinal WAT	585.2 ± 138.5 (6)	575.6 ± 63.0 (5)	655.1 ± 148.7 (5)	962.0 ± 160.2 (6)	4.63 ± 0.85 (6)	4.18 ± 0.27 (5)	3.40 ± 0.73 (5)	4.99 ± 0.82 (6)
Liver	104.2 ± 15.2 (6)	85.5 ± 17.7 (5)	87.6 ± 14.4 (5)	68.0 ± 3.5 (5)	-	-	-	-
Left Ventricle	5159.0 ± 609.2 (6)	3922.9 ± 509.2 (5)	4003.3 ± 434.1 (5)	3983.8 ± 418.1 (6)	-	-	-	-
Masseter	717.6 ± 130.2 (6)	676.9 ± 94.0 (5)	1027.0 ± 153.1 (5)	759.2 ± 91.6 (5)	5.28 ± 0.32 (6)	**4.84 ± 0.38# (5)**	5.26 ± 0.42 (5)	**4.18 ± 0.28# (5)**
Rectus Femoris	695.6 ± 113.0 (6)	666.9 ± 104.5 (5)	768.2 ± 79.5 (5)	578.8 ± 67.2 (6)	**5.22 ± 0.27* (6)**	**4.68 ± 0.22*# (5)**	4.00 ± 0.34 (5)	**3.14 ± 0.40# (6)**
Red Gastrocnemius	511.6 ± 70.8 (6)	542.8 ± 108.6 (5)	562.9 ± 75.3 (5)	447.9 ± 32.4 (6)	4.05 ± 0.54 (6)	**3.74 ± 0.33# (5)**	2.93 ± 0.37 (5)	**2.53 ± 0.45# (6)**
Right Ventricle	1613.9 ± 278.7 (6)	1540.3 ± 264.4 (5)	1646.5 ± 128.8 (5)	1361.0 ± 139.7 (6)	-	-	-	-
Soleus	71.4 ± 9.4 (6)	46.7 ± 5.5 (5)	70.5 ± 17.3 (3)	62.8 ± 7.3 (6)	0.59 ± 0.11 (6)	0.34 ± 0.03 (5)	0.35 ± 0.06 (3)	0.35 ± 0.05 (6)
Semitendinosus	954.8 ± 146.1 (6)	826.0 ± 117.0 (5)	1135.5 ± 180.8 (5)	869.5 ± 111.1 (6)	7.20 ± 0.53 (6)	5.88 ± 0.26 (5)	6.05 ± 1.09 (5)	4.89 ± 0.93 (6)
Tibialis Anterior	273.7 ± 41.2 (6)	**227.5 ± 44.2# (5)**	307.1 ± 29.5 (4)	**195.8 ± 19.8# (6)**	**2.08 ± 0.13* (6)**	**1.62 ± 0.19*# (5)**	1.57 ± 0.09 (4)	**1.06 ± 0.14# (6)**
Trapezius	820.6 ± 105.2 (5)	755.1 ± 106.6 (5)	983.0 ± 221.1 (5)	1173.1 ± 186.9 (6)	8.00 ± 1.10 (6)	5.56 ± 0.76 (5)	5.00 ± 0.82 (5)	6.00 ± 0.56 (6)
Triceps	737.5 ± 99.3 (6)	684.3 ± 179.2 (5)	742.5 ± 100.7 (5)	644.7 ± 77.7 (6)	**5.76 ± 0.67* (6)**	**4.74 ± 0.79* (5)**	3.86 ± 0.38 (5)	3.57 ± 0.56 (6)
Vastus Lateralis	575.1 ± 82.6 (6)	517.8 ± 95.0 (5)	778.5 ± 104.8 (5)	551.8 ± 20.5 (5)	4.41 ± 0.36 (6)	3.60 ± 0.40 (5)	4.03 ± 0.43 (5)	3.31 ± 0.34 (6)
Vastus Medialis	136.9 ± 29.1 (6)	137.1 ± 31.4 (5)	217.7 ± 18.2 (4)	156.5 ± 30.4 (6)	1.02 ± 0.14 (6)	0.93 ± 0.11 (5)	1.09 ± 0.06 (4)	0.80 ± 0.11 (6)
White Gastrocnemius	449.5 ± 72.3 (6)	**315.0 ± 57.5# (5)**	498.1 ± 88.2 (5)	**345.6 ± 33.7# (6)**	3.41 ± 0.42 (6)	**2.27 ± 0.28# (5)**	2.55 ± 0.33 (5)	**1.90 ± 0.26# (6)**

Values for liver *total activity* are $x10^3$. *Significant main population effect ($P < 0.05$). #Significant main acclimation effect ($P < 0.05$). Significant differences in population × acclimation interactions result from Holm Sidak post hoc tests ($P < 0.05$). †Significantly different than lowlanders, within an acclimation. ‡Significantly different than thermoneutral conditions, within a population.

Table 4.2. Statistics summary for data in Table 4.1. *F* and *P* values for 2-way ANOVA for population (Pop), acclimation (Acc) and population × acclimation interaction. Bolded values are statistically significant.

Tissue	Tissue mass (mg)			Specific Activity (CPM mg^{-1})		
	Pop	Acc	Pop × Acc	Pop	Acc	Pop × Acc
Auxiliary BAT	$F_{1,18} = 0.48$ $P = 0.50$	$F_{1,18} = 1.53$ $P = 0.23$	$F_{1,18} = 0.05$ $P = 0.83$	$F_{1,16} = 1.66$ $P = 0.22$	**$F_{1,16} = 8.25$** **$P = 0.01$**	$F_{1,16} = 1.49$ $P = 0.24$
Bicep Brachii	**$F_{1,16} = 9.16$** **$P < 0.01$**	$F_{1,16} = 0.46$ $P = 0.51$	$F_{1,16} = 1.75$ $P = 0.20$	$F_{1,16} = 3.20$ $P = 0.09$	$F_{1,16} = 1.45$ $P = 0.25$	$F_{1,16} = 1.91$ $P = 0.19$
Bicep Femoris	$F_{1,18} = 2.07$ $P = 0.17$	$F_{1,18} = 1.92$ $P = 0.18$	**$F_{1,18} = 6.91$** **$P = 0.02$**	$F_{1,18} = 1.56$ $P = 0.23$	$F_{1,18} = 0.23$ $P = 0.64$	$F_{1,18} = 3.57$ $P = 0.08$
Diaphragm	**$F_{1,18} = 5.37$** **$P = 0.03$**	**$F_{1,18} = 11.21$** **$P < 0.01$**	$F_{1,18} = 2.71$ $P = 0.12$	$F_{1,18} = 0.14$ $P = 0.71$	**$F_{1,18} = 8.19$** **$P = 0.01$**	$F_{1,18} = 0.13$ $P = 0.72$
Extensor Digitorum Longus	$F_{1,18} = 1.72$ $P = 0.21$	$F_{1,18} = 3.26$ $P = 0.09$	$F_{1,18} = 1.24$ $P = 0.28$	$F_{1,18} = 0.85$ $P = 0.37$	$F_{1,18} < 0.01$ $P > 0.99$	$F_{1,18} = 3.33$ $P = 0.09$
Erector Spinae	$F_{1,18} = 3.80$ $P = 0.07$	$F_{1,18} = 0.10$ $P = 0.76$	$F_{1,18} = 1.83$ $P = 0.19$	$F_{1,18} = 0.57$ $P = 0.46$	$F_{1,18} = 0.53$ $P = 0.47$	$F_{1,18} = 2.99$ $P = 0.10$
Gluteus	$F_{1,17} = 1.78$ $P = 0.20$	$F_{1,17} = 3.07$ $P = 0.10$	$F_{1,17} = 1.39$ $P = 0.26$	$F_{1,18} = 2.13$ $P = 0.16$	$F_{1,18} = 1.10$ $P = 0.31$	$F_{1,18} = 2.72$ $P = 0.12$
Gonadal WAT	$F_{1,17} = 2.66$ $P = 0.12$	$F_{1,17} = 0.98$ $P = 0.34$	$F_{1,17} = 2.15$ $P = 0.16$	**$F_{1,17} = 4.89$** **$P = 0.04$**	**$F_{1,17} = 6.39$** **$P = 0.02$**	$F_{1,17} = 3.39$ $P = 0.08$
Interscapular BAT	$F_{1,18} = 1.04$ $P = 0.32$	$F_{1,18} = 1.04$ $P = 0.32$	$F_{1,18} = 0.68$ $P = 0.42$	$F_{1,17} < 0.01$ $P > 0.99$	**$F_{1,17} = 7.22$** **$P = 0.02$**	$F_{1,17} = 0.02$ $P = 0.90$
Inguinal WAT	$F_{1,16} = 3.04$ $P = 0.10$	$F_{1,16} = 0.90$ $P = 0.36$	$F_{1,16} = 0.66$ $P = 0.43$	$F_{1,16} = 2.92$ $P = 0.11$	$F_{1,16} = 2.33$ $P = 0.15$	$F_{1,16} = 3.86$ $P = 0.07$
Liver	**$F_{1,18} = 5.38$** **$P = 0.03$**	**$F_{1,18} = 6.79$** **$P = 0.02$**	$F_{1,18} = 1.53$ $P = 0.23$	$F_{1,18} = 3.47$ $P = 0.08$	**$F_{1,18} = 9.89$** **$P < 0.01$**	$F_{1,18} = 2.19$ $P = 0.16$
Left Ventricle	$F_{1,17} = 0.05$ $P = 0.82$	**$F_{1,17} = 21.14$** **$P < 0.01$**	**$F_{1,17} = 5.99$** **$P = 0.03$**	$F_{1,18} = 0.56$ $P = 0.46$	**$F_{1,18} = 40.06$** **$P < 0.01$**	$F_{1,18} = 2.34$ $P = 0.14$
Masseter	$F_{1,18} = 0.02$ $P = 0.89$	**$F_{1,18} = 9.43$** **$P < 0.01$**	**$F_{1,18} = 4.55$** **$P = 0.05$**	$F_{1,17} = 1.31$ $P = 0.27$	**$F_{1,17} = 4.53$** **$P = 0.05$**	**$F_{1,17} = 4.64$** **$P = 0.05$**
Rectus Femoris	**$F_{1,18} = 4.45$** **$P = 0.05$**	$F_{1,18} = 0.07$ $P = 0.80$	$F_{1,18} = 1.41$ $P = 0.25$	$F_{1,18} = 0.93$ $P = 0.35$	$F_{1,18} = 0.01$ $P = 0.91$	$F_{1,18} = 2.69$ $P = 0.12$
Red Gastrocnemius	**$F_{1,17} = 7.15$** **$P = 0.02$**	$F_{1,17} < 0.01$ $P = 0.94$	$F_{1,17} = 0.86$ $P = 0.37$	$F_{1,18} = 2.33$ $P = 0.14$	$F_{1,18} = 0.54$ $P = 0.47$	$F_{1,18} = 0.28$ $P = 0.60$
Right Ventricle	$F_{1,18} = 0.19$ $P = 0.67$	**$F_{1,18} = 13.03$** **$P < 0.01$**	$F_{1,18} < 0.01$ $P = 0.94$	$F_{1,18} = 0.32$ $P = 0.58$	**$F_{1,18} = 14.07$** **$P < 0.01$**	$F_{1,18} < 0.01$ $P = 0.92$
Soleus	$F_{1,16} = 3.43$ $P = 0.08$	$F_{1,16} = 0.06$ $P = 0.80$	$F_{1,16} = 2.31$ $P = 0.15$	**$F_{1,16} = 4.73$** **$P = 0.05$**	$F_{1,16} = 0.44$ $P = 0.52$	$F_{1,16} = 2.19$ $P = 0.16$
Semitendinosus	$F_{1,18} = 2.62$ $P = 0.12$	$F_{1,18} = 0.31$ $P = 0.58$	$F_{1,18} = 2.24$ $P = 0.15$	$F_{1,17} = 0.77$ $P = 0.39$	$F_{1,17} = 0.77$ $P = 0.39$	$F_{1,17} = 2.29$ $P = 0.15$
Tibialis Anterior	$F_{1,17} = 0.80$ $P = 0.38$	$F_{1,17} = 0.12$ $P = 0.73$	$F_{1,17} = 1.87$ $P = 0.19$	$F_{1,17} = 0.11$ $P = 0.74$	$F_{1,17} = 0.40$ $P = 0.54$	**$F_{1,17} = 5.38$** **$P = 0.03$**
Trapezius	$F_{1,18} = 0.13$ $P = 0.73$	$F_{1,18} = 0.38$ $P = 0.54$	**$F_{1,18} = 7.35$** **$P = 0.01$**	$F_{1,18} = 1.08$ $P = 0.31$	$F_{1,18} = 2.66$ $P = 0.12$	$F_{1,18} = 3.60$ $P = 0.07$
Triceps	$F_{1,18} = 2.78$ $P = 0.11$	$F_{1,18} = 0.42$ $P = 0.52$	$F_{1,18} = 1.17$ $P = 0.29$	$F_{1,18} = 1.45$ $P = 0.24$	$F_{1,18} = 0.37$ $P = 0.55$	$F_{1,18} = 2.58$ $P = 0.13$
Vastus Lateralis	$F_{1,18} = 0.23$ $P = 0.64$	$F_{1,18} = 0.34$ $P = 0.57$	$F_{1,18} = 0.89$ $P = 0.36$	$F_{1,17} = 0.40$ $P = 0.54$	$F_{1,17} = 1.70$ $P = 0.21$	$F_{1,17} = 0.76$ $P = 0.40$
Vastus Medialis	$F_{1,18} < 0.01$ $P = 0.95$	$F_{1,18} = 2.673$ $P = 0.12$	$F_{1,18} < 0.01$ $P = 0.95$	$F_{1,17} = 0.55$ $P = 0.47$	$F_{1,17} = 2.53$ $P = 0.13$	$F_{1,17} = 1.04$ $P = 0.32$
White Gastrocnemius	**$F_{1,17} = 4.86$** **$P = 0.04$**	$F_{1,17} = 1.27$ $P = 0.28$	**$F_{1,17} = 4.82$** **$P = 0.04$**	$F_{1,18} = 1.96$ $P = 0.18$	$F_{1,18} = 0.41$ $P = 0.53$	**$F_{1,18} = 4.68$** **$P = 0.04$**

Table 4.2. ***continued …***

Tissue	Total activity (CPM g^{-1} body weight)			Relative Tissue Uptake (%)		
	Pop	Acc	Pop × Acc	Pop	Acc	Pop × Acc
Auxiliary BAT	**$F_{1,18}$ = 5.07 P = 0.04**	$F_{1,18}$ = 1.15 P = 0.30	$F_{1,18}$ < 0.01 P = 0.99	$F_{1,17}$ = 1.40 P = 0.25	$F_{1,17}$ = 2.10 P = 0.17	$F_{1,17}$ = 0.53 P = 0.48
Bicep Brachii	$F_{1,16}$ = 1.88 P = 0.19	$F_{1,16}$ > 0.01 P = 0.95	$F_{1,16}$ = 0.03 P = 0.87	**$F_{1,16}$ = 8.57 P < 0.01**	$F_{1,16}$ = 0.09 P = 0.76	$F_{1,16}$ = 0.58 P = 0.46
Bicep Femoris	$F_{1,18}$ = 1.54 P = 0.23	$F_{1,18}$ = 2.273 P = 0.15	$F_{1,18}$ = 0.04 P = 0.85	$F_{1,18}$ = 2.92 P = 0.10	**$F_{1,18}$ = 8.32 P < 0.01**	$F_{1,18}$ = 2.02 P = 0.17
Diaphragm	$F_{1,18}$ = 0.75 P = 0.40	$F_{1,18}$ = 0.48 P = 0.50	$F_{1,18}$ = 0.72 P = 0.41	-	-	-
Extensor Digitorum Longus	$F_{1,18}$ = 0.21 P = 0.65	$F_{1,18}$ = 1.74 P = 0.20	$F_{1,18}$ = 0.21 P = 0.66	$F_{1,17}$ = 3.46 P = 0.08	$F_{1,17}$ = 2.37 P = 0.14	$F_{1,17}$ = 3.19 P = 0.09
Erector Spinae	**$F_{1,17}$ = 15.75 P < 0.01**	**$F_{1,17}$ = 5.15 P = 0.04**	$F_{1,17}$ = 0.01 P = 0.91	$F_{1,18}$ = 0.45 P = 0.51	**$F_{1,18}$ = 4.45 P = 0.05**	$F_{1,18}$ = 0.35 P = 0.56
Gluteus	$F_{1,18}$ = 1.84 P = 0.19	$F_{1,18}$ = 0.72 P = 0.41	$F_{1,18}$ = 0.14 P = 0.71	$F_{1,18}$ = 1.57 P = 0.23	$F_{1,18}$ = 0.69 P = 0.42	$F_{1,18}$ = 0.02 P = 0.88
Gonadal WAT	$F_{1,18}$ = 0.08 P = 0.78	$F_{1,18}$ < 0.01 P = 0.96	$F_{1,18}$ = 0.05 P = 0.83	$F_{1,17}$ = 0.78 P = 0.39	$F_{1,17}$ = 0.33 P = 0.57	$F_{1,17}$ = 0.65 P = 0.43
Interscapular BAT	**$F_{1,18}$ = 12.87 P < 0.01**	$F_{1,18}$ = 2.66 P = 0.12	$F_{1,18}$ = 0.10 P = 0.75	**$F_{1,18}$ = 9.14 P < 0.01**	**$F_{1,18}$ = 8.66 P < 0.01**	$F_{1,18}$ = 2.03 P = 0.17
Inguinal WAT	$F_{1,18}$ = 2.74 P = 0.12	$F_{1,18}$ = 1.16 P = 0.30	$F_{1,18}$ = 1.32 P = 0.27	$F_{1,18}$ = 0.08 P = 0.78	$F_{1,18}$ = 0.58 P = 0.46	$F_{1,18}$ = 1.89 P = 0.19
Liver	$F_{1,17}$ = 1.48 P = 0.24	$F_{1,17}$ = 1.87 P = 0.19	$F_{1,17}$ < 0.01 P = 0.97	-	-	-
Left Ventricle	$F_{1,18}$ = 1.16 P = 0.30	$F_{1,18}$ = 1.53 P = 0.23	$F_{1,18}$ = 1.43 P = 0.25	-	-	-
Masseter	$F_{1,17}$ = 2.57 P = 0.13	$F_{1,17}$ = 1.60 P = 0.22	$F_{1,17}$ = 0.87 P = 0.37	$F_{1,17}$ = 0.94 P = 0.35	**$F_{1,17}$ = 4.73 P = 0.04**	$F_{1,17}$ = 0.81 P = 0.38
Rectus Femoris	$F_{1,18}$ < 0.01 P = 0.94	$F_{1,18}$ = 1.35 P = 0.26	$F_{1,18}$ = 0.73 P = 0.40	**$F_{1,18}$ = 18.05 P < 0.01**	**$F_{1,18}$ = 4.74 P = 0.04**	$F_{1,18}$ = 0.27 P = 0.61
Red Gastrocnemius	$F_{1,18}$ = 0.09 P = 0.77	$F_{1,18}$ = 0.32 P = 0.56	$F_{1,18}$ = 0.99 P = 0.33	**$F_{1,18}$ = 6.87 P = 0.02**	$F_{1,18}$ = 0.63 P = 0.44	$F_{1,18}$ = 0.01 P = 0.92
Right Ventricle	$F_{1,18}$ = 0.11 P = 0.74	$F_{1,18}$ = 0.68 P = 0.42	$F_{1,18}$ = 0.24 P = 0.63	-	-	-
Soleus	$F_{1,16}$ = 0.65 P = 0.43	$F_{1,16}$ = 2.92 P = 0.11	$F_{1,16}$ = 0.80 P = 0.38	$F_{1,16}$ = 2.08 P = 0.17	$F_{1,16}$ = 2.47 P = 0.14	$F_{1,16}$ = 2.34 P = 0.15
Semitendinosus	$F_{1,18}$ = 0.64 P = 0.44	$F_{1,18}$ = 1.97 P = 0.18	$F_{1,18}$ = 0.24 P = 0.63	$F_{1,18}$ = 1.90 P = 0.18	$F_{1,18}$ = 2.56 P = 0.13	$F_{1,18}$ = 0.01 P = 0.92
Tibialis Anterior	$F_{1,17}$ < 0.01 P = 0.98	**$F_{1,17}$ = 4.80 P = 0.04**	$F_{1,17}$ = 0.82 P = 0.38	**$F_{1,17}$ = 12.40 P < 0.01**	**$F_{1,17}$ = 10.49 P < 0.01**	$F_{1,17}$ = 0.02 P = 0.88
Trapezius	$F_{1,17}$ = 3.02 P = 0.10	$F_{1,17}$ = 0.14 P = 0.71	$F_{1,17}$ = 0.59 P = 0.45	$F_{1,18}$ = 2.29 P = 0.15	$F_{1,18}$ = 0.72 P = 0.41	$F_{1,18}$ = 4.13 P = 0.06
Triceps	$F_{1,18}$ = 0.02 P = 0.88	$F_{1,18}$ = 0.42 P = 0.52	$F_{1,18}$ = 0.04 P = 0.85	**$F_{1,18}$ = 6.09 P = 0.02**	$F_{1,18}$ = 1.11 P = 0.31	$F_{1,18}$ = 0.34 P = 0.57
Vastus Lateralis	$F_{1,17}$ = 2.04 P = 0.17	$F_{1,17}$ = 2.92 P = 0.11	$F_{1,17}$ = 1.04 P = 0.32	$F_{1,18}$ = 0.78 P = 0.39	$F_{1,18}$ = 4.08 P = 0.06	$F_{1,18}$ = 0.01 P = 0.91
Vastus Medialis	$F_{1,17}$ = 2.84 P = 0.11	$F_{1,17}$ = 1.06 P = 0.32	$F_{1,17}$ = 1.07 P = 0.32	$F_{1,17}$ = 0.09 P = 0.76	$F_{1,17}$ = 2.66 P = 0.12	$F_{1,17}$ = 0.76 P = 0.40
White Gastrocnemius	$F_{1,18}$ = 0.37 P = 0.55	**$F_{1,18}$ = 4.90 P = 0.04**	$F_{1,18}$ = 0.02 P = 0.89	$F_{1,18}$ = 3.37 P = 0.08	**$F_{1,18}$ = 7.17 P = 0.02**	$F_{1,18}$ = 0.52 P = 0.48

Figure 4.3

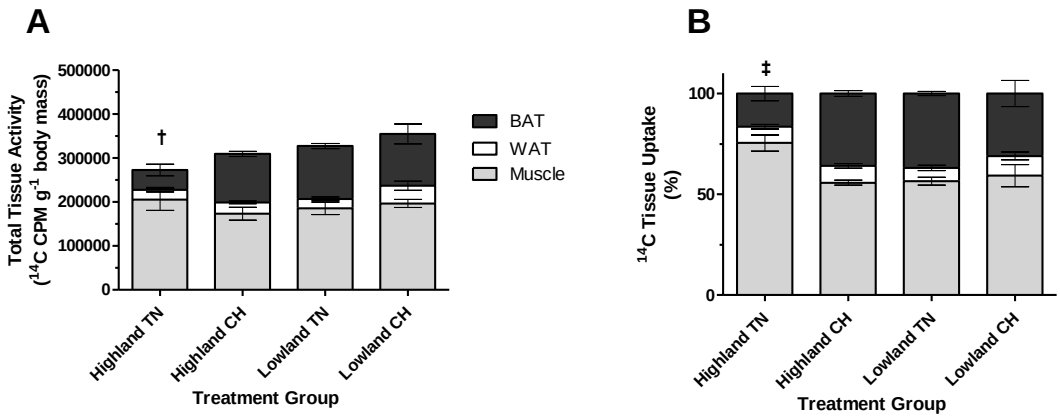
A
Total Tissue Activity
(14C CPM g-1 body mass)
500000
400000
300000
200000
100000
0
†
BAT
WAT
Muscle
Highland TN
Highland CH
Lowland TN
Lowland CH
Treatment Group
B
14C Tissue Uptake
(%)
100
50
0
‡
Highland TN
Highland CH
Lowland TN
Lowland CH
Treatment Group

Figure 4.3. The absolute (A) and relative uptake (B) of ^{14}C-bromopalmitic acid into muscle (light grey bar), white adipose tissue (WAT, white bar) and brown adipose tissue (BAT, dark grey bar) of highland and lowland deer mice acclimated to thermoneutral conditions (TN, 30ºC, 21kPa) or cold hypoxia (CH, 5ºC, 12kPa) exposed to a maximal cold challenge. Sample sizes for TN and CH were *N*=6 and *N*=5 for highlanders, and *N*=5 and *N*=6 for lowlanders, respectively. †TN highlander BAT are significantly different than CH highlander BAT ($P < 0.05$). ‡WN highlander muscle and BAT are significantly different than CH highlander muscle and BAT ($P < 0.05$). Data are reported as means ± s.e.m.

Figure 4.4

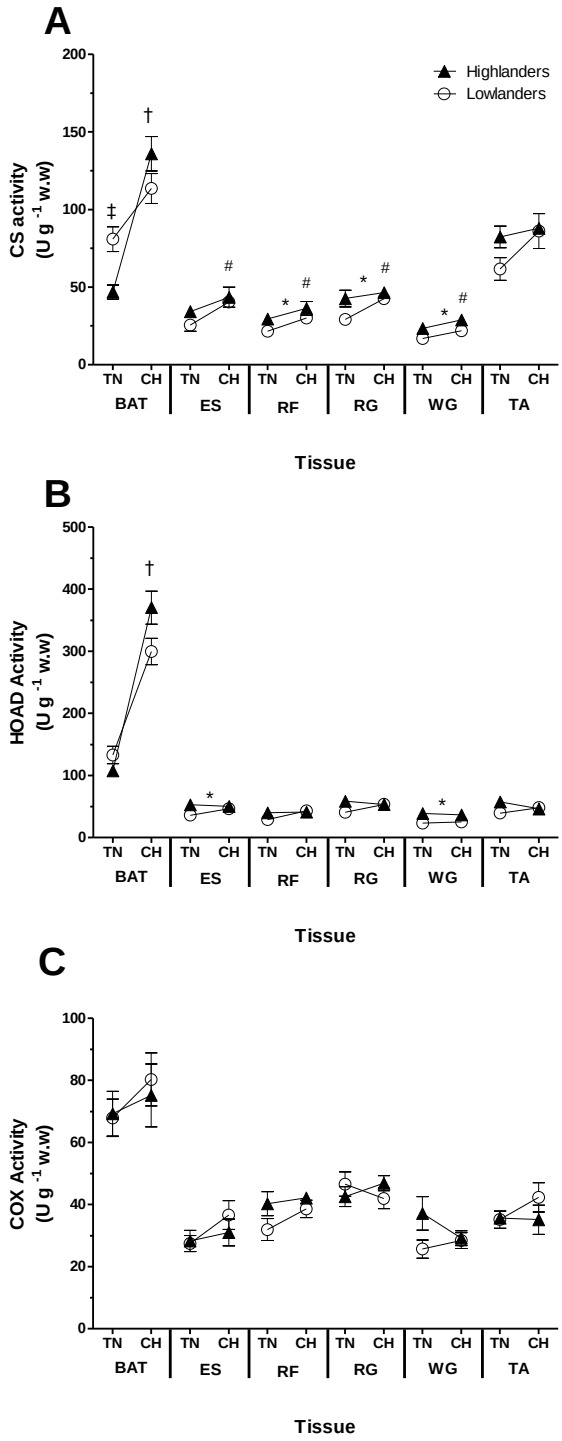
A
Highlanders
Lowlanders
CS activity (U g -1 w.w)
200
150
100
50
0
TN CH TN CH TN CH TN CH TN CH TN CH
BAT ES RF RG WG TA
Tissue
B
HOAD Activity (U g -1 w.w)
500
400
300
200
100
0
TN CH TN CH TN CH TN CH TN CH TN CH
BAT ES RF RG WG TA
Tissue
C
COX Activity (U g -1 w.w)
100
80
60
40
20
0
TN CH TN CH TN CH TN CH TN CH TN CH
BAT ES RF RG WG TA
Tissue

Figure 4.4. Apparent maximal enzyme activities (Vmax) of citrate synthase (CS) (A), ß-hydroxyacyl-CoA dehydrogenase (HOAD) (B), and cytochrome c oxidase (COX) (C) in the brown adipose tissue (BAT), erector spinae (ES), rectus femoris (RF), red gastrocnemius (RG), white gastrocnemius (WG) and tibialis anterior (TA). Second-generation laboratory born and raised highland and lowland deer mice (*Peromyscus maniculatus*), acclimated to thermoneutral (TN, 30^{o}C, 21 kPa O_2) or cold hypoxia (CH, 5^{o}C, 12 kPa O_2) conditions. All enzyme activities were standardized to g^{-1} of tissue wet weight (w.w). Symbols represent significant differences resulting from Holm Sidak post hoc tests ($P < 0.05$). *Significant difference between populations. #Significant difference between acclimations. ‡TN highlanders are different than TN lowlanders. †CH highlanders are different than WN highlanders. Sample sizes for TN and CH were N=9 and N=6 for highlanders, and N=9 and N=6 for lowlanders, respectively. Data are reported as means ± s.e.m.

Figure 4.5

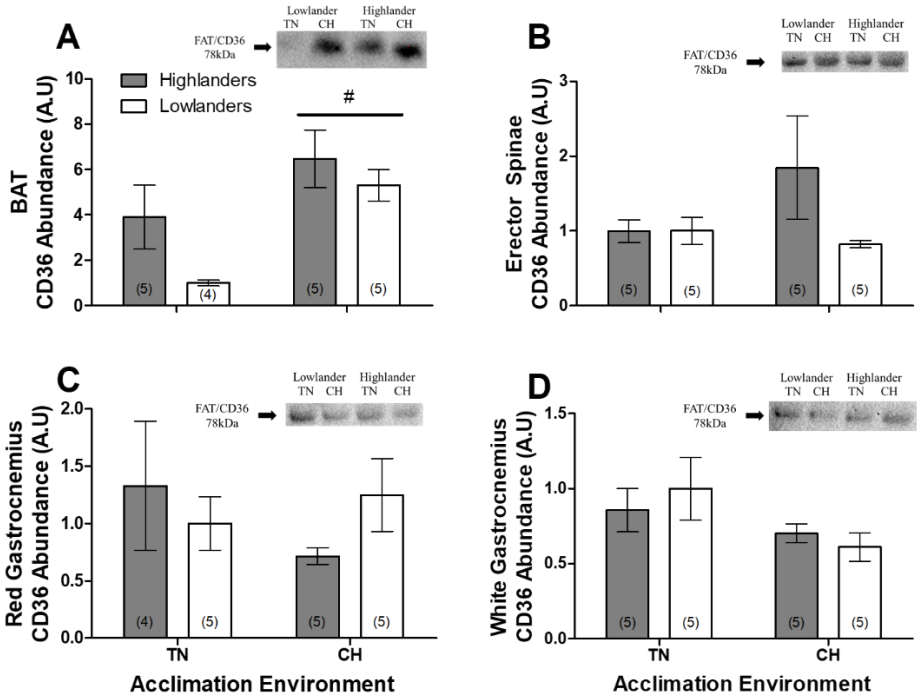
A
Lowlander TN CH
Highlander TN CH
FAT/CD36 78kDa
BAT CD36 Abundance (A.U)
Highlanders
Lowlanders
#
(5)
(4)
(5)
(5)
B
Erector Spinae CD36 Abundance (A.U)
C
Red Gastrocnemius CD36 Abundance (A.U)
D
White Gastrocnemius CD36 Abundance (A.U)
TN
CH
Acclimation Environment

Figure 4.5. Relative protein abundance of fatty acid translocase (FAT/CD36) in (A) interscapular brown adipose tissue (BAT), (B) erector spinae, (C) red gastrocnemius and (D) white gastrocnemius. Second-generation laboratory born and raised highland and lowland deer mice (*Peromyscus maniculatus*), acclimated to thermoneutral (TN, 30^{o}C, 21 kPa O_2) or cold hypoxia (CH, 5^{o}C, 12 kPa O_2) conditions. Representative western blots are shown for each tissue. #Significant difference between acclimations ($P < 0.05$). Sample sizes for each treatment group are shown in parentheses at the bottom of the bar. Data are reported as means ± s.e.m.

4.9 REFERENCES

1. **Armstrong RB, Essén-Gustavsson B, Hoppeler H, Jones JH, Kayar SR, Laughlin MH, Lindholm A, Longworth KE, Taylor CR, Weibel ER.** O2 delivery at VO2max and oxidative capacity in muscles of standardbred horses. *J Appl Physiol* 73:2274–82, 1992. doi: 10.1152/jappl.1992.73.6.2274.

2. **Beaudry JL**, **McClelland GB**. Thermogenesis in CD-1 mice after combined chronic hypoxia and cold acclimation. *Comp Biochem Physiol - B Biochem Mol Biol* 157: 301–309, 2010. doi: 10.1016/j.cbpb.2010.07.004.

3. **Blondin DP**, **Tingelstad HC**, **Mantha OL**, **Gosselin C**, **Haman F**. Maintaining thermogenesis in cold exposed humans: Relying on multiple metabolic pathways. *Compr Physiol* 4: 1383–1402, 2014. doi: 10.1002/cphy.c130043.

4. **Blondin DP**, **Tingelstad HC**, **Noll C**, **Frisch F**, **Phoenix S**, **Guérin B**, **Turcotte ÉE**, **Richard D**, **Haman F**, **Carpentier AC**. Dietary fatty acid metabolism of brown adipose tissue in cold-acclimated men. *Nat Commun* 8, 2017. doi: 10.1038/ncomms14146.

5. **Cannon B**, **Nedergaard J**. Brown Adipose Tissue: Function and Physiological Significance. *Physiol Rev* 84: 277–359, 2004. doi: 10.1152/physrev.00015.2003.

6. **Cheviron ZA**, **Bachman GC**, **Connaty AD**, **McClelland GB**, **Storz JF**. Regulatory changes contribute to the adaptive enhancement of thermogenic capacity in high-altitude deer mice. *Proc Natl Acad Sci* 109: 8635–8640, 2012. doi: 10.1073/pnas.1120523109.

7. **Coulson SZ**, **Robertson CE**, **Mahalingam S**, **McClelland GB**. Plasticity of non-shivering thermogenesis and brown adipose tissue in high-altitude deer mice. *J Exp Biol* 224, 2021. doi: 10.1242/jeb.242279.

8. **Foster DO**, **Frydman ML**. Tissue distribution of cold-induced thermogenesis in conscious warm- or cold-acclimated rats reevaluated from changes in tissue blood flow: The dominant role of brown adipose tissue in the replacement of shivering by nonshivering thermogenesis. *Can J Physiol Pharmacol* 57: 257–270, 1979. doi: 10.1139/y79-039.

9. **Furler SM**, **Cooney GJ**, **Hegarty BD**, **Lim-Fraser MY**, **Kraegen EW**, **Oakes ND**. Local factors modulate tissue-specific NEFA utilization: Assessment in rats using 3H-(R)-2-Bromopalmitate. *Diabetes* 49: 1427–1433, 2000. doi: 10.2337/diabetes.49.9.1427.

10. **Hauton D**, **Coney AM**, **Egginton S**. Both substrate availability and utilisation contribute to the defence of core temperature in response to acute cold. *Comp Biochem Physiol - A Mol Integr Physiol* 154: 514–522, 2009. doi: 10.1016/j.cbpa.2009.08.008.

11. **Hayward L**, **Robertson CE**, **McClelland GB**. Phenotypic plasticity to chronic

cold exposure in two species of Peromyscus from different environments. *J Comp Physiol B Biochem Syst Environ Physiol* 192: 335–348, 2022. doi: 10.1007/s00360-021-01423-4.

12. **Hegarty BD**, **Cooney GJ**, **Kraegen EW**, **Furler SM**. Increased efficiency of fatty acid uptake contributes to lipid accumulation in skeletal muscle of high fat-fed insulin-resistant rats. *Diabetes* 51: 1477–1484, 2002. doi: 10.2337/diabetes.51.5.1477.

13. **Jastroch M**, **Polymeropoulos ET**, **Gaudry MJ**. Pros and cons for the evidence of adaptive non-shivering thermogenesis in marsupials. *J Comp Physiol B Biochem Syst Environ Physiol* 191: 1085–1095, 2021. doi: 10.1007/s00360-021-01362-0.

14. **Lau DS**, **Connaty AD**, **Mahalingam S**, **Wall N**, **Cheviron ZA**, **Storz JF**, **Scott GR**, **McClelland GB**. Acclimation to hypoxia increases carbohydrate use during exercise in high-altitude deer mice. *Am J Physiol - Regul Integr Comp Physiol* 312: R400–R411, 2017. doi: 10.1152/ajpregu.00365.2016.

15. **Laughlin MH**, **Armstrong RB**. Muscular blood flow distribution patterns as a function of running speed in rats. *Am J Physiol - Hear Circ Physiol* 12, 1982. doi: 10.1152/ajpheart.1982.243.2.h296.

16. **Lui MA**, **Mahalingam S**, **Patel P**, **Connaty AD**, **Ivy CM**, **Cheviron ZA**, **Storz JF**, **McClelland GB**, **Scott GR**. High-altitude ancestry and hypoxia acclimation have distinct effects on exercise capacity and muscle phenotype in deer mice. *Am J Physiol - Regul Integr Comp Physiol* 308: R779–R791, 2015. doi: 10.1152/ajpregu.00362.2014.

17. **Lyons SA**, **McClelland GB**. Thermogenesis is supported by high rates of circulatory fatty acid and triglyceride delivery in highland deer mice. *J Exp Biol* 225, 2022. doi: 10.1242/jeb.244080.

18. **Lyons SA**, **Tate KB**, **Welch Jr. KC**, **McClelland GB**. Lipid oxidation during thermogenesis in high-altitude deer mice (Peromyscus maniculatus) . *Am J Physiol Integr Comp Physiol* 320: R735–R746, 2021. doi: 10.1152/ajpregu.00266.2020.

19. **Mahalingam S**, **Cheviron ZA**, **Storz JF**, **McClelland GB**, **Scott GR**. Chronic cold exposure induces mitochondrial plasticity in deer mice native to high altitudes. *J Physiol* 598: 5411–5426, 2020. doi: 10.1113/JP280298.

20. **McClelland GB**, **Hochachka PW**, **Weber J-M**. Carbohydrate utilization during exercise after high-altitude acclimation: A new perspective. *Proc Natl Acad Sci U S A* 95: 10288–10293, 1998. doi: 10.1073/pnas.95.17.10288.

21. **McClelland GB**, **Scott GR**. Evolved Mechanisms of Aerobic Performance and Hypoxia Resistance in High-Altitude Natives. *Annu Rev Physiol* 81: 561–583, 2019. doi: 10.1146/annurev-physiol-021317-121527.

22. **McKie GL**, **Medak KD**, **Knuth CM**, **Shamshoum H**, **Townsend LK**, **Peppler WT**, **Wright DC**. Housing temperature affects the acute and chronic metabolic adaptations to exercise in mice. *J Physiol* 17: 4581–4600, 2019. doi: 10.1113/JP278221.

23. **Oakes ND**, **Kjellstedt A**, **Forsberg GB**, **Clementz T**, **Camejo G**, **Furler SM**, **Kraegen EW**, **Ölwegård-Halvarsson M**, **Jenkins AB**, **Ljung B**. Development and initial evaluation of a novel method for assessing tissue-specific plasma free fatty acid utilization in vivo using (R)-2- bromopalmitate tracer. *J Lipid Res* 40: 1155–1169, 1999.

24. **Oakes ND**, **Thalén P**, **Aasum E**, **Edgley A**, **Larsen T**, **Furler SM**, **Ljung B**, **Severson D**. Cardiac metabolism in mice: Tracer method developments and in vivo application revealing profound metabolic inflexibility in diabetes. *Am J Physiol - Endocrinol Metab* 290: 870–881, 2006. doi: 10.1152/ajpendo.00233.2005.

25. **Saari TJ**, **Raiko J**, **U-Din M**, **Niemi T**, **Taittonen M**, **Laine J**, **Savisto N**, **Haaparanta-Solin M**, **Nuutila P**, **Virtanen KA**. Basal and cold-induced fatty acid uptake of human brown adipose tissue is impaired in obesity. *Sci Rep* 10: 1–11, 2020. doi: 10.1038/s41598-020-71197-2.

26. **Schippers MP**, **LeMoine CMR**, **McClelland GB**. Patterns of fuel use during locomotion in mammals revisited: The importance of aerobic scope. *J Exp Biol* 217: 3193–3196, 2014. doi: 10.1242/jeb.099432.

27. **Schönke M**, **Massart J**, **Zierath JR**. Effects of high-fat diet and AMP-activated protein kinase modulation on the regulation of whole-body lipid metabolism. *J Lipid Res* 59: 1276–1282, 2018. doi: 10.1194/jlr.D082370.

28. **Tate KB, Ivy CM, Velotta JP, Storz JF, McClelland GB, Cheviron ZA, Scott GR.** Circulatory mechanisms underlying adaptive increases in thermogenic capacity in high-altitude deer mice. *J Exp Biol* 220(20): 3616-3620, 2017. doi: 10.1242/jeb.164491.

29. **Tate KB**, **Wearing OH**, **Ivy CM**, **Cheviron ZA**, **Storz JF**, **McClelland GB**, **Scott GR**. Coordinated changes across the O2 transport pathway underlie adaptive increases in thermogenic capacity in high-altitude deer mice. *Proceedings Biol Sci* 287: 20192750, 2020. doi: 10.1098/rspb.2019.2750.

30. **u Din M**, **Raiko J**, **Saari T**, **Kudomi N**, **Tolvanen T**, **Oikonen V**, **Teuho J**, **Sipilä HT**, **Savisto N**, **Parkkola R**, **Nuutila P**, **Virtanen KA**. Human brown adipose tissue [15O]O2 PET imaging in the presence and absence of cold stimulus. *Eur J Nucl Med Mol Imaging* 43: 1878–1886, 2016. doi: 10.1007/s00259-016-3364-y.

31. **Vaillancourt E**, **Haman F**, **Weber JM**. Fuel selection in Wistar rats exposed to cold: Shivering thermogenesis diverts fatty acids from re-esterification to

oxidation. *J Physiol* 587: 4349–4359, 2009. doi: 10.1113/jphysiol.2009.175331.

32. **Van Sant MJ**, **Hammond KA**. Contribution of Shivering and Nonshivering Thermogenesis to Thermogenic Capacity for the Deer Mouse (*Peromyscus maniculatus*). *Physiol Biochem Zool* 81: 605–611, 2008. doi: 10.1086/588175.

CHAPTER 5: GENERAL DISCUSSION

The overall objective of my thesis was to understand how lipid metabolism has evolved to sustain the high rates of thermogenesis observed in deer mice living at high altitude. Furthermore, my goal was to elucidate whether the adaptations sustaining lipid metabolism at high altitude are due to fixed genetic traits and/or environmentally induced plasticity. Prior to my thesis work, the following **questions** were either unclear or unanswered: ***1*)** What are the rates of lipid oxidation in deer mice during submaximal and maximal intensities of thermogenesis? What proportion of total energy expenditure do lipids represent? How do thermogenic lipid oxidation rates compare to those observed during exercise? **2)** Which components of the lipid metabolic pathway contribute to differences in lipid oxidative capacity between populations of highland and lowland deer mice? **3)** What are the contributions of various thermo-effector tissues to maximal heat production in deer mice, and does this proportion change with acclimation to either thermoneutral or cold hypoxic conditions? My overarching hypothesis was that highland native deer mice are adapted to survive in the cold high alpine because there has been selection for high lipid oxidation to power heat production. In ***Chapter 2***, I determined that lipids are the primary fuel source for both submaximal and maximal intensities of thermogenesis in deer mice. The normoxic whole-animal lipid oxidation rates of maximally cold-challenged deer mice, especially cold hypoxia acclimated highlanders, were higher than those observed during running exercise. In fact, lipid oxidation at normoxic cold-induced $\dot{V}O_2max$ are the highest mass-specific rates of mammalian lipid oxidation recorded in the literature to date. Assessment of various key steps along the

lipid metabolic pathway in ***Chapter 3*** revealed that high rates of circulatory NEFA and TG delivery may dictate the high lipid oxidation rates observed in thermoregulating high-altitude deer mice. In ***Chapter 4***, I examined the relative distribution of circulating fatty acids during maximal heat production in deer mice by measuring fatty acid uptake into 24 tissues. I found that highland deer mice acclimated to cold hypoxia increased uptake of fatty acids into brown adipose tissue while decreasing uptake into shivering skeletal muscle. This acclimation response, observed only in highland BAT, provides further evidence that highlanders have overcome the inhibitory effects of hypoxia on the cold response, in contrast with what is commonly observed in lowland mice. Altogether, the data chapters of this thesis provide thorough evidence for how highland deer mice evolved increased capacities for lipid oxidation during thermogenesis, which has served to increase their survival in montane environments.

5.1 THE EVOLUTION OF LIPID USE AT HIGH ALTITUDE IN DEER MICE

Deer mice inhabiting the cold and hypoxic environment of high altitude face selective pressure to enhance heat producing capacities to ensure survival (Hayes and O'Connor, 1999). In Colorado, mountaintop summer temperatures peak at 10^{o}C and fall below -25^{o}C during the winter, temperatures far below the thermoneutral zone of deer mice (Hayward *et al.*, 2022). For mammals, lipids are a major fuel source for sustaining daily physical activities as lipids are largely abundant and provide high amounts of energy (Weber, 2011). Heat production has been reported to be primarily fuelled by lipids in an array of mammals, including humans (Ouellet *et al.*, 2012; Blondin *et al.*, 2014, 2015; Saari *et al.*, 2020), lab rats (Hauton *et al.*, 2009; Vaillancourt *et al.*, 2009; Labbé *et*

al., 2015), and deer mice (Cheviron *et al.*, 2012; Lyons *et al.*, 2021; Hayward *et al.*, 2022). An advantage of relying on lipids for long term thermogenesis is that carbohydrates are spared for more intense locomotory activity. Despite the lower ATP yield per mol O_2 in lipids compared to carbohydrates, deer mice faced with limited oxygen availability still use lipids to power thermogenesis (Cheviron *et al.*, 2012; Lyons *et al.*, 2021), highlighting the importance of using this metabolic substrate at high altitude (Figure 5.S1).

The deer mouse model used in this thesis provides a very powerful system for studying high-altitude physiology. Deer mice bred in common conditions, and acclimated to conditions simulating high altitude, allow us analyze traits associated with genetic ancestry and phenotypic plasticity in isolation. Highlanders that have been acclimated to high-altitude conditions display the highest thermogenic capacities and whole-animal lipid oxidation rates during cold-induced $\dot{V}O_2max$ compared to warm-acclimated highlanders, and lowlanders acclimated to warm normoxic and cold hypoxic conditions (Cheviron *et al.*, 2012; Tate *et al.*, 2020; Lyons *et al.*, 2021, Chapter 4). Interestingly, my main findings infer that circulatory lipid transport far exceeds the lipid supply required for thermogenic lipid oxidation (Figure 5.S2; Lyons and McClelland, 2022). High rates of lipid use are the end product of a complex and integrated response have been highlighted both in previous studies and in this thesis. In brief, the higher thermogenic capacities and lipid oxidation rates observed in highlanders can be attributed to the higher rates of fat-fuelled NST (Coulson *et al.*, 2021) and ST (Robertson and McClelland, 2019). The mechanisms that make whole-animal thermogenesis greater in highlanders are likely

linked to their increased cardiac output and plasma flow (Tate *et al.*, 2017, 2020), increased circulatory delivery of lipids to BAT and skeletal muscle (Lyons and McClelland, 2022; Chapter 4), higher BAT activity, respiration, and fatty acid uptake (Coulson *et al.*, 2021; Chapter 4), and increased skeletal muscle capillarity (Lui *et al.*, 2015), proportion of oxidative fibres (Lui *et al.*, 2015; Mahalingam *et al.*, 2017), and mitochondrial density/activity (Lau *et al.*, 2017; Mahalingam *et al.*, 2017; Mahalingam *et al.*, 2020; Dawson and Scott, 2022). These adaptations all serve to contribute to the high lipid oxidation rates observed in highland deer mice during maximal heat production.

In Chapter 3 (Lyons and McClelland, 2022), I proposed that high circulatory delivery of lipids plays a critical role in contributing to the high lipid oxidation rates observed during thermogenesis in highland deer mice. These findings may be supported by the fact that lipid and O_2 transport are both predominately dictated by the cardiovascular system. Because O_2 is more limited than metabolic substrates in mammals, O_2 delivery is a major determinant of cardiovascular function and as such, the circulatory transport pathway has most likely evolved to favour O_2 transport given how limiting O_2 is in mammalian metabolism (Weibel *et al.*, 1996). Interestingly, many of the adaptations associated with increased circulatory O_2 delivery may also benefit circulatory lipid transport. In highlanders, cardiac outputs and left ventricle ejection fractions are greater than those observed in lowland conspecifics, allowing for higher rates of blood transport throughout the body to working tissues (Tate *et al.*, 2017, 2020; Wearing *et al.*, 2022). Highlanders also have higher hemoglobin O_2-binding affinities (Storz *et al.*, 2010), which allow for higher arterial O_2 saturations in hypoxia and lower hematocrits (Lui *et al.*, 2015), and

increased plasma flow rates compared to lowlanders (Tate *et al.*, 2020; Lyons and McClelland, 2022). Increased plasma flow also serves to increase lipid transport, as NEFAs and TGs are circulated bound to albumin and lipoproteins in the circulation. Furthermore, increased tissue capillarity of highlanders offers increased diffusion surface area and uptake capacity for both O_2 and metabolic substrates (Lui *et al.*, 2015). Finally, the increased subsarcolemmal mitochondrial volume density of highland skeletal muscle decreases substrate diffusion distances and has been associated with increased fatty acid oxidative capacities (Mahalingam *et al.*, 2020; Dawson and Scott, 2022). Therefore, given the determining role of circulatory lipid transport in the high lipid oxidation rates observed in highland native deer mice, it may have evolved in concert with increasing O_2 transport in a hypoxic environment.

Remarkably, all these adaptations associated with increased fuel and O_2 transport coincide with the evolved physiology of migratory birds, the champions of metabolism. High O_2 extraction, high rates of O_2 and lipid (TGs and NEFAs) transport, high number of oxidative fibres, increased capillarity, high mitochondrial densities, high membrane/cytosolic concentrations of fatty acid binding protein and increased oxidation of lipids are all identified in migrating bar headed geese, which migrate over the Himalayas (Scott et al., 2015). Given the similarities of fuel use and O_2 transport between migrating birds and high-altitude deer mice, it becomes more impressive how these deer mice can achieve and sustain such high metabolic rates for thermogenesis and lipid metabolism.

High lipid oxidation rates during cold-induced $\dot{V}O_2max$ may be a performance trait not only important for maximal heat production. In the wild, it is unlikely that highland deer mice are constantly burning lipids at the high maximal rates measured in this thesis; however, they must be able to consistently sustain thermogenesis to maintain constant body temperatures. Both highland and lowland deer mice acclimated to either warm normoxia or cold hypoxia oxidize lipids at the same rate in moderate cold (0^{o}C, ~50-30% of normoxic cold-induced $\dot{V}O_2max$), suggesting a specific metabolic cost for submaximal thermogenesis (Lyons et al., 2021). Having a high maximal capacity for lipid oxidation allows submaximal thermogenesis to be sustained at low to moderate lipid oxidation rates. Given the increased capacity for lipid oxidation with cold hypoxia acclimation, wild highland deer mice are most likely sustaining rates of thermogenesis about 50% of cold-induced $\dot{V}O_2max$. This sustained and elevated metabolism would undoubtably be matched by an increase in food consumption, but unfortunately the highland deer mouse diet has not yet been identified. Food availability appears to be scarce at high altitude, and yet highland deer mice are well-nourished and thrive in this environment. These mice must have ecological strategies and physiological adaptations that allow them to effectively sustain fat reserves for heat production. Matching highland deer mouse diet to digestive physiology is a fruitful area for future research.

5.2 CIRCULATORY VS INTRACELLULAR TGS DURING THERMOGENESIS

TGs are energy dense lipid substrates that can be stored intracellularly in tissues like adipose tissue, liver, and muscle, or transported in the circulation bound to lipoproteins (very low-density lipoproteins, low-density lipoproteins, high-density lipoproteins, and

chylomicrons). Intracellular TGs have been reported to be the main source of fat for powering BAT activity in lab rats (Ouellet *et al.*, 2012; Blondin *et al.*, 2015; Labbé *et al.*, 2015), while circulating TGs demonstrate the greatest source of TG replenishment in the BAT of lab rats and humans (Bartelt *et al.*, 2011; Blondin *et al.*, 2017). Highland deer mice had greater plasma concentrations of TGs compared to lowlanders acclimated to both warm normoxia or cold hypoxic conditions. Interestingly, only highlanders acclimated to cold hypoxia demonstrated a massive increase in plasma TGs during cold-induced $\dot{V}O_2$max. These findings resulted in higher TG delivery rates during cold-induced $\dot{V}O_2$max in hypoxia (Lyons and McClelland, 2022). Two potential explanations for these elevated TG levels include 1) highlanders having an increased reliance on intracellular BAT TGs (Blondin *et al.*, 2015) and/or 2) highlanders having an increased reliance on circulatory uptake of NEFAs into BAT and skeletal muscle (Chapter 4). Both explanations could account for a decreased reliance of circulating TG during cold-induced $\dot{V}O_2$max and would allow for a pre-emptive increase of circulatory TGs in preparation for replenishing BAT TG stores (Bartelt *et al.*, 2011; Labbé *et al.*, 2015; Blondin *et al.*, 2017). A limitation for the studies performed in this thesis is that blood samples were taken at two specific time points (i.e., at rest or at $\dot{V}O_2$max) rather than multiple time points throughout the course of an experimental trial. As such, it remains unclear if the observed changes in plasma lipid content is associated with an increased rate of appearance or a decrease in lipid uptake.

If the contribution of circulatory lipids to support maximal thermogenesis is equivalent in highlanders compared to lowlanders, then plasma lipid delivery rates should

scale with whole-animal lipid oxidation. However, circulatory delivery of NEFAs and TGs were 1.8-fold and 2.3-fold greater in highlanders, well above what would be expected from simple scaling with lipid oxidation. These differences become even more pronounced following cold hypoxia acclimation, with NEFA delivery and TG delivery being 2.8-fold and 5.6-fold greater in highlanders, respectively (Figure 5.S2). This observation suggests that maximally thermoregulating highland deer mice have an abundance of circulatory lipids to satisfy maximal heat production. Perhaps the excess of highland circulatory NEFAs and TGs observed during cold-induced $\dot{V}O_2max$ indicate an increased NEFA-TG cycling as a supplementary form of NST (McClelland *et al.*, 2001; Reidy and Weber, 2002); however, NEFA-TG cycling has been shown to decrease during increased cold exposure in rats (Vaillancourt *et al.*, 2009).

Manipulating components of the lipid metabolic pathway to induce changes in thermogenesis can be a powerful way to test the relationship between lipid oxidation and lipid partitioning for thermogenesis. One way to study the effects of intracellular TG lipolysis on thermogenesis is by using nicotinic acid (NiAc), which binds to G_i protein-coupled receptors primarily expressed on adipocytes, and mediates an anti-lipolytic response (Tunaru *et al.*, 2003). Previous studies in rats and humans have demonstrated that with oral administration of NiAc, BAT activity, intracellular lipolysis, and NEFA uptake all decrease (Labbé *et al.*, 2015; Blondin *et al.*, 2017). Using these methods, I completed some preliminary work to better understand TG's role in whole-animal heat production and maintaining stable body temperatures in highland deer mice. I predicted that deer mice given NiAc would not be able to maintain their body temperatures during a

moderate cold exposure because intracellular BAT lipolysis would be hindered. In brief, post-absorptive (~3hours) highlanders acclimated to either thermoneutral or cold hypoxic conditions were exposed to 5ºC for 30 minutes, followed by an oral dose of NiAc or saline and placed back in 5ºC conditions for another 1.5 hours.

During a moderate cold challenge, respirometry indicated no differences in whole-animal lipid oxidation with NiAc administration, which was confirmed by no changes in plasma glycerol (an indicator for whole-animal lipolysis) (Figure 5.S3 and 5.S4A). Body temperature also remained stable throughout the entire trial, regardless of treatment or acclimation (Figure 5.S3). Plasma TG concentration at the end of the trial trended to be lower in CH highlanders, which may suggest increased TG use, though this finding was not statistically significant ($P = 0.07$). Additionally, NiAc administration had no effect on plasma TG concentration ($P > 0.05$; Figure 5.S4B). These preliminary findings suggest that 1) NiAc dosing used in lab rats may be insufficient to significantly inhibit intracellular lipolysis in deer mice, 2) the metabolic demands may not have been sufficient to elicit any differences in the measured parameters, or 3) intracellular BAT TG lipolysis and oxidation may not contribute to thermogenesis in deer mice to the same extent observed in lab rats and human BAT. RERs remained the same throughout the entire trial for both treatment and acclimation groups (Figure 5.S3C and 5.3D) showing no indication of a shift in substrate oxidation. In cold-exposed humans, individuals dosed with NiAc showed decreased BAT intracellular TG oxidation; however, total whole-body lipid oxidation did not change compared to saline controls, similar to the findings in my preliminary study (Figure 5.S3E and 5.S3F). Interestingly, there was an increase in

muscle shivering in NiAc-dosed humans (Blondin *et al.*, 2017). Perhaps circulating TGs and NEFAs provided was sufficient substrate supply for shivering muscle and maintaining body temperature, despite the inhibition of BAT intracellular lipolysis. More works needs to be done to fully understand the role of intracellular BAT TGs during thermogenesis and a more thorough understanding of NiAc dose-response relationships is required in deer mice to extrapolate these preliminary findings.

Lipoprotein lipase (LPL) is an extracellular enzyme located on the endothelial surface of the vasculature and is responsible for breaking down TGs in the circulation for tissue uptake (Pirahanchi *et al.*, 2021). This protein is highly expressed in BAT, liver, and muscle and has been reported to play an important role in the uptake of TG-liberated fatty acids during thermogenesis (Jensen *et al.*, 2008; Bartelt *et al.*, 2011). Lab mice with higher LPL protein abundance demonstrate increased thermal tolerance during cold challenge; however, it is unknown whether LPL abundance or activity is greater in highland deer mice compared to lowlanders. I hypothesize that higher LPL abundance and activity allows highlanders to use circulatory TG stores and minimize reliance on circulating NEFAs and/or intracellular stores of TGs for thermogenesis, compared to lowlanders. I measured LPL activity by injecting mice with heparin, which causes LPLs bound to the endothelial wall to be released into the circulation. Plasma samples were collected, and LPL activities were quantified using an enzyme-linked immunosorbent assay in highlanders and lowlanders acclimated to thermoneutral and cold hypoxic conditions. Surprisingly, there were no significant differences between populations or acclimations for LPL activity (Figure 5.S5). A limitation of this method is that LPL

acquired from the plasma cannot be specifically linked to any tissue, as it can originate from anywhere throughout the organism. Additionally, tissue blood flow during the heparin injection may effect the levels of LPL measured. Therefore, an assessment of both tissue specific LPL activity and protein abundance will provide a more thorough understanding for LPL's role in TG metabolism in thermoregulating deer mice.

To observe the impact of LPL function on whole-animal lipid oxidation during thermogenesis, I adapted methods from Bartelt *et al*., (2011), and injected an LPL inhibitor (tetrahydrolipstatin; THL) in highland deer mice immediately before a cold-induced $\dot{V}O_2max$ trial and then assessed thermogenic capacity. During maximal cold challenge, THL had no affect on maximal oxygen consumption, RER, whole-animal lipid oxidation, plasma glycerol or TG concentrations (Figure 5.S6). The lack of changes at the whole-animal level for LPL function might suggest that 1) THL concentrations may not have been sufficiently high enough to effectively inhibit LPL, or 2) highland deer mice are primarily using circulating NEFAs and/or intracellular stores of TGs during cold-induced $\dot{V}O_2max$. If the latter is true, this would support the conclusions from the NiAc study. Perhaps the high TGs concentrations observed in highlanders are serving predominately as a recovery response after intense bouts of thermogenesis rather than a direct fuel source during thermogenesis. Future studies should focus on TG metabolism in the context of thermogenesis, to deepen our understanding of lipid metabolism in deer mice, and in mammals in general.

5.3 LIMITATIONS

In this thesis, the projects use a wide array of experimental designs and techniques to study the challenging topic of lipid metabolism, from the whole-animal level to the tissue level. As with all experiments, some limitations and assumptions were made for select experiments performed in this thesis. In chapter 2 and 4, whole-animal lipid oxidation rates during thermogenesis were quantified; however, the contribution of protein oxidation was ignored, given the negligible contribution of protein oxidation at high metabolic rates (<5%). As such, whole-animal lipid oxidation rates may have been slightly overestimated. Cold-induced $\dot{V}O_2max$ was used as a performance metric for thermogenic capacity and survival at high altitude, although, mice in the wild are rarely working at such a high metabolic rate. To compensate for this extreme view, measurements should also be taken at more ecologically relevant temperatures, as performed in chapter 2 at 0^oC. Additionally, the blood measurements in all three data chapters were taken from mice either at rest or during cold-induced $\dot{V}O_2max$, providing an instantaneous measure of NEFA and TG concentrations. Taking blood measurements over the course of the experimental trial would provide a better understanding of blood metabolite kinetics; however, given the size and nature of the deer mice, this protocol was not possible. This limitation was also the reason tissue specific uptake rates of ^{14}C-bromopalmitic acid were not quantified, as multiple blood measurements over the course of the trial was required. Lastly, in chapter 3 and 4, while the enzyme assays performed in select tissues provided maximal rates of enzyme activities, it is important to remember that they are not reflecting enzymatic activity in vivo.

5.4 CONCLUDING REMARKS

Highland native deer mice have evolved an enhanced energy supply to sustain heat production. These small endotherms have evolved amazing capacities for lipid oxidation to power heat production, which has undoubtably served to enhance their survival in what lowland natives consider to be an extremely challenging environment. Highlander lipid oxidation rates are likely greater than lowlanders because of their ability to overcome the limitations associated with hypoxia on NST-BAT activity, all the while increasing their lipid delivery to thermo-effector tissues through adaptations associated with O_2 transport. Furthermore, thermogenic lipid oxidation rates are likely greater than rates observed during running exercise because of the greater recruitment of working muscle required for shivering and an increased uptake of circulatory fatty acids into BAT and muscle. While the role of circulatory TGs in highland thermoregulating deer mice is unclear, preliminary findings may suggest that high circulatory TGs in highlanders are being used to replenish intracellular TGs stores in thermo-active tissues, presumably BAT. Altogether, the findings of this thesis demonstrate the unique adaptations along the lipid metabolic pathway that highlanders have adapted to survive the cold and hypoxic conditions of high altitude.

Future work should further elucidate how circulatory and intracellular TGs contribute to total heat production in deer mice. In addition, determining the diet and the dietary preferences of wild highland deer mice is imperative for understanding how high rates of metabolism can be sustained in montane environments. This work demonstrates the importance of studying animals from extreme environments as it allows us to deepen our

understanding about the evolution of metabolic pathways and how these pathways have been designed to function in extraordinary physiological conditions.

5.4 REFERENCES

Bartelt, A., Bruns, O. T., Reimer, R., Hohenberg, H., Ittrich, H., Peldschus, K., ... & Heeren, J. (2011). Brown adipose tissue activity controls triglyceride clearance. *Nature medicine*, 17(2), 200-205. doi:10.1038/nm.2297.

Blondin, D. P., Tingelstad, H. C., L. Mantha, O., Gosselin, C., & Haman, F. (2011). Maintaining thermogenesis in cold exposed humans: relying on multiple metabolic pathways. *Comprehensive Physiology*, 4(4), 1383-1402. doi: 10.1002/cphy.c130043.

Blondin, D. P., Labbé, S. M., Phoenix, S., Guérin, B., Turcotte, E. E., Richard, D., ... & Haman, F. (2015). Contributions of white and brown adipose tissues and skeletal muscles to acute cold-induced metabolic responses in healthy men. *The Journal of physiology*, 593(3), 701-714. doi: 10.1113/jphysiol.2014.283598.

Blondin, D. P., Frisch, F., Phoenix, S., Guérin, B., Turcotte, É. E., Haman, F., ... & Carpentier, A. C. (2017). Inhibition of intracellular triglyceride lipolysis suppresses cold-induced brown adipose tissue metabolism and increases shivering in humans. *Cell metabolism*, 25(2), 438-447. doi: 10.1016/j.cmet.2016.12.005.

Cheviron, Z. A., Bachman, G. C., Connaty, A. D., McClelland, G. B., & Storz, J. F. (2012). Regulatory changes contribute to the adaptive enhancement of thermogenic capacity in high-altitude deer mice. *Proceedings of the National Academy of Sciences*, 109(22), 8635-8640. doi: 10.1073/pnas.1120523109.

Coulson, S. Z., Robertson, C. E., Mahalingam, S., & McClelland, G. B. (2021). Plasticity of non-shivering thermogenesis and brown adipose tissue in high-altitude deer mice. *Journal of Experimental Biology*, 224(10), jeb242279. doi: 10.1242/jeb.242279.

Dawson, N. J., & Scott, G. R. (2022). Adaptive increases in respiratory capacity and O2 affinity of subsarcolemmal mitochondria from skeletal muscle of high-altitude deer mice. T*he FASEB Journal*, 36(7), e22391. doi: 10.1096/fj.202200219R.

Hauton, D., Coney, A. M., & Egginton, S. (2009). Both substrate availability and utilisation contribute to the defence of core temperature in response to acute cold. *Comparative Biochemistry and Physiology Part A: Molecular & Integrative Physiology*, 154(4), 514-522. doi: 10.1016/j.cbpa.2009.08.008.

Hayes, J. P., & O'Connor, C. S. (1999). Natural selection on thermogenic capacity of high-altitude deer mice. *Evolution*, 53(4), 1280-1287. doi: 10.2307/2640830.

Hayward, L., Robertson, C. E., & McClelland, G. B. (2022). Phenotypic plasticity to chronic cold exposure in two species of Peromyscus from different environments. *Journal of Comparative Physiology B*, 192(2), 335-348. doi: 10.1007/s00360-021-01423-4.

Jensen, D. R., Knaub, L. A., Konhilas, J. P., Leinwand, L. A., MacLean, P. S., & Eckel,

R. H. (2008). Increased thermoregulation in cold-exposed transgenic mice overexpressing lipoprotein lipase in skeletal muscle: an avian phenotype? *Journal of lipid research*, 49(4), 870-879. doi: 10.1194/jlr.M700519-JLR200.

Labbe, S. M., Caron, A., Bakan, I., & Laplante, M. M., Carpentier, AC, Lecomte, R., and D. Richard. (2015). In vivo measurement of energy substrate contribution to cold induced brown adipose tissue thermogenesis. *The FASEB Journal*, 29, 2046-2058. doi: 10.1096/fj.14-266247.

Lau, D. S., Connaty, A. D., Mahalingam, S., Wall, N., Cheviron, Z. A., Storz, J. F., ... & McClelland, G. B. (2017). Acclimation to hypoxia increases carbohydrate use during exercise in high-altitude deer mice. *American Journal of Physiology-Regulatory, Integrative and Comparative Physiology*, 312(3), R400-R411. doi: 10.1152/ajpregu.00365.2016.

Lui, M. A., Mahalingam, S., Patel, P., Connaty, A. D., Ivy, C. M., Cheviron, Z. A., ... & Scott, G. R. (2015). High-altitude ancestry and hypoxia acclimation have distinct effects on exercise capacity and muscle phenotype in deer mice. *American Journal of Physiology-Regulatory, Integrative and Comparative Physiology*, 308(9), R779-R791. doi: 10.1152/ajpregu.00362.2014.

Lyons, S. A., Tate, K. B., Welch Jr, K. C., & McClelland, G. B. (2021). Lipid oxidation during thermogenesis in high-altitude deer mice (Peromyscus maniculatus). *American Journal of Physiology-Regulatory, Integrative and Comparative Physiology*, 320(5), R735-R746. doi: 10.1152/ajpregu.00266.2020.

Lyons, S. A., & McClelland, G. B. (2022). Thermogenesis is supported by high rates of circulatory fatty acid and triglyceride delivery in highland deer mice. *Journal of Experimental Biology*. doi: 10.1242/jeb.244080.

Mahalingam, S., Cheviron, Z. A., Storz, J. F., McClelland, G. B., & Scott, G. R. (2020). Chronic cold exposure induces mitochondrial plasticity in deer mice native to high altitudes. *The Journal of Physiology*, 598(23), 5411-5426. doi: 10.1113/JP280298.

Mahalingam, S., McClelland, G. B., & Scott, G. R. (2017). Evolved changes in the intracellular distribution and physiology of muscle mitochondria in high-altitude native deer mice. *The Journal of Physiology*, 595(14), 4785-4801. doi: 10.1113/JP274130.

McClelland, G. B., Hochachka, P. W., Reidy, S. P., & Weber, J. M. (2001). High-altitude acclimation increases the triacylglycerol/fatty acid cycle at rest and during exercise. *American Journal of Physiology-Endocrinology And Metabolism*, 281(3), E537-E544. doi: 10.1152/ajpendo.2001.281.3.E537.

Ouellet, V., Labbé, S. M., Blondin, D. P., Phoenix, S., Guérin, B., Haman, F., ... & Carpentier, A. C. (2012). Brown adipose tissue oxidative metabolism contributes to energy expenditure during acute cold exposure in humans. *The Journal of Clinical Investigation*, 122(2), 545-552. doi: 10.1172/JCI60433DS1.

Pirahanchi, Y., Anoruo, M., & Sharma, S. (2022). Biochemistry, lipoprotein lipase. *StatPearls Publishing* [Internet].

Reidy, S. P., & Weber, J. M. (2002). Accelerated substrate cycling: a new energy-wasting role for leptin in vivo. *American Journal of Physiology-Endocrinology and Metabolism*, 282(2), E312-E317. doi: 10.1152/ajpendo.00037.2001.

Robertson, C. E., & McClelland, G. B. (2019). Developmental delay in shivering limits thermogenic capacity in juvenile high-altitude deer mice (Peromyscus maniculatus). *Journal of Experimental Biology*, 222(21), jeb210963. doi: 10.1242/jeb.210963.

Saari, T. J., Raiko, J., U-Din, M., Niemi, T., Taittonen, M., Laine, J., ... & Virtanen, K. A. (2020). Basal and cold-induced fatty acid uptake of human brown adipose tissue is impaired in obesity. *Scientific Reports*, 10(1), 1-11. doi: 10.1038/s41598-020-71197-2.

Scott, Graham R., Lucy A. Hawkes, Peter B. Frappell, Patrick J. Butler, Charles M. Bishop, and William K. Milsom. "How bar-headed geese fly over the Himalayas." *Physiology* 30 (2), (2015): 107-115. https://doi.org/10.1152/physiol.00050.2014

Storz, J. F., Runck, A. M., Moriyama, H., Weber, R. E., & Fago, A. (2010). Genetic differences in hemoglobin function between highland and lowland deer mice. *Journal of Experimental Biology*, 213(15), 2565-2574. doi: 10.1242/jeb.042598.

Tate, K. B., Ivy, C. M., Velotta, J. P., Storz, J. F., McClelland, G. B., Cheviron, Z. A., & Scott, G. R. (2017). Circulatory mechanisms underlying adaptive increases in thermogenic capacity in high-altitude deer mice. *Journal of Experimental Biology*, 220(20), 3616-3620. doi: 10.1242/jeb.164491.

Tate, K. B., Wearing, O. H., Ivy, C. M., Cheviron, Z. A., Storz, J. F., McClelland, G. B., & Scott, G. R. (2020). Coordinated changes across the O2 transport pathway underlie adaptive increases in thermogenic capacity in high-altitude deer mice. *Proceedings of the Royal Society B*, 287(1927), 20192750. doi: 10.1098/rspb.2019.2750.

Tunaru, S., Kero, J., Schaub, A., Wufka, C., Blaukat, A., Pfeffer, K., and Offermanns, S. (2003) Nat. Med. 9, 352–355. doi: 10.1038/nm824.

Vaillancourt, E., Haman, F., & Weber, J. M. (2009). Fuel selection in Wistar rats exposed to cold: shivering thermogenesis diverts fatty acids from re-esterification to oxidation. *The Journal of Physiology*, 587(17), 4349-4359. doi: 10.1113/jphysiol.2009.175331.

Wearing, O. H., Nelson, D., Ivy, C. M., Crossley II, D. A., & Scott, G. R. (2022). Adrenergic control of the cardiovascular system in deer mice native to high altitude. *Current Research in Physiology*, 5, 83-92. doi: 10.1016/j.crphys.2022.01.006.

Weber, J. M. (2011). Metabolic fuels: regulating fluxes to select mix. *Journal of Experimental Biology*, 214(2), 286-294. doi: 10.1242/jeb.047050.

Weibel, E. R., Taylor, C. R., Weber, J. M., Vock, R. U. T. H., Roberts, T. J., & Hoppeler, H. A. N. S. (1996). Design of the oxygen and substrate pathways. VII. Different structural limits for oxygen and substrate supply to muscle mitochondria. *The Journal of Experimental Biology*, 199(8), 1699-1709. doi: 10.1242/jeb.199.8.1699

APPENDIX A
Table 2.S1

Table S1. Breathing frequency (f_R), tidal volume (V_T), total ventilation (V_I), and pulmonary oxygen extraction efficiency (ELO_2) of first-generation laboratory born and raised highland and lowland *Peromyscus* mice, acclimated to control (warm normoxia) or cold hypoxia, exposed to ambient temperatures of 30°C and 0°C. Values are means ± SEM.

	Lowland (*P. leucopus*)				Lowland (*P. maniculatus*)				Highland (*P. maniculatus*)			
	Warm Normoxia		Cold Hypoxia		Warm Normoxia		Cold Hypoxia		Warm Normoxia		Cold Hypoxia	
	30°C	0°C	30°C	0°C	30°C	0°C	30°C	0°C	30°C	0°C	30°C	0°C
f_R (min^{-1})	125 ± 6	303 ± 10^a	112 ± 7	276 ± 20^a	165 ± 7	305 ± 16^a	139 ± 15	288 ± 14^a	115 ± 6^c	271 ± 21^a	114 ± 10^c	267 ± 7^a
V_T (µl g^{-1})	6.6 ± 0.4	9.4 ± 1.0^a	8.1 ± 0.8^b	9.9 ± 1.0^a	6.4 ± 0.4	9.7 ± 0.1^a	8.6 ± 0.7^b	10.4 ± 0.7^a	8.5 ± 0.4^d	10.3 ± 0.9^a	9.7 ± 0.8^{bd}	11.6 ± 0.7^a
V_I (ml g^{-1} min^{-1})	0.8 ± 0.1^c	2.8 ± 0.2^a	0.9 ± 0.1^c	2.7 ± 0.2^a	1.0 ± 0.1	2.9 ± 0.2^a	1.1 ± 0.1	2.9 ± 0.1^a	1.0 ± 0.1	2.7 ± 0.2^a	1.1 ± 0.1	3.1 ± 0.1^a
ELO_2 (%)	21.6 ± 1.6	16.5 ± 1.9^c	17.1 ± 2.3	16.6 ± 0.7^c	22.9 ± 1.4	23.0 ± 2.1	23.7 ± 1.6	22.4 ± 1.3^c	23.2 ± 1.9	22.1 ± 1.9	22.8 ± 2.3	18.7 ± 1.6

Symbols representing significant differences result from post-tests ($p<0.05$).
[a]Significantly different from 30°C
[b]Significantly different from warm normoxia within a given temperature
[c]Significantly different than lowland deer mice within a given temperature
[d]Significantly different than lowland deer mice and lowland white-footed mice within a given temperature

Table 2.S2

Table S2. Average breathing frequency (f_R), tidal volume (V_T), total ventilation (V_I), oxygen extraction efficiency (E_{LO_2}), and change in body temperature (ΔT_b) of first-generation laboratory born and raised highland and lowland *Peromyscus* mice, acclimated to control (warm normoxia) or cold hypoxia, during maximal cold challenge tested in normoxia using Heliox. Values are means ± SEM.

	Warm Normoxia			Cold Hypoxia		
	Highland Deer Mice	Lowland Deer Mice	White-Footed Mice	Highland Deer Mice	Lowland Deer Mice	White-Footed Mice
f_R (min^{-1})	494.14 ± 12.95	510.51 ± 21.06	399.41 ± 21.03	545.34 ± 29.13*	533.61 ± 21.51*	485.24 ± 15.31*
V_T ($\mu l\ g^{-1}$)	10.68 ± 0.87	10.56 ± 0.99	12.54 ± 0.93	12.78 ± 0.81*	14.14 ± 1.11*	11.05 ± 0.52*
V_I ($ml\ g^{-1}\ min^{-1}$)	5.21 ± 0.32	5.30 ± 0.47	5.02 ± 0.50	6.90 ± 0.42*	7.44 ± 0.50*	5.34 ± 0.22*
E_{LO_2} (%)	22.72 ± 1.90	24.67 ± 1.55	20.54 ± 2.62	27.73 ± 2.36	23.19 ± 1.82	23.68 ± 1.03
ΔT_b (°C)	-5.71 ± 0.49	-6.30 ± 0.58	-9.28 ± 0.66†	-4.22 ± 1.15*	-3.90 ± 0.54*	-7.08 ± 1.00*†

Symbols representing significant differences result from post-tests ($p<0.05$)
*Significant effect of acclimation
†Significantly different from high and lowland deer mice

Figure 2.S1

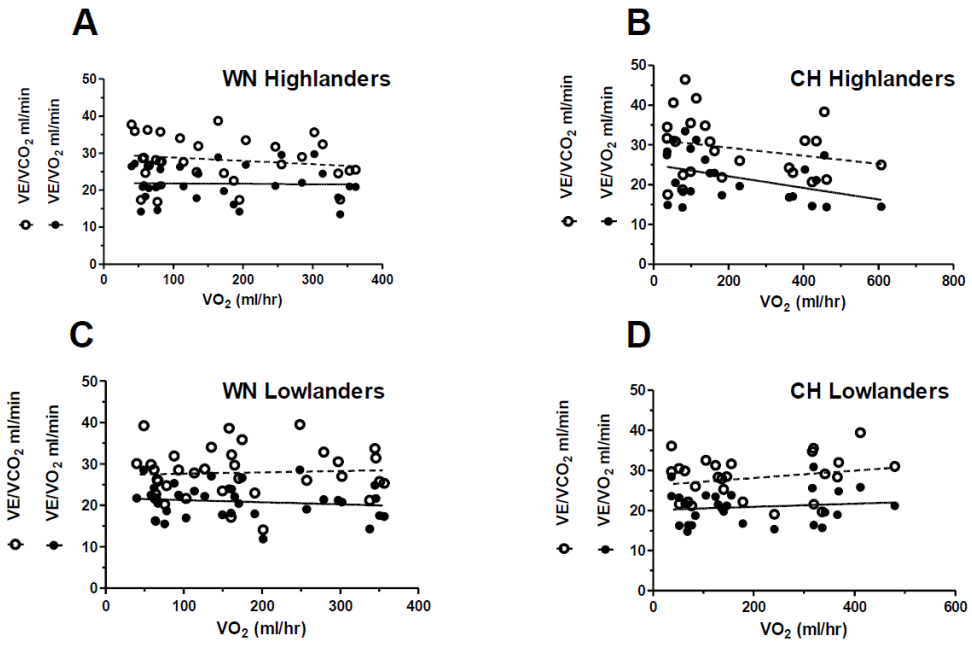
A
WN Highlanders
B
CH Highlanders
C
WN Lowlanders
D
CH Lowlanders
VE/VCO2 ml/min
VE/VO2 ml/min
VO2 (ml/hr)

Figure 2.S1. Ventilatory equivalent of first-generation laboratory born and raised highland and lowland native deer mice (*Peromyscus maniculatus)* acclimated to either control warm normoxic (WN) or cold hypoxic (CH) conditions, exposed to various temperatures from 30ºC to maximal cold-induced $\dot{V}O_2$max. Values compare the ratio of total ventilation (VE) to either $\dot{V}O_2$ (solid circles with solid regression line) or $\dot{V}CO_2$ (open circles with dashed regression line) at a given $\dot{V}O_2$. A) WN Highlanders; B) CH Highlanders; C) WN Lowlanders; D) CH Lowlanders. Data for $\dot{V}O_2$ (ml hr^{-1}) utilized temperatures from 30ºC, 20ºC, 15ºC, 10ºC, 5ºC, 0ºC and cold induced $\dot{V}O_2$max for WN animals, and 30ºC, 0ºC, and $\dot{V}O_2$max for CH animals. All measurements were performed in normoxia. All VE/$\dot{V}O_2$ and VE/$\dot{V}CO_2$ slopes are close to 0, and do not differ between populations or acclimations ($p>0.05$).

Figure 3.S1

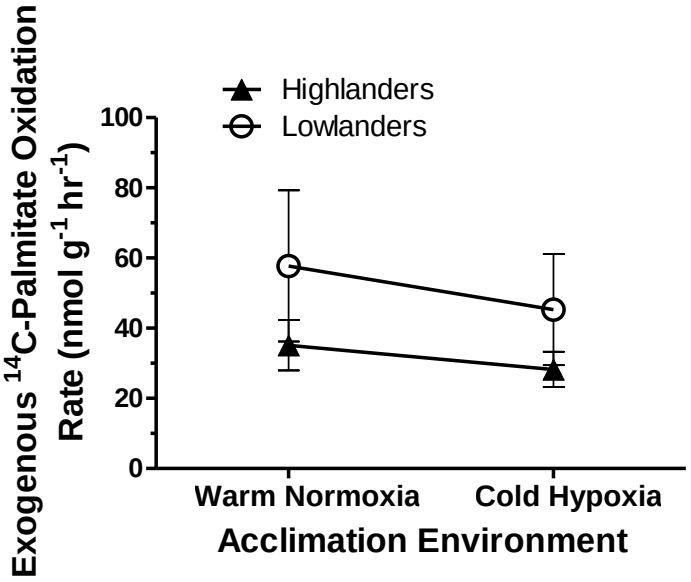
Highlanders
Lowlanders
Exogenous ^{14}C-Palmitate Oxidation Rate (nmol g^{-1} hr^{-1})
100
80
60
40
20
0
Warm Normoxia
Cold Hypoxia
Acclimation Environment

Figure 3.S1. Exogenous fatty acid oxidation rates of soleus muscle. First-generation laboratory born and raised highland and lowland deer mice (*Peromyscus maniculatus*), acclimated to control warm normoxia (23^{o}C, 21 kPa O_2) or cold hypoxia (5^{o}C, 12 kPa O_2) conditions. The oxidation of palmitate was determined by placing freshly intact soleus muscle into incubation buffer containing ^{14}C-palmitic acid. After one hour, incubation buffer $^{14}CO_2$ was released, trapped, and counted using a scintillation counter. Sample sizes for warm normoxia and cold hypoxia were *N*=11 and *N*=9 for highlanders, and *N*=7 and *N*=6 for lowlanders, respectively. Data are reported as mean ± s.e.m.

Figure 5.S1

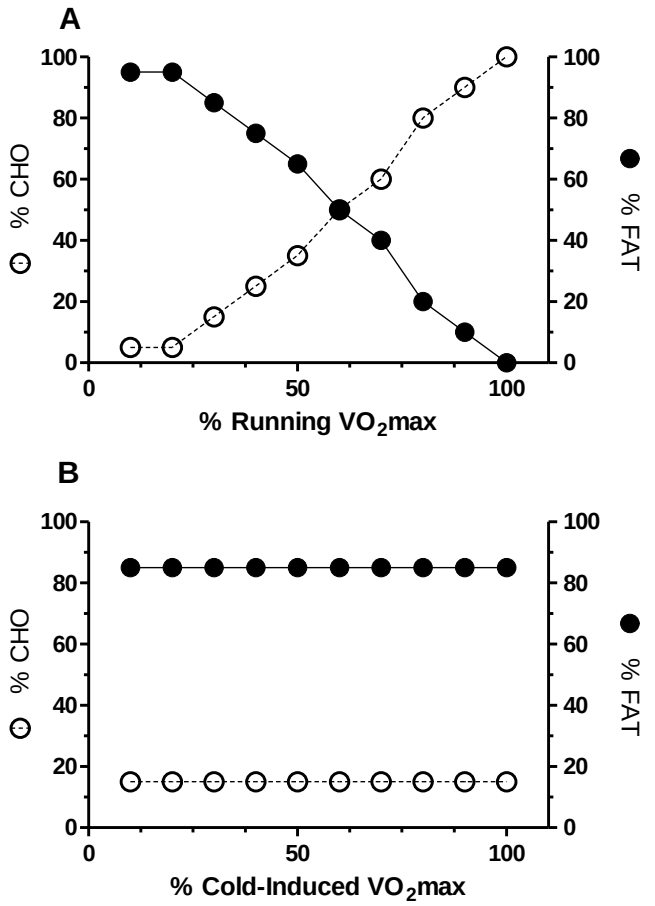
A
100
80
60
40
20
0
% CHO
% FAT
0
50
100
% Running VO2max
B
% Cold-Induced VO2max

Figure 5.S1. A comparison of the proportion use of metabolic fuels (as % total VO_2) during running exercise (A) and thermogenesis (B). Fats (closed circles) are the main source of metabolic substrate for running exercise during low to moderate exercise intensities. As exercise intensities increases towards running VO_2max, the proportion of fat oxidation decreases with a corresponding increase in the proportion of carbohydrates oxidized (CHO; open circles). Unlike exercise, however, as thermogenic demands increase towards cold-induced VO_2max, the proportion of fat remains dominant at across all thermogenic intensities.

Figure 5.S2

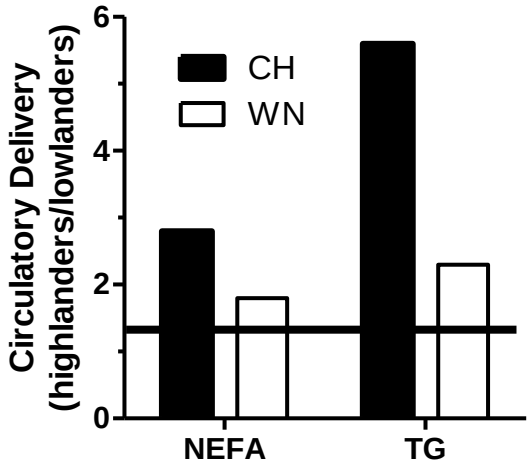
Circulatory Delivery
(highlanders/lowlanders)
6
4
2
0
CH
WN
NEFA
TG

Figure 5.S2. Ratios of highland-to-lowland deer mouse circulatory non-esterified fatty acid (NEFA) and triglyceride (TG) delivery rates during cold-induced VO_2max. First-generation deer mice (*Peromyscus maniculatus*) were acclimated to either warm normoxia (WN; 21 kPa O_2, 23^oC) or cold hypoxia (CH; 12 kPa O_2, 5^oC) conditions for ~6-8 weeks. Solid horizontal line indicates a highland-to-lowland whole-animal lipid oxidation rate ratio of 1.35. When compared to lowlanders, circulatory lipid transport for highland deer mice is much higher than what would be expected if circulatory lipid transport scaled with whole-animal lipid oxidation rate. Acclimation to CH further exacerbates these observations.

Figure 5.S3

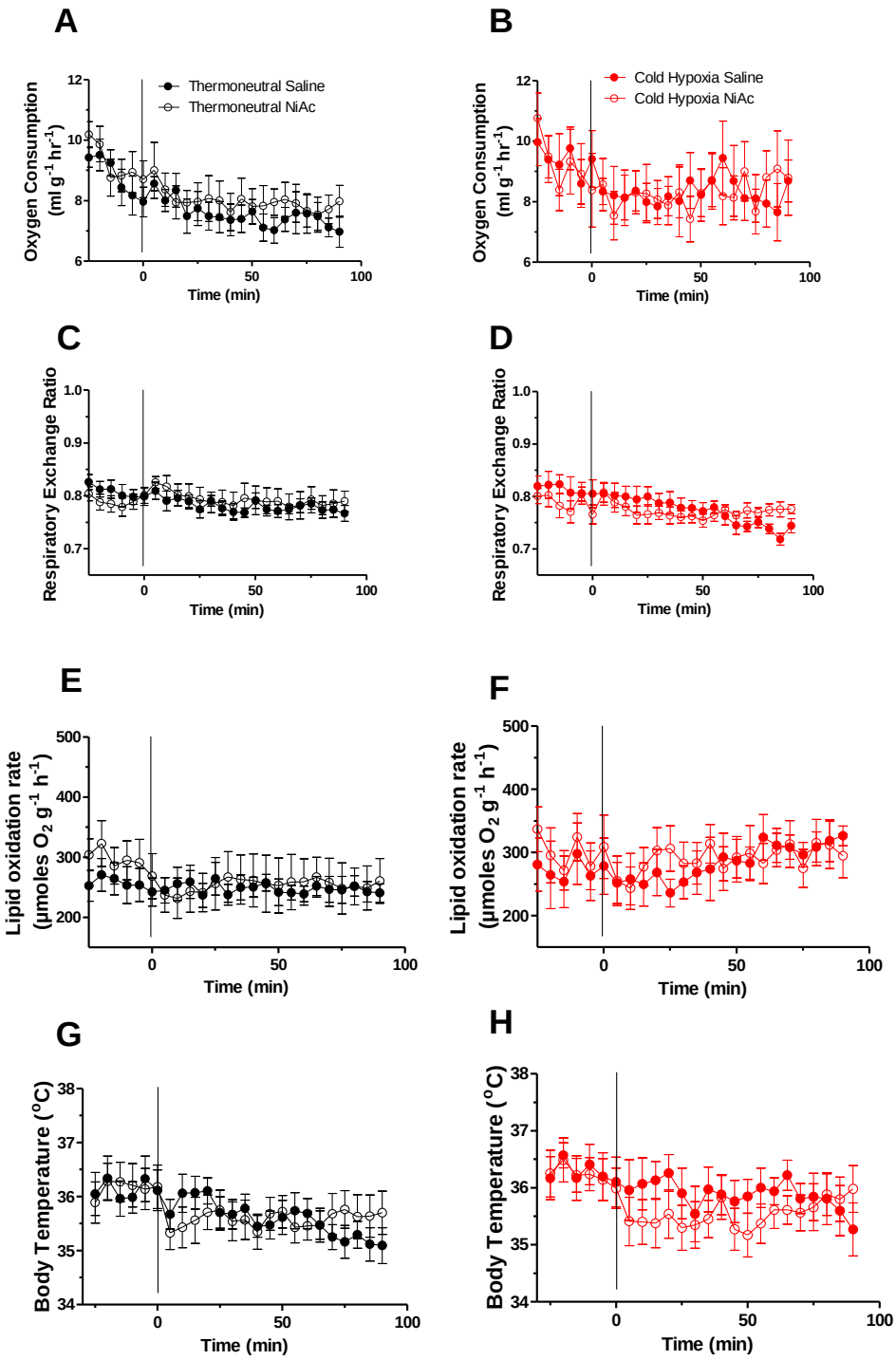
A
Thermoneutral Saline
Thermoneutral NiAc
Oxygen Consumption (ml g-1 hr-1)
Time (min)
B
Cold Hypoxia Saline
Cold Hypoxia NiAc
Oxygen Consumption (ml g-1 hr-1)
Time (min)
C
Respiratory Exchange Ratio
Time (min)
D
Respiratory Exchange Ratio
Time (min)
E
Lipid oxidation rate (µmoles O2 g-1 h-1)
Time (min)
F
Lipid oxidation rate (µmoles O2 g-1 h-1)
Time (min)
G
Body Temperature (°C)
Time (min)
H
Body Temperature (°C)
Time (min)

Figure 5.S3. The effects of an inhibitor of intracellular lipolysis (nicotinic acid; NiAc) on highland deer mice (*Peromyscus maniculatus*) exposed to a moderate cold challenge (5ºC) for 2 hours. Second-generation highland deer mice were acclimated to either thermoneutral (black; 21 kPa O_2, 30ºC) or cold hypoxia (red; 12 kPa O_2, 5ºC) conditions for ~6-8 weeks. Mice were fasted for 2.5 hours before the start of the trial. 30 minutes into the trial (vertical line), mice were either given an oral dose of NiAc (150µg g^{-1}; open circles) or saline (5µL g^{-1}; filled circles). Oxygen consumption ($\dot{V}O_2$) (in ml g^{-1} hr^{-1}) (A, B), with the corresponding Respiratory Exchange Ratios (RER= $\dot{V}CO_2/\dot{V}O_2$) (C, D), whole-animal lipid oxidation rates (in µmol g^{-1} hr^{-1}) (E, F) and core body temperatures (G, H) were measured. No effects of population or acclimation were observed ($P > 0.05$). N = 10 for each treatment group. Data are presented as means ± s.e.m.

Figure 5.S4

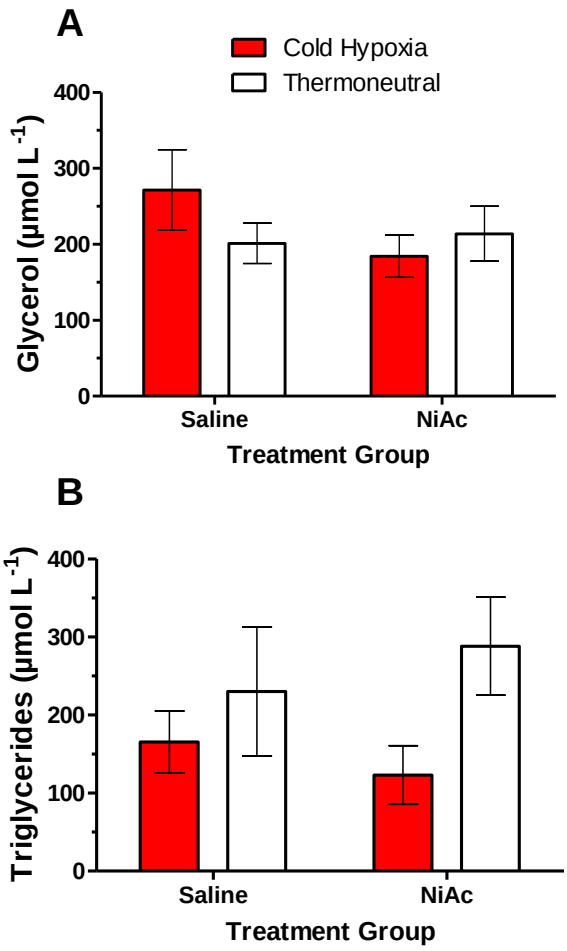
A
Cold Hypoxia
Thermoneutral
Glycerol (µmol L-1)
400
300
200
100
0
Saline
NiAc
Treatment Group
B
Triglycerides (µmol L-1)
400
300
200
100
0
Saline
NiAc
Treatment Group

Figure 5.S4. The effects of an inhibitor of intracellular lipolysis (nicotinic acid; NiAc) on plasma glycerol (μmol L^{-1}) (A) and plasma triglycerides (μmol L^{-1}) (B) in highland deer mice (*Peromyscus maniculatus*) exposed to a moderate cold challenge (5ºC) for 2 hours. Second-generation highland deer mice were acclimated to either thermoneutral (white bars; 21 kPa O_2, 30ºC) or cold hypoxia (red bars; 12 kPa O_2, 5ºC) conditions for ~6-8 weeks. Mice were fasted for 2.5 hours before the start of the trial. 30 minutes into the trial (vertical line), mice were either given an oral dose of NiAc (150μg g^{-1}) or saline (5μL g^{-1}). Blood was collected immediately after the trial and plasma was separated. There was a trend for an acclimation effect for plasma triglyceride concentration, but it did not reach significance ($P = 0.07$). $N = 5$ for each treatment group. Data are presented as means ± s.e.m.

Figure 5.S5

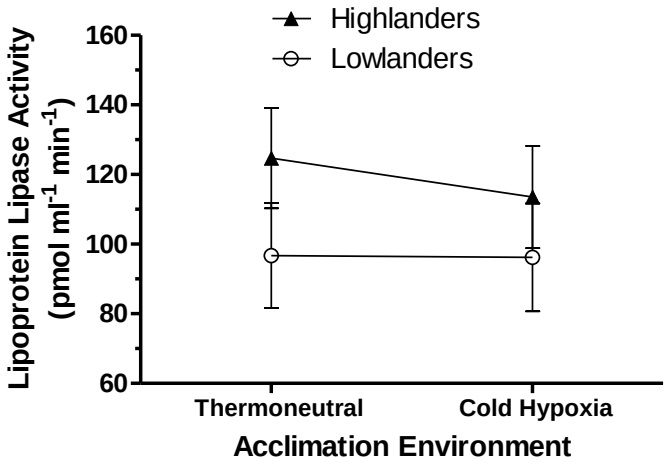
Highlanders
Lowlanders
Lipoprotein Lipase Activity
(pmol ml-1 min-1)
160
140
120
100
80
60
Thermoneutral
Cold Hypoxia
Acclimation Environment

Figure 5.S5. Lipoprotein lipase (LPL) activity (pmol ml^{-1} min^{-1}) in the plasma of highland and lowland deer mouse (*Peromyscus maniculatus*) acclimated to either thermoneutral (21 kPa O_2, 30ºC) or cold hypoxia (12 kPa O_2, 5ºC) conditions for ~6-8 weeks. Deer mice were injected with 0.2 U g^{-1} heparin via tail vein to liberate tissue bound LPL into the plasma. After 10 minutes, blood was collected via facial vein and plasma was separated. An enzyme-linked immunosorbent assay was used to quantify LPL activity. No main effects of population or acclimation were observed ($P > 0.05$). Sample sizes for thermoneutral and cold hypoxia were N = 4 and 6 for highlanders, and N = 5 and 6 for lowlanders. Data are presented as means ± s.e.m.

Figure 5.S6

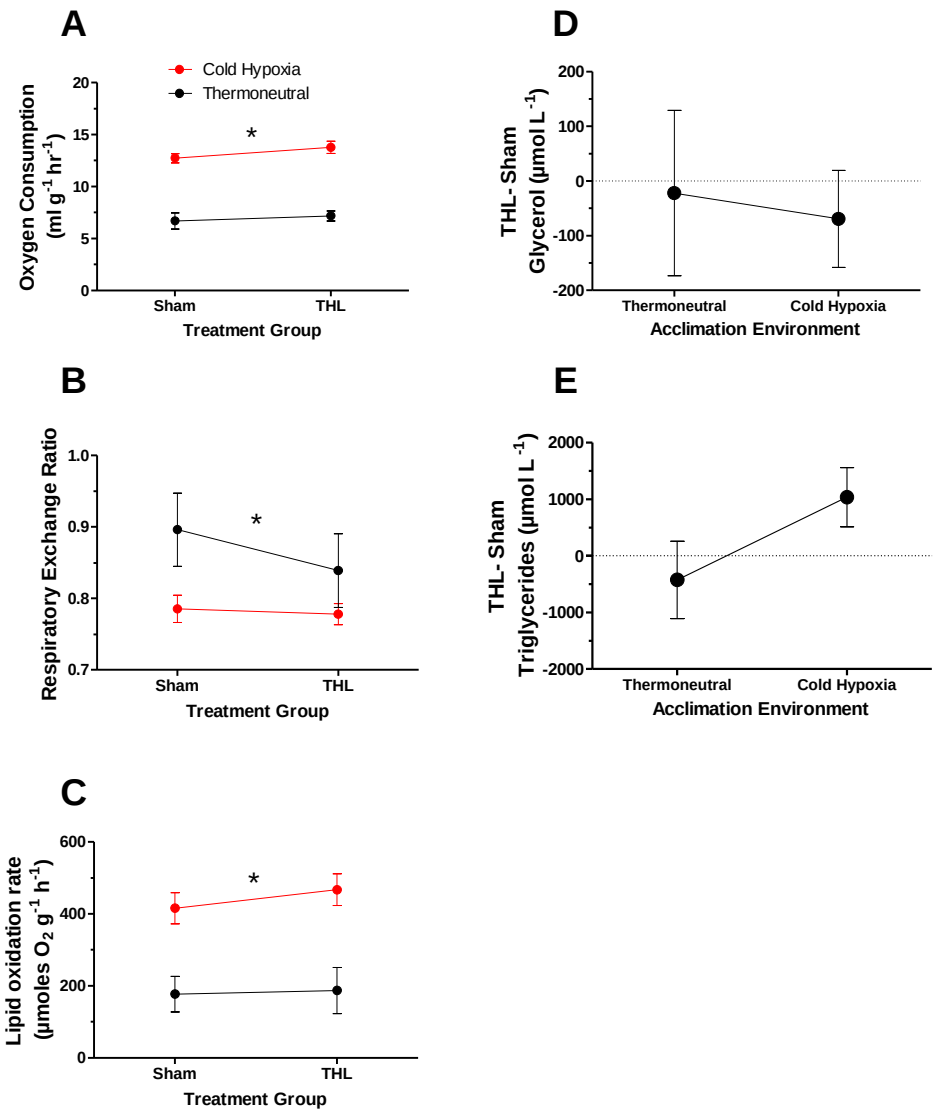
A
Cold Hypoxia
Thermoneutral
Oxygen Consumption (ml g-1 hr-1)
20
15
10
5
0
*
Sham
THL
Treatment Group
D
THL- Sham Glycerol (µmol L-1)
200
100
0
-100
-200
Thermoneutral
Cold Hypoxia
Acclimation Environment
B
Respiratory Exchange Ratio
1.0
0.9
0.8
0.7
*
Sham
THL
Treatment Group
E
THL- Sham Triglycerides (µmol L-1)
2000
1000
0
-1000
-2000
Thermoneutral
Cold Hypoxia
Acclimation Environment
C
Lipid oxidation rate (µmoles O2 g-1 h-1)
600
400
200
0
*
Sham
THL
Treatment Group

Figure 5.S6. The effects of a lipoprotein lipase inhibitor, tetrahydrolipstatin (THL), on second-generation highland deer mice (*Peromyscus maniculatus*) acclimated to either thermoneutral (black; 21 kPa O_2, 30ºC) or cold hypoxia (red; 12 kPa O_2, 5ºC) conditions for ~6-8 weeks. Deer mice were either injected with 100 µL of THL (2.5 mg mL^{-1}) or 100 µL of vehicle (Sham- 10% DMSO in PBS) via tail vein immediately before a hypoxic cold-induced $\dot{V}O_2max$ trial. Plasma samples were taken immediately after the end of the trial via facial vein. Each mouse received both treatments, with 10 days between each trial. (A) Oxygen consumption ($\dot{V}O_2$) (in ml g^{-1} hr^{-1}), (B) Respiratory Exchange Ratios (RER= $\dot{V}CO_2/\dot{V}O_2$) and (C) whole-animal lipid oxidation rates (in µmol g^{-1} hr^{-1}) all demonstrated a significant main effect of acclimation ($P < 0.05$); however, there were no significant main effects of treatment ($P > 0.05$). Changes in plasma concentrations of glycerol (D) and triglycerides (E) were determined in each mouse. There were no significant differences observed. *Significant effect of population. N = 7 for sham cold hypoxia mice and thermoneutral mice. N = 7 for THL cold hypoxia mice and 5 for THL thermoneutral mice. Data are presented as means ± s.e.m.